RESEARCH MEMORANDUM

for the

U. S. Air Force

FLUTTER TESTS OF A 1/25-SCALE MODEL OF THE B-36J/RF-84F TIP-COUPLED AIRPLANE CONFIGURATION IN THE LANGLEY 19-FOOT PRESSURE TUNNEL

By Robert H. Neely

Langley Aeronautical Laboratory
Langley Field, Va.

NATIONAL ADVISORY COMMITTEE
FOR AERONAUTICS

WASHINGTON

C[redacted]L

NACA RM SL56A25b [redacted] UNCLASSIFIED

NATIONAL ADVISORY COMMITTEE FOR AERONAUTICS

RESEARCH MEMORANDUM

for the

U. S. Air Force

CLASSIFICATION CHANGED To UNCLASSIFIED By authority of NASA Date 3-5-71 V.9 No.1

CLASSIFICATION CHANGED To CONFIDENTIAL By authority of TPA 55, Sept 28, 1961 Date

FLUTTER TESTS OF A 1/25-SCALE MODEL OF THE B-36J/RF-84F TIP-COUPLED AIRPLANE CONFIGURATION IN THE LANGLEY 19-FOOT PRESSURE TUNNEL

CLEARANCE NO. AF-218

By Robert H. Neely

SUMMARY

Tests of a 1/25-scale model of a B-36J/RF-84F tip-coupled airplane were made in the Langley 19-foot pressure tunnel in order to evaluate the flutter characteristics where bomber-body freedoms are allowed and to obtain an indication of the dynamic stability characteristics of the configuration. The bomber model was supported by a gimbal which moved on a vertical rod and permitted four degrees of body freedom. Both the fighter and bomber models were scaled in geometry, mass, and inertia; in addition, the bomber model was elastically scaled. The variables studied in the investigation were the skew angle of the fighter-bomber coupling, fighter longitudinal position, fighter and bomber loading, angle of sideslip, degrees of body freedom, and the number of fighters. In this report, the flight technique employed is described in some detail. The overall flight behavior is discussed, and certain limitations in interpreting the results in terms of full-scale flight behavior are noted. Data pertaining to flutter characteristics and to the motion of the fighter relative to the bomber are presented and discussed briefly.

[redacted]

INTRODUCTION

[redacted]

Free-to-roll coupling of fighter airplanes to the wing tips of another airplane poses dynamic stability problems including those associated with flutter which are more complex than those encountered with single airplanes. In reference 1 it was found that, for satisfactory flight behavior of coupled airplanes, a certain amount of restoring moment must be supplied by the fighter when it is displaced in bank

[redacted] UNCLASSIFIED

C[redacted]

relative to the bomber. One method of producing this moment is to skew the hinge axis so that, when the fighter is banked up, its angle of attack is decreased. A current project where the fighters are coupled to the wing tips of a bomber by a skewed hinge coupling is the B-36J/RF-84F airplane configuration. Some of the dynamic problems associated with this configuration have been investigated at the David Taylor Model Basin using a 1/25-scale semispan model which was cantilevered from the tunnel sidewall. (See ref. 2.) In the investigation of reference 2 the dynamic behavior of the configuration below flutter speed and the flutter speed itself were determined for various skew angles of the hinge.

At the request of the United States Air Forces, tests have been made in the Langley 19-foot pressure tunnel of a 1/25-scale full-span model configuration in which the bomber model was supported by a gimbal which moved on a vertical rod and permitted four degrees of rigid-body freedom - roll, yaw, pitch, and vertical translation. The purpose of these tests was to evaluate the flutter characteristics where bomber-body motion is allowed and to obtain an indication of the dynamic lateral and longitudinal stability characteristics of the configuration. Both the fighters and bomber were scaled in geometry, mass, and inertia; in addition, the bomber was elastically scaled. The most important configuration variable in the present investigation was the hinge skew angle. Other variables investigated were fighter longitudinal position, fighter weight, bomber weight, angle of sideslip, degrees of bomber body freedom, and number of fighters.

In this report the flight technique employed during the investigation is described in some detail because of its nonroutine nature. The general flight behavior is discussed and certain limitations in interpreting the results in terms of full-scale flight behavior are noted. Data pertaining to flutter characteristics and to the fighter motion relative to the bomber are presented and discussed briefly.

SYMBOLS

V	free-stream velocity, mph
V_c	flutter velocity, mph
q	free-stream dynamic pressure, lb/sq ft
β	sideslip angle, deg (positive nose left)
α_f	angle of attack of bomber fuselage, deg

W	weight, lb
ΔL	incremental lift, L-W, lb
D	drag, lb
L_β	derivative of rolling moment due to sideslip, ft-lb/deg
N_β	derivative of yawing moment due to sideslip, ft-lb/deg
$\bar{c}$	mean aerodynamic chord of bomber wing
X,Y,Z	reference axes, direction and sign of axes are same as stability system of axes but origin is located at gimbal
x,z	coordinates of bomber center of gravity, ft
δ	hinge skew angle, angle between bomber center line and projection of hinge line on chord plane, deg
ϕ_b	bomber bank angle, deg (positive, right wing down)
ϕ	fighter roll angle relative to bomber wing tip, deg (measured in a plane perpendicular to hinge center line)
f	frequency, cps
f_c	flutter frequency, cps
f_ϕ	fighter roll frequency, cps
f_x	bomber-wing chordwise-bending (fore and aft) frequency, cps
f_{x_1}	first symmetric chordwise-bending (fore and aft) frequency, cps
$f_{\bar{x}_1}$	first antisymmetric chordwise-bending (fore and aft) frequency, cps
f_z	bomber-wing vertical-bending frequency, cps
f_{α_1}	first symmetric torsional frequency, cps
EI	bending rigidity, lb-in.^{2}

GJ	torsional rigidity, lb-in.^{2}
I_X, I_Y, I_Z	mass moments of inertia, lb-in.^{2}
h	decrement coefficient, determined from $\frac{\text{Amplitude at } t}{\text{Amplitude at } t = 0} = e^{-ht}$
g	structural damping constant
t	time, sec
CB	chordwise bending
VB	vertical bending
T	torsion
A	accelerometer

Subscripts:

u	up
d	down
l	left
r	right
m	model
a	airplane

MODEL AND TESTS

Model Characteristics

The general arrangement of the model configuration is shown in figure 1. A 1/25-scale model of the bomber airplane was supplied by Convair, Ft. Worth Division, and was intended to simulate the B-36J airplane. The elastic and mass properties of the model were scaled from calculated characteristics of the airplane; however, it is not known to what extent these characteristics match the actual airplane characteristics. In scaling the model, the relative density, the Froude number, and reduced

frequency were matched. The mass of the model at the average air density of the tests was scaled to represent that of the airplane flying at approximately 27,500 feet. The geometric scale was 1:25 which fixes the velocity scale V_m/V_a at 1:5 and the frequency scale f_m/f_a at 5:1. A number of scale factors are listed below:

	Model:Airplane
Length	1:25
Air density	1:0.4097
Mass	1:6401
Mass moments of inertia	1:4000625
Velocity	1:5
Frequency	5:1
Time	1:5
Acceleration	1:1

The Mach number and Reynolds number were not duplicated. The design requirements, details of construction and detailed mass, inertia, and elastic properties of the B-36J model are given in reference 3. Some of the characteristics of the Convair B-36J airplane are given in table I. Briefly, the wing and fuselage structure of the model consisted of a spar assembly representing the elastic characteristics, balsa box fairings, and various concentrated masses. Thin rubber was used to seal the gaps between the balsa pods. Some photographs indicating the type of structure employed are shown in figure 2.

Measurements of the rigidity of the bomber wing were made before the tests were begun. The results of these measurements are presented in figure 3. The measurements were generally made with the balsa pods attached to the wing spar but hinged open as in figure 2. The values of EI and GJ were computed from measurements of the slope of deflection curve of the wing spar when subjected to a tip load.

The two bomber loading conditions - designated as light and heavy - are defined in figure 4. Different loading conditions were obtained by varying lead weights representing fuel in the wings and bombs in the fuselage. Center-of-gravity locations and mass moments of inertia for $\alpha_f = 0^\circ$ are also given in figure 4. These characteristics were calculated from measured characteristics of configurations not greatly different from those shown in figure 4. Values of I_X and I_Y were measured by the pendulum method using an arm of approximately 6 inches. Values of I_Z were measured using a calibrated steel torsion rod. Small errors exist in the values of moment of inertia presented as evidenced by the fact that $I_Z > I_X + I_Y$.

The fighter models were supplied by Thieblot Aircraft Company, Incorporated, and were intended to be models of the RF-84F airplane scaled with respect to geometry, mass, inertia, and center-of-gravity location. The models were essentially rigid. Mass and moment-of-inertia characteristics measured by Thieblot Aircraft Company are listed in table II. The mass characteristics of the fighters were changed by adding external fuel tanks and additional weight within the fuselage.

The fighters were hinged to the bomber through a coupling, the hinge axis of which was skewed relative to a longitudinal plane. The positions of the fighters relative to the bomber for the two longitudinal positions of the fighter are shown in figure 5. A drawing of the coupling is shown in figure 6 and a photograph in figure 7. The fighters were free only in roll about the hinge axis but could be pitched about an axis normal to the hinge axis using a remotely controlled screw-block mechanism. The angles of the hinge axis were nominally 8° and 15°. The skew angles were generally within a few tenths of a degree of these values but in some cases they were more. The bearing surfaces of the rolling axis of the hinge were magnesium and were lubricated.

Test Setup and Flight Technique

Two methods of supporting the model were employed during the investigation which was conducted in the Langley 19-foot pressure tunnel. One method allowed four degrees of bomber body freedom and is designated the bomber-free condition. The other method of supporting the model allowed the bomber to be free in roll only and is designated the bomber-fixed condition.

The test setup for the bomber-free condition is shown in figure 8. The bomber-free test setup and flight technique employed in the present investigation are nearly the same as those used in reference 4. The bomber model was attached to a vertical rod by means of a gimbal arrangement which allowed the model to be free in vertical translation, pitch, yaw, and roll. The rod was 1/4 inch in diameter and 40 inches long between the stops. The spring constant of the support assembly for load applied at the center of the rod was 12.5 lb/in. for drag loads and 18.2 lb/in. for side loads. It should be noted that the vertical rod passed through the bomber model behind its center of gravity. (See fig. 1.)

The various cables used in controlling the bomber model are shown in figures 8 and 9. The various controls and their functions are summarized in table III. The main longitudinal control was obtained through operation of cables attached to the model at points close to the surface of the fuselage and directly above and below the bomber center of gravity. These cables were used to position the model, restrict vertical translation,

and excite the model by jerking. Longitudinal trim was maintained by a horizontal stabilizer which was remotely controlled during flight. Lateral trim was obtained by adjusting the ailerons and rudder before flight. During the course of the investigation, a small remotely controlled flap was added to the right wing to provide fine lateral trim. The sideslip angle of the bomber was restricted to $\pm 5^{\circ}$ by vertical cables passing near the nose of the fuselage as shown in figure 8. A single cable was attached to each wing in order to restrain the model in rolling and also to excite the model asymmetrically.

The only control for the fighters was the drive mechanism used to change fighter angle of attack relative to the bomber and thereby the fighter roll angle.

At each airspeed, the bomber and fighters were trimmed level and the bomber was excited by first jerking one of the vertical control cables for symmetric excitation and then, somewhat later, one of the roll control cables for asymmetric excitation. Data were recorded and the procedure repeated for the next speed.

The particular method of mounting used for testing the model does not provide for good simulation of the airplane flight behavior and probably contributes to the difficulties which were encountered in flying the model. For the longitudinal mode locating the gimbal behind the center of gravity introduces several additional forces (see fig. 10) which affect trim and stability; however, the magnitude of these forces has not been determined. The first of these forces is the frictional force between the gimbal and the vertical rod which produces a destabilizing pitching moment if the incremental lift force acts forward of gimbal. The second force is the reaction of the rod to the drag which, as shown in figure 10, produces a destabilizing pitching moment. Other forces result from the constraining effect of the vertical rod on pitching motions. During flight, the bomber had a tendency to diverge in pitch and vertical translation so that frequent adjustment of the vertical control cable was required.

For the lateral mode, the directional stability parameter C_{n_β} about the center of rotation is approximately 20 percent lower than the value about the center of gravity. Furthermore, weight moments which affect lateral stability are introduced for combined yawing and rolling motions. An analysis of the static equilibrium condition for combined sideslip and bank in figure 11(a) indicates the effect of the weight moments on stability. In figure 11(a), the lateral-moment equations are shown and the boundary of center-of-gravity locations for static stability is expressed. The location of the bomber center of gravity relative to the approximate static-stability boundary is shown in figure 11(b). The stability derivatives used in defining this boundary were obtained from

reference 5. The center of gravity is located in a region where a combined roll and yaw divergence would be expected. For the heavy bomber case, such a divergence was generally encountered; however, for the light bomber, the lateral flight behavior was generally good. This difference in flight behavior may perhaps be ascribed to the larger weight moments of the heavy bomber. Judgment of the flight characteristics for some runs was difficult because the model was not trimmed laterally. In addition to the limitations imposed by the location of the center of gravity, the lack of lateral freedom of the configuration does not allow for accurate simulation of complete configuration flight behavior. Because of the aforementioned limitations on flight simulation, the primary emphasis during the investigation was on the motion of the fighters relative to the bomber.

In addition to tests with the bomber free in four directions, a number of special runs were made with the model free in roll only. The other degrees of freedom were eliminated for reasons of model safety. The setup for this condition, designated the bomber-fixed condition, is shown in figure 12. The bomber fuselage was at approximately zero angle of attack. Vertical and horizontal cables were run from the fuselage nose to the tunnel wall in order to restrain yawing and pitching. With the fuselage restrained in this manner the natural frequency of the structure in the yaw direction was within the range of fighter roll frequencies. In order to increase the natural frequency in yaw, the forward part of the fuselage was stiffened by clamping steel bars to the spar and by adding an aluminum shell (fig. 12). A few tests were made, however, with the fuselage stiffened by taping 1/8-inch-thick balsa strips to the fuselage surface. Excitation was provided by the roll-control cables shown in figure 8. Both cables were jerked simultaneously for symmetric excitation; one cable was jerked for asymmetric excitation. In order to determine the influence of air gusts on fighter behavior, gusts were produced by deflecting an airfoil located ahead and below the left fighter. The airfoil installation is shown in figure 13. The airfoil trailing edge was about 1/2 inch ahead of the fighter nose and about 4 inches below the fighter.

A listing of the measurements made and the associated instrumentation used during the tests are given in table IV. A recording oscillograph was used to record the data. The outputs of the strain gages were monitored during each flight.

The bulk of the test program consisted of 16 runs of the model with four rigid-body degrees of freedom. Two hinge skew angles, two fighter positions, two fighter weights, and two bomber weights were investigated. The effects of sideslip angle, the removal of one fighter, and gusts on fighter behavior were determined from tests with the bomber free in roll only. The airspeed was varied from about 65 miles per hour to 75 miles per hour up to the flutter speed or to some speed in excess of the maximum scaled speed of the configuration. Each run was normally terminated by

shutting off the tunnel-fan drive motor. This operation proved to be an effective means in limiting the amplitude of flutter.

Measurements of Vibration Frequencies

Measurements were made at zero airspeed of the vibration frequencies of the complete model and, for comparison, the cantilever wing. The results are presented in tables V and VI. The identifying modes given in these tables are only approximate and indicate the predominant motion.

The vibration frequencies of the complete model were measured with the model mounted on the support rod. The frequencies given in table V(a) were measured with the model fastened to the rod so that it was restrained in the translational degrees of freedom but was free in the rotational degrees of freedom. The frequencies presented in table V(b) were measured with the model mounted as shown in figure 12. The fighters were supported by strings attached to the top of the tunnel so that little longitudinal restraint of the fighters was present. Resonant frequencies were determined by hand-driving the model.

For the cantilever wing tests (table VI), the wing was mounted horizontally, and the fighter was supported at its center of gravity by a string and a soft coil spring (spring constant is 0.125 lb/in.). The natural frequencies were determined by resonance testing except for some of the chordwise-bending frequencies which were determined by plucking the wing.

Damping characteristics at zero airspeed were measured from decay records of the strain-gage outputs for a few of the configurations. These characteristics are presented in table VII. The decrement coefficient was constant for all amplitudes.

PRESENTATION OF RESULTS

A sample record showing the response of the fighters and the bomber wing to disturbances is presented in figure 14. The frequencies and amplitudes of the roll oscillation of the fighter are plotted as functions of the tunnel airspeed in figure 15 for four basic configurations - two skew angles and two fighter weights. The amplitudes plotted are those for the oscillation which was present after the oscillation produced by control excitation had decayed. Representative time histories are given in figures 16 to 19.

A summary of the maximum speeds and corresponding values of dynamic pressure and air density is presented in tables VIII and IX for all the

configurations investigated. Oscillograms showing the bomber wing and fighter response during flutter are presented in figure 20. Only one run was made which indicates the reproducibility of the flutter speed. This is shown at the bottom of table VIII. The flutter speeds are plotted as a function of skew angle in figure 21. For comparative purposes, flutter speeds measured in the semispan tests in reference 2 are presented also.

The effects of sideslip angle on the fighter roll frequency are shown in figure 22. These results were obtained with the bomber free in roll only. Data for the single-fighter configuration with 15° skew angles are presented in figures 23 and 24.

Data pertaining to the response of fighter due to gusts are given in figures 25 and 26 and table X. Figure 25 presents typical oscillograph records for the four different fighter configurations at $V = 75$ mph and defines the amplitudes and frequencies used in figure 26 and table X. The amplitude of the roll oscillations as plotted in figure 26 are averages of about four test points for pulse times below 0.3 second. For large pulse times, the plotted data are averages of one to three test points. The amplitudes plotted in figure 26 are for comparative purposes only. A schematic diagram illustrating the fighter-bomber roll oscillation encountered with the fighters banked up is presented in figure 27.

DISCUSSION

The basic points of interest in the present investigation are the motions of the fighter relative to the bomber at normal flying speeds, the flutter characteristics of the combination, and the overall configuration dynamic stability characteristics (rigid-body modes). The greater amount of information was obtained on the first two points inasmuch as the flying behavior of the combination, as discussed previously, makes any evaluation of overall configuration stability uncertain.

Flight Behavior of Fighters and Flutter Characteristics

General comments.- The response of the fighters relative to the bomber as a result of excitation of the combination consisted of a short-period lateral oscillation and irregular displacements from a wings-level attitude. A record of the rolling response of the fighters which illustrates this response is presented in figure 14. It should be noted that, after the response due to excitation by the control cables had decayed, a response of the fighters resulting from random tunnel disturbances existed.

[redacted]

The frequencies and amplitudes of the short-period oscillation of the fighter are plotted as functions of the tunnel airspeed in figure 15 for four basic configurations - two skew angles and two fighter weights. The frequencies were measured by counting cycles over a portion of the record both during the decay from control excitation and during the response due to tunnel disturbances. The frequencies measured in this manner may not be the true frequency of the short-period roll oscillation. The frequencies vary linearly with airspeed over most of the speed range for which data are presented and their values are consistent with the values reported in reference 2.

The amplitudes plotted in figure 15 are roughly average values of the roll angle response of the fighters to tunnel disturbances. Data for both left and right fighters are plotted. These data may give some indication of the effect of increasing airspeed on the relative rolling response of the fighter to disturbances. The average amplitude of the roll oscillation was nearly constant over an appreciable speed range in some cases. (See figs. 15(b) and 15(d).) For most of the configurations, the magnitude of the oscillation increased significantly as the instability speed was approached. For speeds close to instability, the fighter roll oscillation was nearly constant in amplitude or exhibited beats. The oscillograms of figures 16 to 19 indicate that the roll oscillation is well damped at the lower speeds and is only lightly damped at the higher speeds.

Flutter characteristics.- Oscillograms which illustrate the flutter behavior are shown in figure 20. The flutter mode was symmetrical in all cases. Some differences in the flutter mode were observed which appear to be primarily a function of the fighter mass. For light fighters, instability was manifested by a slowly increasing oscillation involving, predominantly, fighter roll and bomber-wing chordwise bending. (See fig. 20(a).) The fighter roll frequency was very close to the natural chordwise-bending frequency of the bomber wing at a speed only slightly smaller than the flutter speed. (See table VIII.) The flutter frequency was also close to this frequency. In figure 20(a) it may be seen that a second harmonic in chordwise bending exists. In these tests, however, flutter seemed to occur when the fighter roll frequency was close to the fundamental chordwise-bending frequency.

For heavy fighters instability occurred rather abruptly and was very violent, as shown in figure 20(b). From visual observations the flutter mode appeared to involve, predominantly, flapping motions or vertical bending of the bomber wing and fighter roll. The fighter roll frequency approached closely the natural chordwise-bending frequency of the wing at speeds a little less than the flutter speeds for the two basic heavy fighter configurations where flutter was obtained (fighters aft; $\delta = 15^{\circ}$). The roll frequency for some configurations, however, was considerably different from the chordwise bending frequency. (See table VIII.) For

all heavy fighter configurations, the roll frequency dropped significantly when instability occurred.

Attention is called to an unusual flutter experience which was encountered when the model was partially restrained by the vertical control cables. An oscillogram is presented in figure 20(c) which shows the change in flutter characteristics when up-elevator is applied and the lower vertical control cable is tightened. It may be seen that the flutter characteristics which were similar to those shown in figure 20(a) were changed to the type shown in figure 20(b).

Effect of body freedoms on flutter characteristics.- An important question concerns the effect of the introduction of body freedoms on the flutter speed. The data of the present investigation are compared with the semispan data of reference 2 in figure 21. Different models were used in the two investigations, and the fighters were farther rearward during the semispan tests by about 0.2 inch for the fighter-aft configurations. The measured vibration frequencies of the configurations for comparable mounting are approximately the same, however, so that the results should be comparable. On the whole, the results of the present tests are consistent with the results of reference 2. It thus appears that the introduction of the four body freedoms had no large effect on the flutter speed. In flight, however, additional longitudinal and lateral freedoms will be introduced so that the results obtained herein may not apply directly.

Effect of skew angle and longitudinal position of fighter on flutter.- The effect of skew angle on general fighter behavior and the flutter speed is very pronounced. Decreasing the skew angle from 15° to 8° raises the speed at which the forced fighter oscillations are encountered (fig. 15) and increases the flutter speed (fig. 21). For the aft fighters, the flutter speed is about 85 miles per hour for a 15° skew angle and is above 110 miles per hour for an 8° skew angle.

Moving the fighter aft increased the flutter speed by about 6 miles per hour for configurations with 15° skew angle. (See table VIII.) Appreciable increases are also indicated for heavy bomber configurations with 8° skew angles.

Effect of bomber and fighter mass on flutter.- As shown in table VIII and figure 21, increasing bomber mass had little effect on the flutter speed. Configurations with light fighters had a lower flutter speed than those with heavy fighters for hinge skew angles of 15°. For the single case available with 8° skew angle (fighters forward and bomber heavy), the light fighters gave a higher flutter speed than the heavy fighters. As shown in figure 21(d), the flutter speed of this heavy fighter configuration was not consistent with the results of reference 2.

Effect of sideslip angle on fighter behavior.- The effects of sideslip angle on the frequency of the fighter roll oscillation and the flutter speed of the symmetrical fighter configuration are indicated in figure 22. When the sideslip angle is positive, the right (leading) and left (trailing) fighters have aerodynamic restoring moments due to roll angle which are smaller and greater, respectively, than those obtained for the zero sideslip condition. The difference in frequencies obtained below 74 miles per hour for the two fighters follows directly from this fact. Above 74 miles per hour, the left and right fighter frequencies coincide and increase in magnitude to a value considerably in excess of the bomber chordwise-bending frequency. For part of the speed range, the disturbances damped out very quickly. Instability in the form of a symmetric fighter oscillation occurred at a speed only slightly less than that attained in unyawed flow.

Results for single-fighter configuration.- When one of the fighters was removed, the mode of flutter was changed somewhat from that which had been obtained with two fighters. (Compare figs. 23 and 20(a).) As shown in figure 24 the fighter roll frequencies exceeded the chordwise-bending frequency of the left wing (left fighter attached) given in table V. In addition, the flutter speed with one fighter attached was considerably greater than that attained with two fighters. (See data on 15° light-fighter configuration in table IX.) Because of the restraints imposed in the tunnel tests (only roll freedom was allowed), it is ~~now~~ not known to what extent this result will be applicable in free flight. For a bomber sideslip angle such that the fighter was rearward, the flutter speed for the 15° light-fighter configuration was considerably lower than that for the zero sideslip case. (See fig. 24(a).) It should be noted that for the heavy-fighter configuration at a sideslip angle of 5° an approximately constant chordwise oscillation of the left bomber wing (fighter attached) was obtained between 83 and approximately 90 miles per hour. The fighter was rolling also but the amplitude of the roll angle was not large.

Response of fighters to artificially produced gusts.- As shown in figure 25 for a test velocity of 75 miles per hour, the motion of the fighter relative to the bomber following a gust was a well damped oscillation which decreased to half amplitude in less than one cycle. The magnitude of the fighter roll angle increases with increase of pulse time or gust length. (See fig. 26.) Light fighters reach greater roll angles than heavy fighters. In addition, fighters with 8° skew angles reach slightly greater roll angles than fighters with 15° skew angles. The full-scale gust length corresponding to a V of 75 miles per hour and a pulse time of 0.3 second is 830 feet.

Observations on Overall Configuration Stability

Previous discussions have suggested that the usefulness of results on rigid-body stability characteristics of the combination is limited; however, there are a few observations on these characteristics which should be noted.

For the free-bomber configurations with heavy fighters at $\delta = 8^{\circ}$, an instability in roll and yaw was encountered at airspeeds below about 75 miles per hour. The instability appeared to be a simple divergence; however, the motion was difficult to evaluate because the bomber hit the yaw restraining cables. The flying characteristics of the configuration appeared to be better at speeds above 80 miles per hour. For 15° fighters, no lateral instability was obtained. With the exception noted above, there did not appear to be any large difference between the flying characteristics of the bomber alone and bomber with fighters.

An interesting result was obtained with the bomber fixed except in roll and with the fighters ($\delta = 8^{\circ}$) trimmed so that they were banked up. A rolling oscillation involving essentially rigid-body motions of the bomber and the fighters occurred. A sketch describing the motion for light fighters with $\delta = 8^{\circ}$ is shown in figure 27. It may be seen that the bomber leads the fighter. The amplitude of the oscillation built up slowly and occasionally damped out for the lowest initial roll angle of the fighter (10°). The oscillation was very pronounced for the highest initial roll angle (30°). The frequency varied from 0.8 and 0.9 cycles per second, and the total amplitude of the fighter roll angle varied from 15° to 30°.

Tests of the same configuration as above but with the fighters banked down indicated no unusual behavior. Additional tests with fighters banked down 24° and the bomber free showed that the configuration was steady with no applied disturbance.

SUMMARY OF RESULTS

The main results of the subject investigation are summarized as follows:

1. For symmetric flight conditions, flutter occurred, with some exceptions, when the fighter roll frequency was near the natural chordwise-bending frequency of the bomber wing. The flutter mode was symmetrical.

2. The introduction of the four degrees of body freedom in the present tests had only a small effect on the flutter speed.

3. Decreasing the hinge skew angle from 15° to 8° increased the flutter speed from about 85 miles per hour to above 110 miles per hour. The response of the fighters to gusts in the vicinity of left fighter was not much greater for a hinge skew angle of 8° than for a hinge skew angle of 15° for gust lengths less than 900 feet full scale. For a hinge skew angle of 8°, however, a roll and yaw divergence of the complete configuration occurred at the lower speeds which was not obtained with a hinge skew angle of 15°.

4. Little effect on the flutter speed was obtained when the configuration with two fighters was flown at a fixed sideslip angle of 5° and with the bomber free in roll only.

Langley Aeronautical Laboratory,
National Advisory Committee for Aeronautics,
Langley Field, Va., January 11, 1956.

Lawrence K. Loftin, Jr. for

Robert H. Neely
Aeronautical Research Scientist

Approved:

Eugene C. Draley
Chief of Full Scale Research Division

ecc

[redacted]

REFERENCES

1. Bennett, Charles V., and Boisseau, Peter C.: Free-Flight Tunnel Investigation of the Dynamic Lateral Stability and Control Characteristics of a High-Aspect-Ratio Bomber Model With a Sweptback-Wing Fighter Model Attached to Each Wing Tip. NACA RM L52E08, 1952.

2. Smith, Roger K.: Preliminary Report. Partial Reduction of Data From Wind Tunnel Tests on a Cantilevered Flexible Wing Coupled to Solid Fighter Model. Tech. Rep. No. TR-39-047, Thieblot Aircraft Co. Inc., Nov. 29, 1954.

3. Elrod, J. C., and Morgan, J. E.: B-36J Flutter Model Design and Basic Data. Rep. FZS-36-405 (Contract AF33(600)-5793), Convair, Ft. Worth Div., May 5, 1954.

4. Elrod, J. C.: B-36J Flutter Model Wind Tunnel Test. Rep. FZS-36-303 (Contract AF33(600)-5793), Consolidated Vultee Aircraft Corp., Ft. Worth Div., Sept. 11, 1953.

5. Alexander, S. R., and Pepper, Edward: Tests of a $\frac{1}{14}$- Scale Model of the XB-36 Airplane in the Langley 19-Foot Pressure Tunnel. III - Lateral Stability and Control Characteristics. NACA MR L5D23a, Army Air Forces, 1945.

TABLE I.- CHARACTERISTICS OF THE 1/25-SCALE MODEL

OF THE CONVAIR B-36J AIRPLANE

Wing:	
Span, in.	110.46
Area, sq ft	7.645
Aspect ratio	11.09
Taper ratio	4.0
Mean aerodynamic chord, in.	11.230
Dihedral, deg	2
Incidence, deg	3
Sweep of the $29\frac{1}{2}$ percent chord line, deg	11.62
Fuselage:	
Length, in.	78.00
Diameter (maximum), in.	6.00
Complete model:	
Light bomber:	
Weight, lb	37.3
I_X, lb-in.^{2}	15,397
I_Y, lb-in.^{2}	5,987
I_Z, lb-in.^{2}	22,300
Heavy bomber:	
Weight, lb	56.6
I_X, lb-in.^{2}	19,978
I_Y, lb-in.^{2}	6,028
I_Z, lb-in.^{2}	26,695

TABLE II.- CHARACTERISTICS OF THE 1/25-SCALE MODEL OF THE REPUBLIC RF-84F AIRPLANE

Wing:	
Span (projected), ft	1.341
Area (except inlets), sq ft	0.520
Aspect ratio (except inlets)	3.45
Taper ratio	0.578
Mean aerodynamic chord, in.	4.819
Dihedral, deg	3.5
Incidence, deg	1.5
Sweep of 0.25c line, deg	40
Twist, deg	0
Complete model:	
Light fighter:	
Weight, lb	2.37
I_X, lb-in.^{2}	15.22
I_Y, lb-in.^{2}	35.72
I_Z, lb-in.^{2}	48.39
Heavy fighter:	
Weight, lb	4.01
I_X, lb-in.^{2}	24.51
I_Y, lb-in.^{2}	44.65
I_Z, lb-in.^{2}	64.13

TABLE III.- LIST OF CONTROLS AND THEIR FUNCTIONS

Control	Actuation	Function
Vertical cables	Manual	Control vertical translation Excite model symmetrically for bomber-free condition
Horizontal stabilizer	Electric motor	Longitudinal trim
Roll cables	Manual	Control bomber bank angle Excite model asymmetrically Excite model symmetrically for bomber-fixed condition
Lateral trimmer	Pneumatic	Final lateral trim adjustment
Sideslip restraining cables	Electric motor	Limit bomber yaw angle to $\pm 5^{\circ}$
Fighter pitch	Electric motor	Lateral trim of fighters

TABLE IV.- MEASUREMENTS AND INSTRUMENTATION

Measurement	Instrumentation
Fighter roll angle relative to bomber wing tips	NACA angular position pickoff
Fighter pitch angle relative to bomber wing tip	Slide wire potentiometer
Vertical acceleration of bomber center of gravity	Accelerometer
Bomber spar strains	Vertical bending, chordwise bending, and torsion strain gages
Motions of complete configuration	Synchronized side, rear, and top view movie cameras

TABLE V.- VIBRATION FREQUENCIES FOR COMPLETE MODEL MOUNTED ON SUPPORT SYSTEM

(a) Bomber free; fighters in aft position

Hinge skew angle, deg	Fighter weight	Bomber weight	Frequency, cps	
			f_{x_1}	$f_{\bar{x}_1}$
15	Light	Light	2.30	4.00
15	Heavy	Light	1.89	3.71
8	Heavy	Light	----	----
--	No fighter	Heavy	----	----
8	Light	Heavy	2.23	3.73
8	Heavy	Heavy	1.83	----
15	Heavy	Heavy	1.87	3.45

(b) Bomber fixed; fighters in aft position

Hinge skew angle, deg	Fighter weight	Bomber weight	Other conditions	Frequency, cps		
				f_{x_1}	f_x (left wing)	f_x (right wing)
15	Light	Light	----------	2.34	----------	----------
8	Light	Light	Left fighter only	----	2.22	4.31
15	Heavy	Light	Left fighter only	----	1.72	4.30

TABLE VI.- VIBRATION FREQUENCIES FOR CANTILEVER WING

(a) Light bomber without fighter; frequencies determined by resonance testing

Configuration	Frequency, cps		
	f_x	f_z	f_{α_1}
Left wing without seals and couplings	[a]5.77	[a]5.77	11.04
Right wing without seals and couplings	[a]5.73	[a]5.73	11.03
Right wing with seals; no couplings	[a]5.71	[a]5.71	11.18
Right wing with seals and couplings	4.93	5.06	11.11

[a]Vertical bending and chordwise bending modes could not be separated.

(b) Light bomber with fighters attached; frequencies determined by resonance testing unless otherwise noted; right wing with seals

Hinge skew angle, deg	Fighter weight	Fighter position	Frequency, cps		
			f_{x_1}	f_z (vertical bending, fighter roll)	f_z (vertical bending, fighter pitch)
8	Light	Aft	2.31	4.52	----
15	Light	Aft	2.33		
			[a]2.36	4.25	5.79
8	Heavy	Aft	[a]1.89	4.52	5.31
15	Heavy	Aft	[a]1.86	4.30	5.44
8	Light	Forward	[a]2.31	4.43	5.20
8	Heavy	Forward	[a]1.86	4.55	5.41

[a]Measured by plucking.

TABLE VII.- DAMPING CHARACTERISTICS AT ZERO AIRSPEED

Configuration	Mount	Vibration mode	h (a)	g (b)
Plain wing	Cantilever	Chordwise bending Vertical bending	0.117 .120	0.0073 .0077
Wing and light fighter	Cantilever	Chordwise bending Vertical bending fighter roll	0.372 .656	0.051 .046
Complete model and heavy fighters	Model mounted in tunnel at bottom of support rod	Chordwise bending	0.31	0.052

[a]Determined from $\frac{\text{Amplitude at } t}{\text{Amplitude at } t = 0} = e^{-ht}$.

[b]Determined from $g = \frac{h}{\pi f}$.

TABLE VIII.- SUMMARY OF RESULTS FOR BOMBER-FREE CONDITION

Hinge skew angle, deg	Fighter weight	Fighter position	Bomber weight	Maximum test speed, mph	Maximum q, lb/sq ft	ρ, slugs/cu ft	f_ϕ, cps (a)	f_c, cps
15	Light	Aft	Light	[b]83.2	17.42	0.002340	2.28	2.45
15	Heavy	Aft	Light	[b]87.3	19.07	.002326	1.73	1.48
8	Light	Aft	Light	[c]105.8	28.63	.002377	----	----
8	Heavy	Aft	Light	[c]104.8	28.09	.002378	----	----
15	Light	Aft	Heavy	[b]88.3	19.08	.002275	2.30	2.32
15	Heavy	Aft	Heavy	[b]89.1	19.43	.002275	1.86	1.63
8	Light	Aft	Heavy	[c]112.1	30.73	.002272	----	----
8	Heavy	Aft	Heavy	[c]112.1	30.92	.002288	----	----
15	Light	Forward	Light	[b]80.1	16.25	.002353	2.26	----
15	Heavy	Forward	Light	[b]81.2	16.43	.002319	1.60	1.43
8	Light	Forward	Light	[b]111.3	30.56	.002295	2.26	----
8	Heavy	Forward	Light	[c]94.9	22.39	.002312	----	----
15	Light	Forward	Heavy	[b]82.2	17.00	.002341	2.32	2.29
15	Heavy	Forward	Heavy	[b]82.7	17.58	.002392	1.61	1.35
8	Light	Forward	Heavy	[b]108.8	30.11	.002364	2.15	2.00
8	Heavy	Forward	Heavy	[b]103.3	27.01	.002351	1.87	1.71
8	Heavy	Forward	Heavy	[b]101.0	26.18	.002384	1.78	1.60

[a]Fighter roll frequency at a speed within 2 miles per hour of critical speed.

[b]Flutter speed.

[c]No instability.

TABLE IX.- SUMMARY OF RESULTS FOR BOMBER-FIXED CONDITION

[Light bomber; fighters in aft position; $\alpha_f = 0^\circ$]

Hinge skew angle, deg	Fighter weight	β, deg	Other conditions	Maximum speed, mph	Maximum q, lb/sq ft	ρ, slugs/cu ft	f_ϕ, cps (a)	f_c, cps
15	Light	0	----------	[b]86.2	18.56	0.002321	----	2.26
15	Light	5	----------	[b]84.8	17.70	.002291	2.56	2.63
15	Light	0	Left fighter only	[b]109.3	29.18	.002270	2.65	2.80
15	Light	5	Left fighter only	[b]94.0	22.15	.002329	----	2.86
15	Heavy	0	Left fighter only	[c]103.2	26.19	.002287	----	----
15	Heavy	5	Left fighter only	[c]103.0	26.18	.002294	----	----
8	Light	0	Left fighter only	[c]109.4	30.37	.002357	----	----

[a]Fighter roll frequency at a speed within 2 miles per hour of critical speed.

[b]Flutter speed.

[c]No instability.

TABLE X.- FREQUENCIES OF FIGHTER ROLL OSCILLATIONS DUE TO GUSTS

Configuration		Frequency, cps, for -			
Skew angle, deg	Fighter weight	V = 60 mph	V = 65 mph	V = 70 mph	V = 75 mph
15	Light	1.49	1.64	1.72	1.75
15	Heavy	----	1.02	1.27	1.35
8	Light	.88	1.00	1.04	1.15
8	Heavy	----	.62	.70	.89

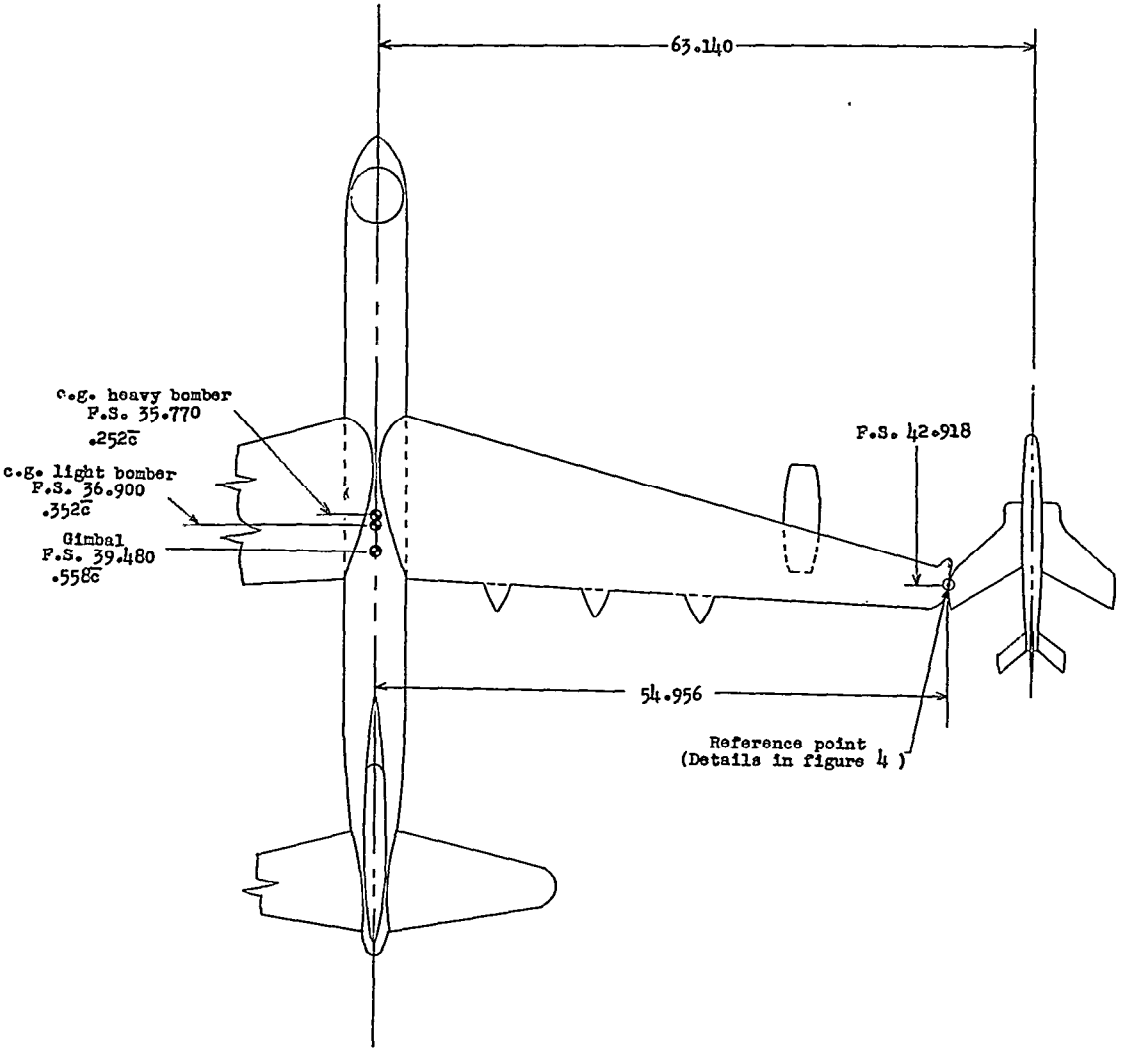

Figure 1.- General arrangement of model. Fuselage station (F.S.) 0 is 0.80 inch ahead of nose. All dimensions are in inches.

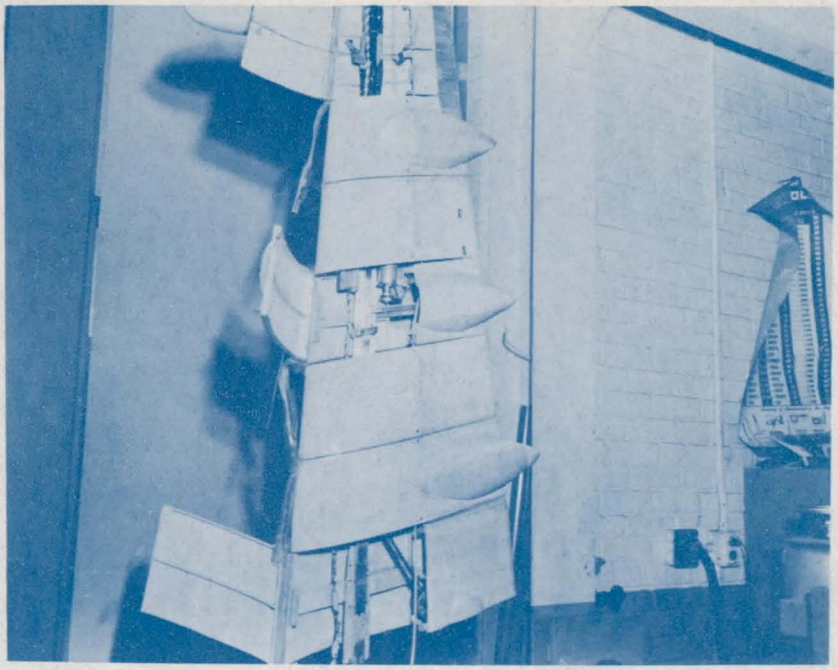

L-92439

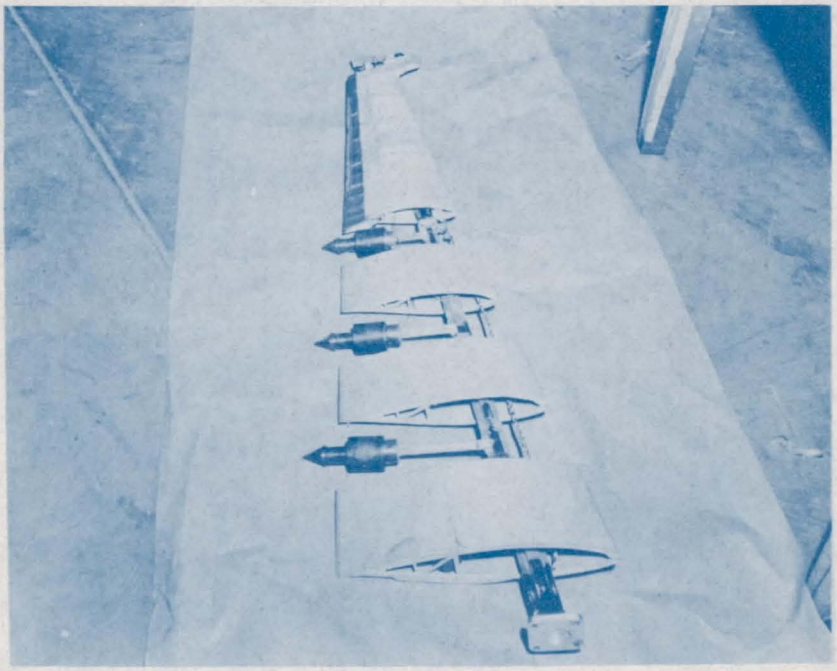

L-92440

Figure 2.- Details of model construction.

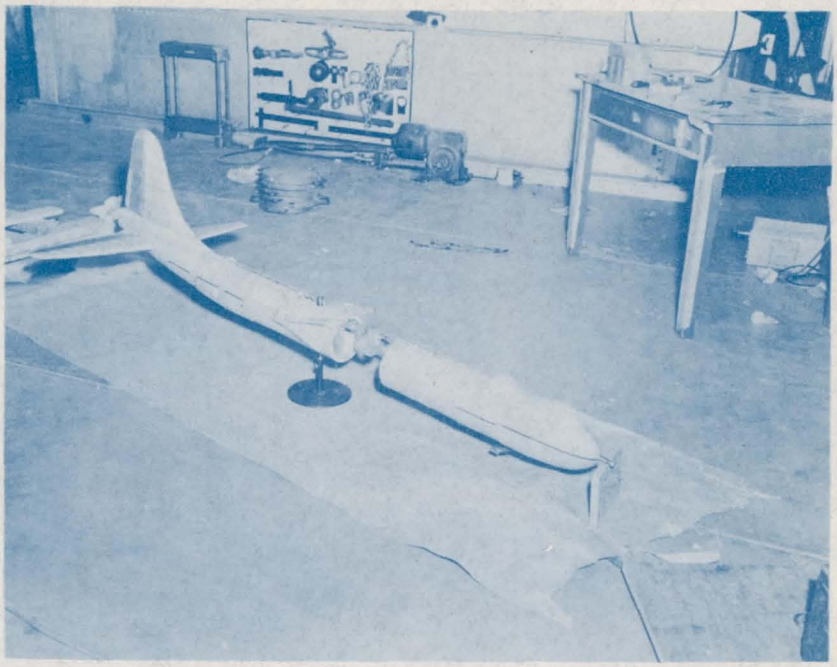

L-92441

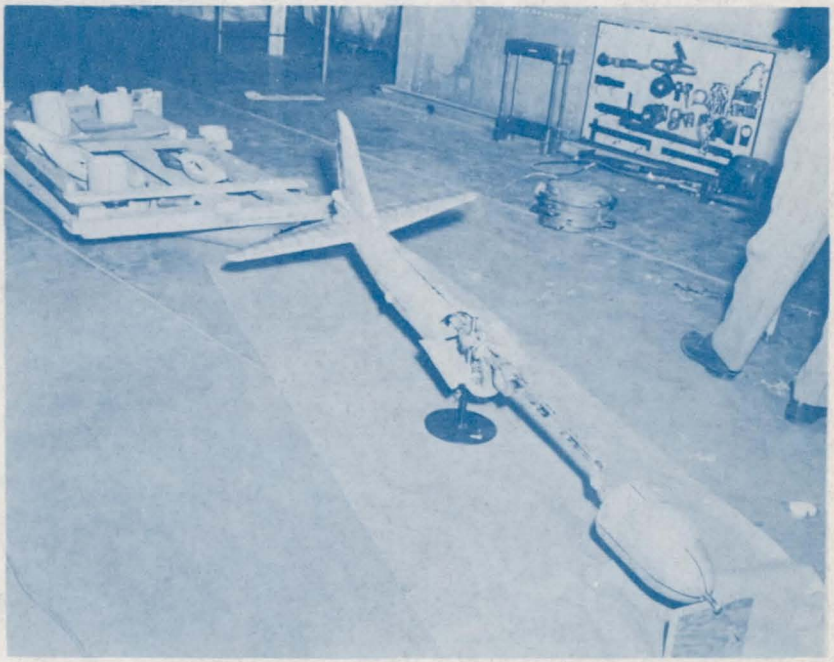

Figure 2.- Concluded. L-92442

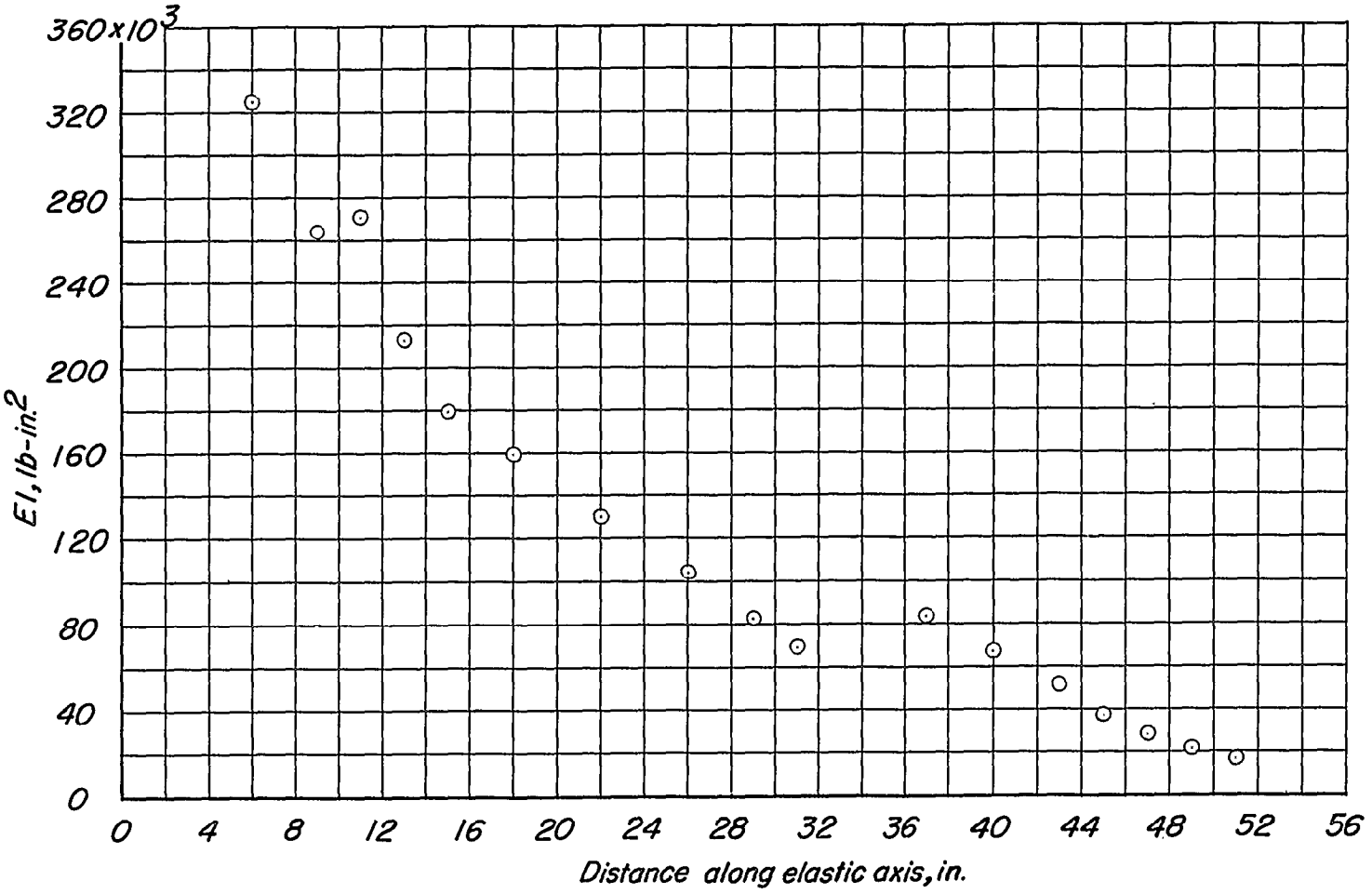

(a) Chordwise-bending rigidity.

Figure 3.- Rigidity characteristics of bomber wing. Distance along elastic axis measured from fuselage center line.

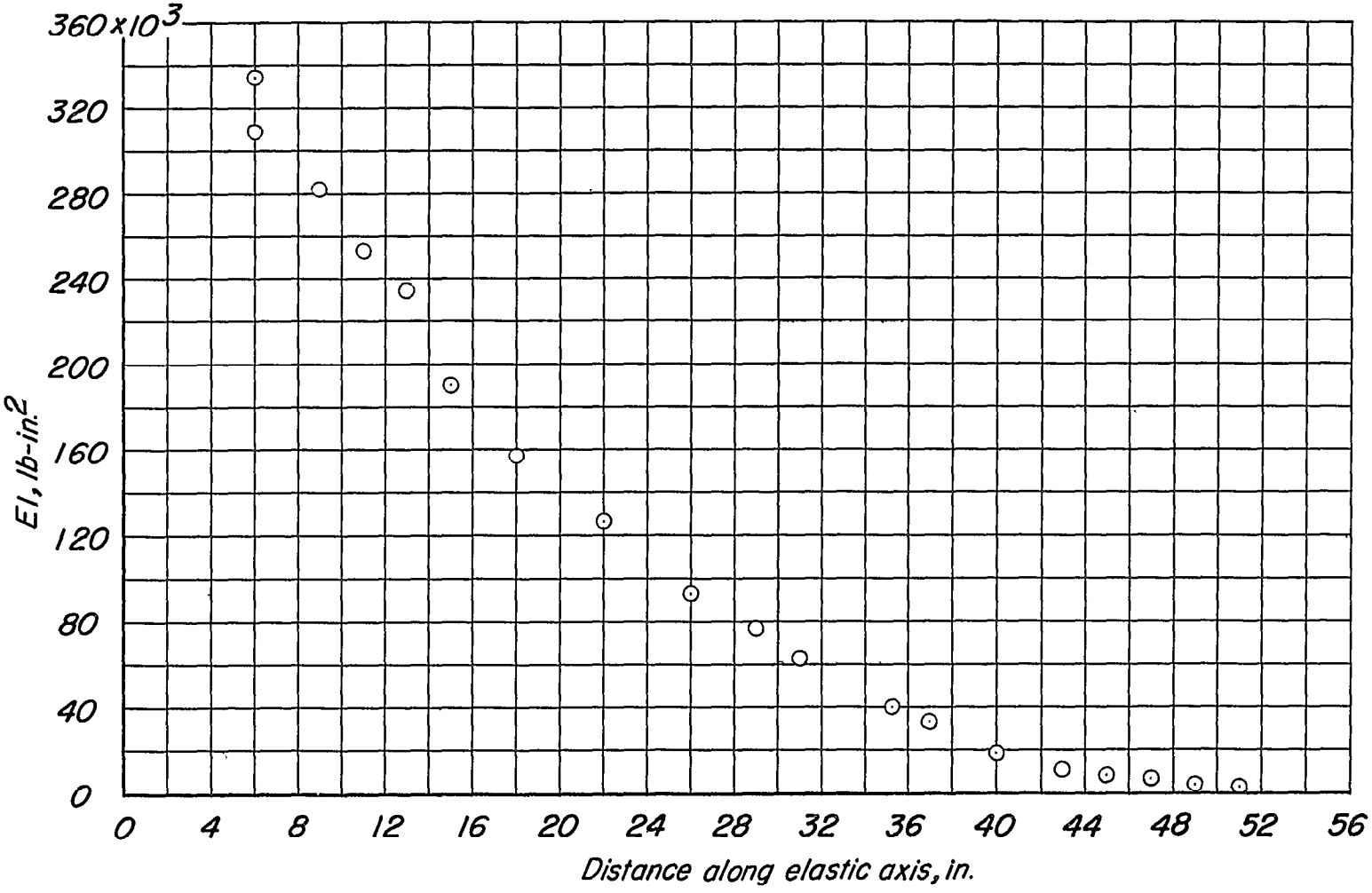

(b) Vertical-bending rigidity.

Figure 3.- Continued.

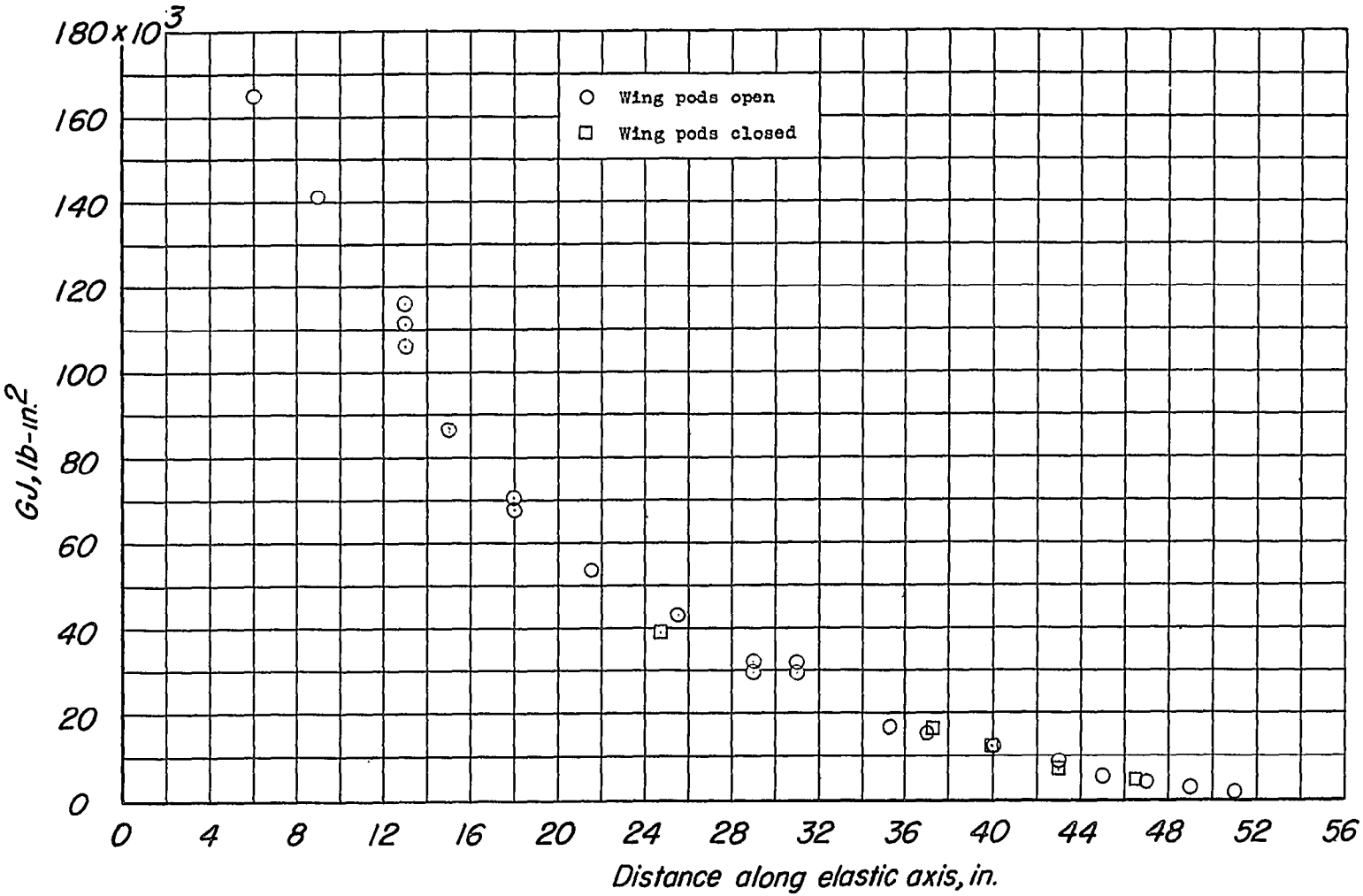

(c) Torsional rigidity.

Figure 3.- Concluded.

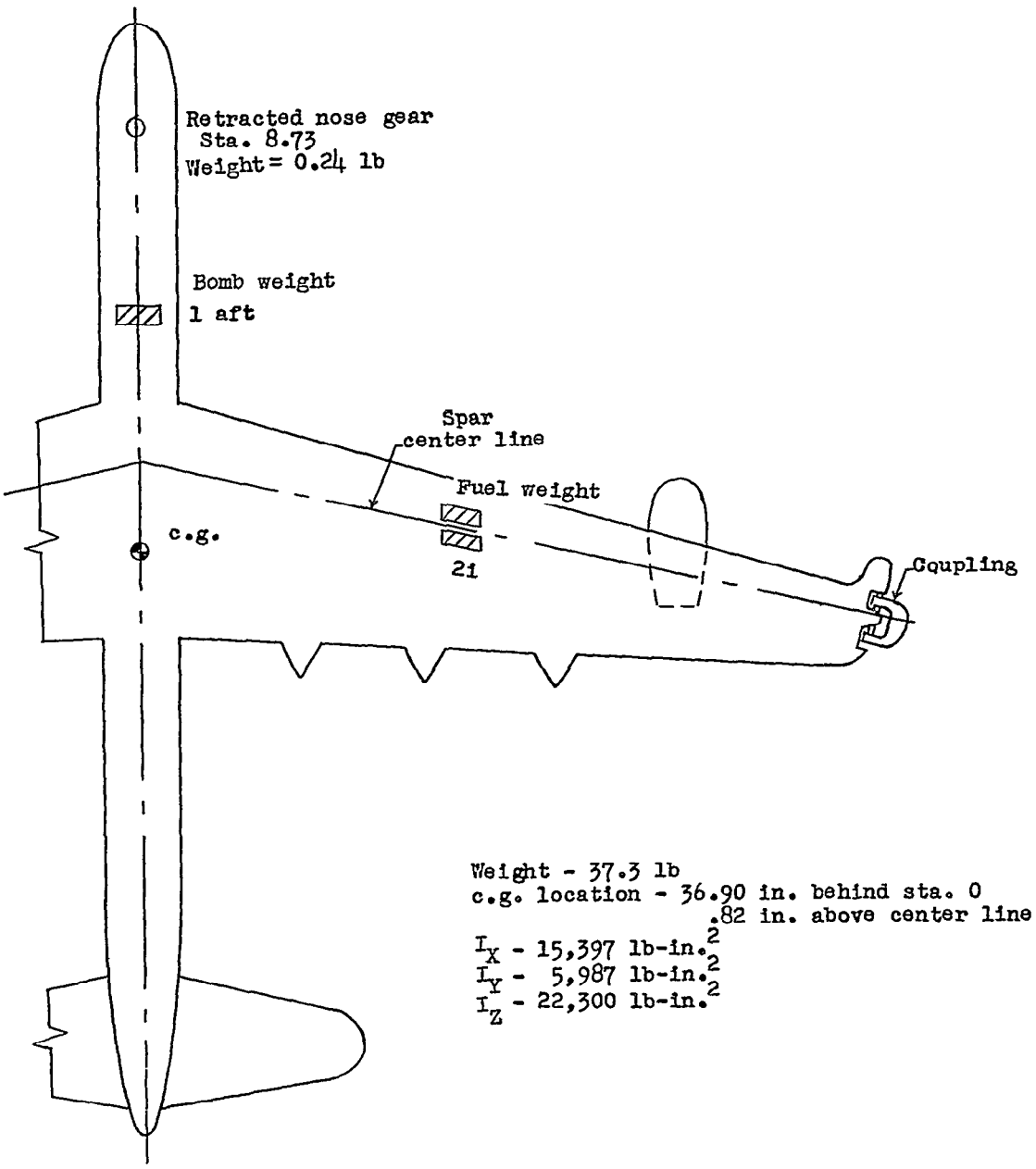

(a) Light bomber.

Figure 4.- Bomber loading conditions.

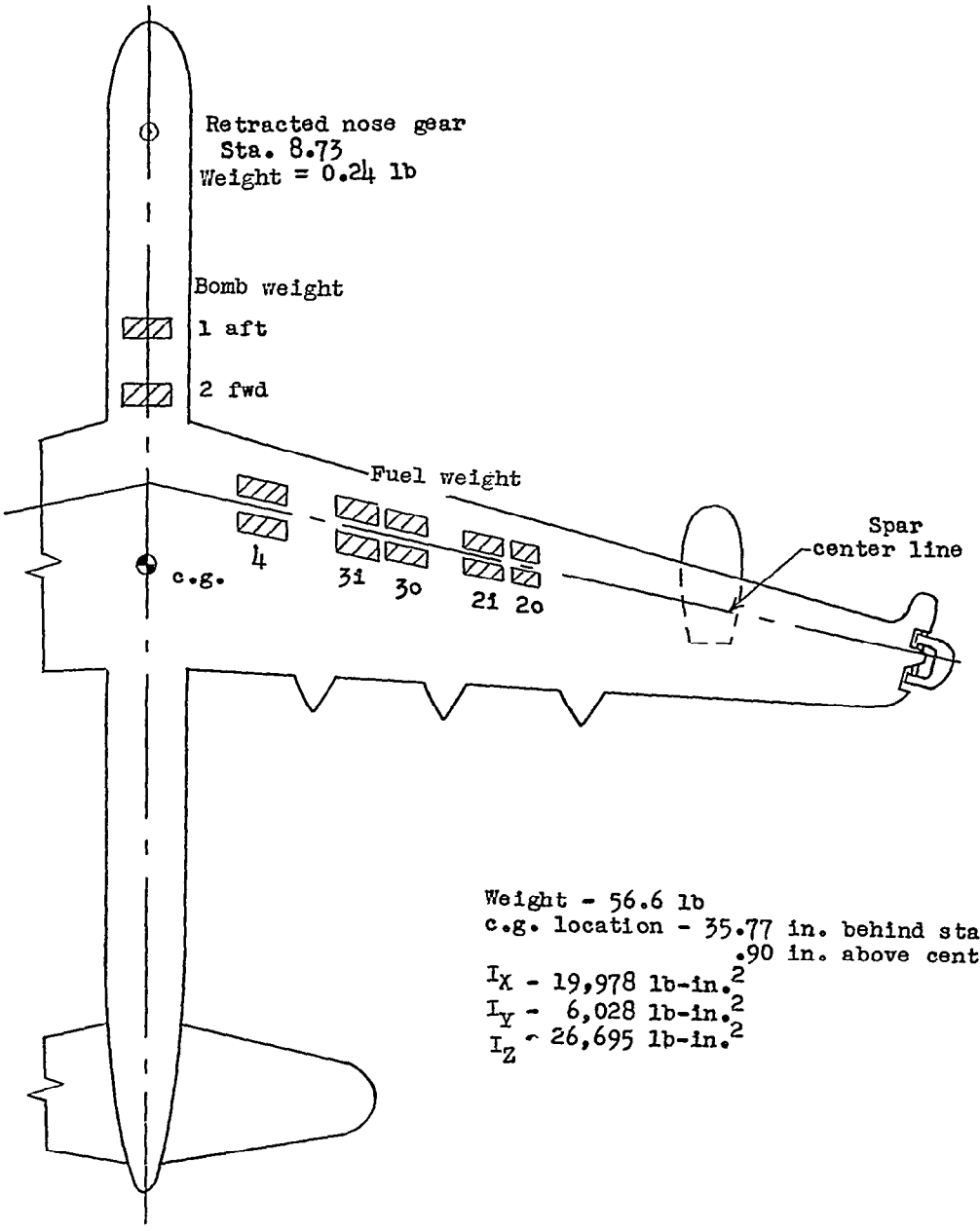

(b) Heavy bomber.

Figure 4.- Concluded.

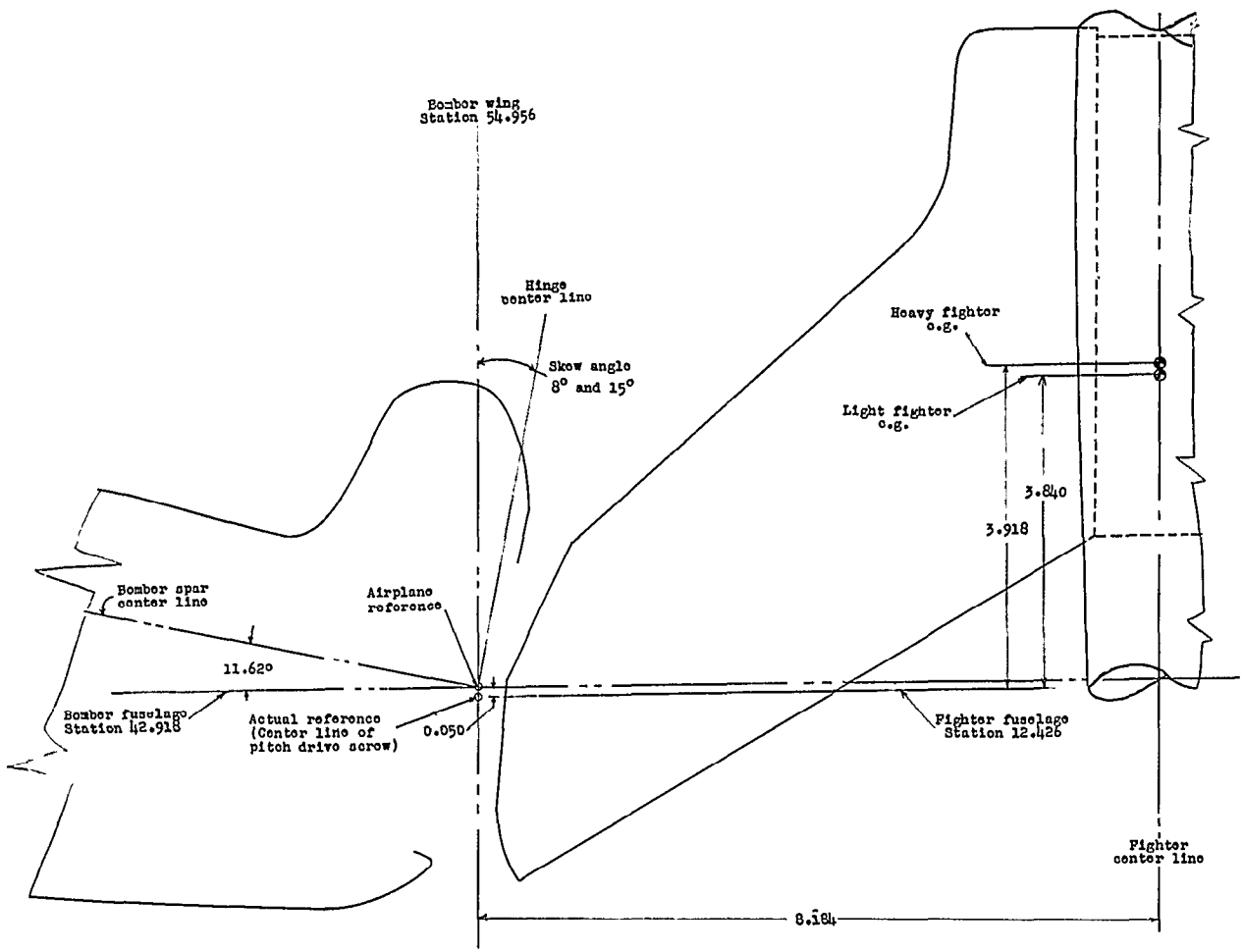

(a) Forward fighter position.

Figure 5.- Geometry of fighter attachment. All linear dimensions are in inches.

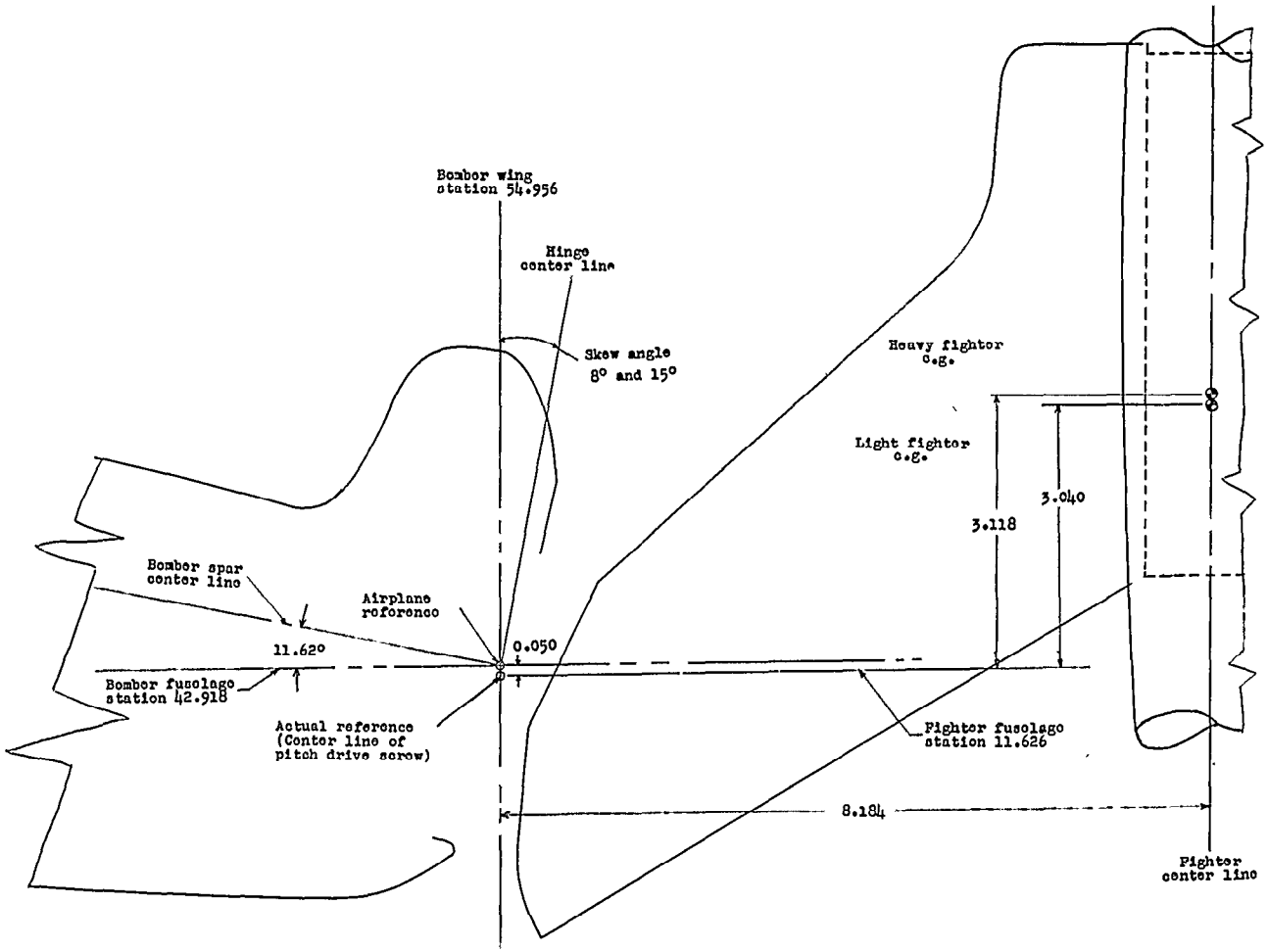

(b) Aft fighter position.

Figure 5.- Concluded.

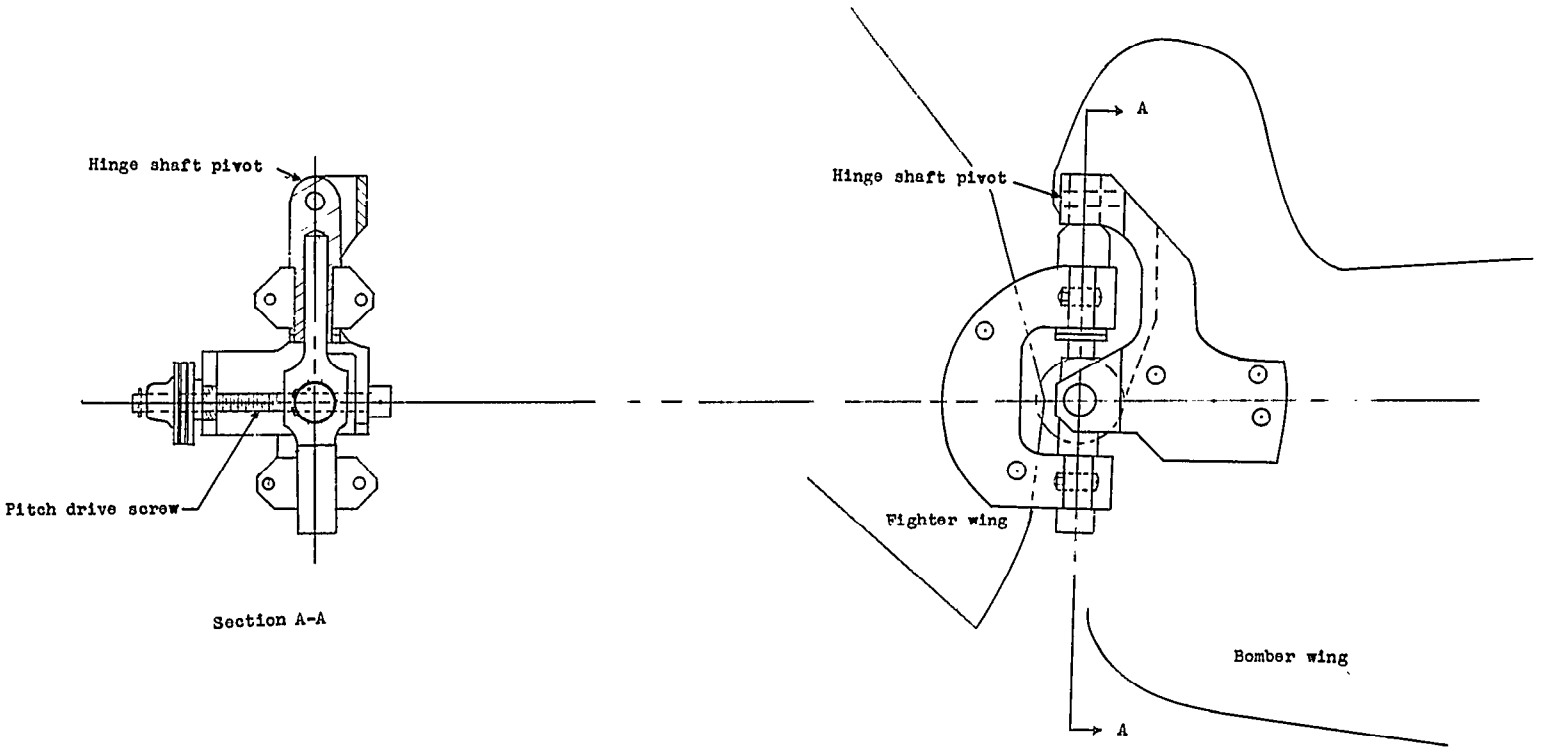

Figure 6.- Coupling details.

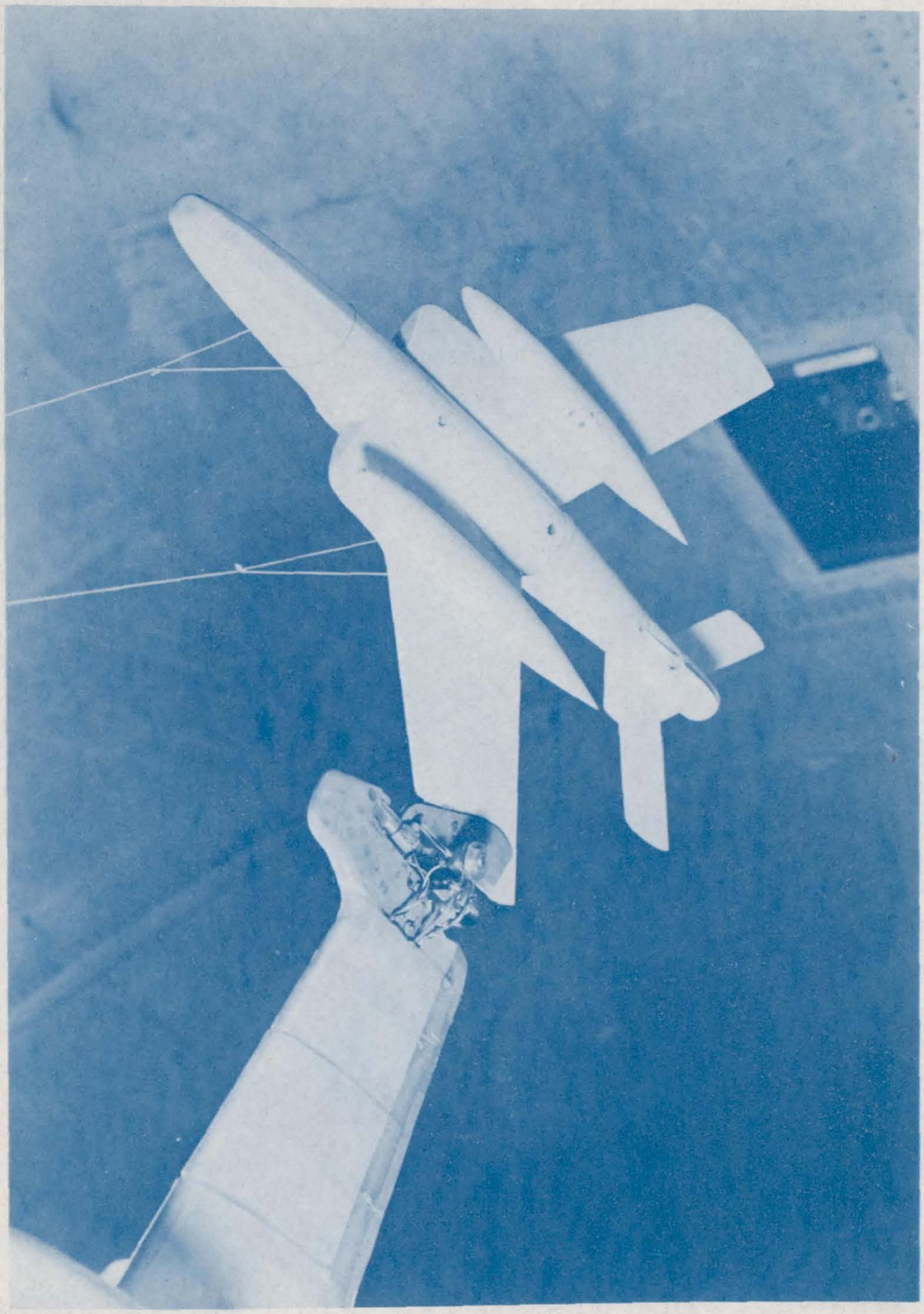

L-88500

Figure 7.- Photograph of bomber-fighter coupling.

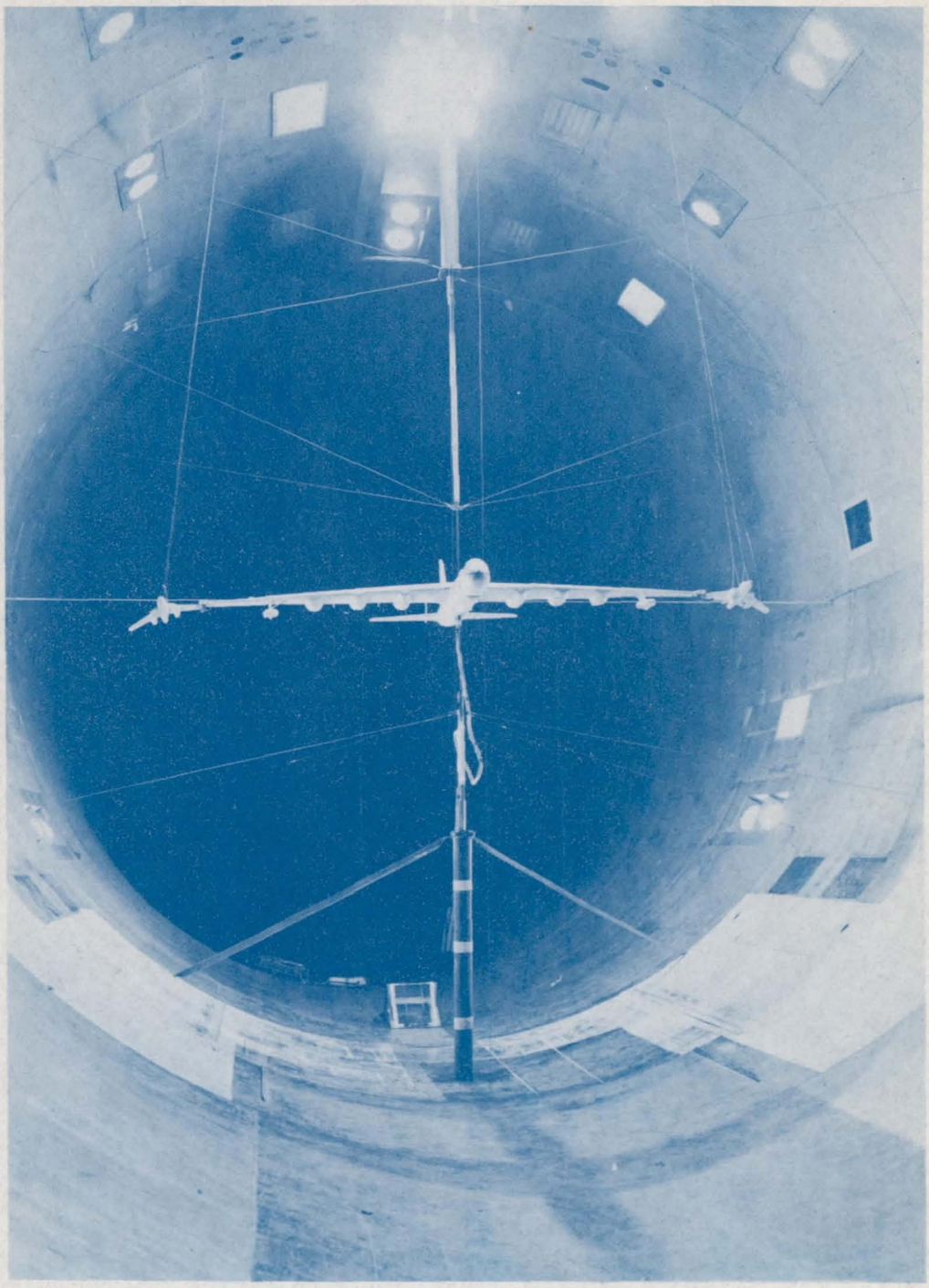

L-88499

Figure 8.- Model installation for bomber-free condition. Bomber is free in roll, yaw, pitch, and vertical translation.

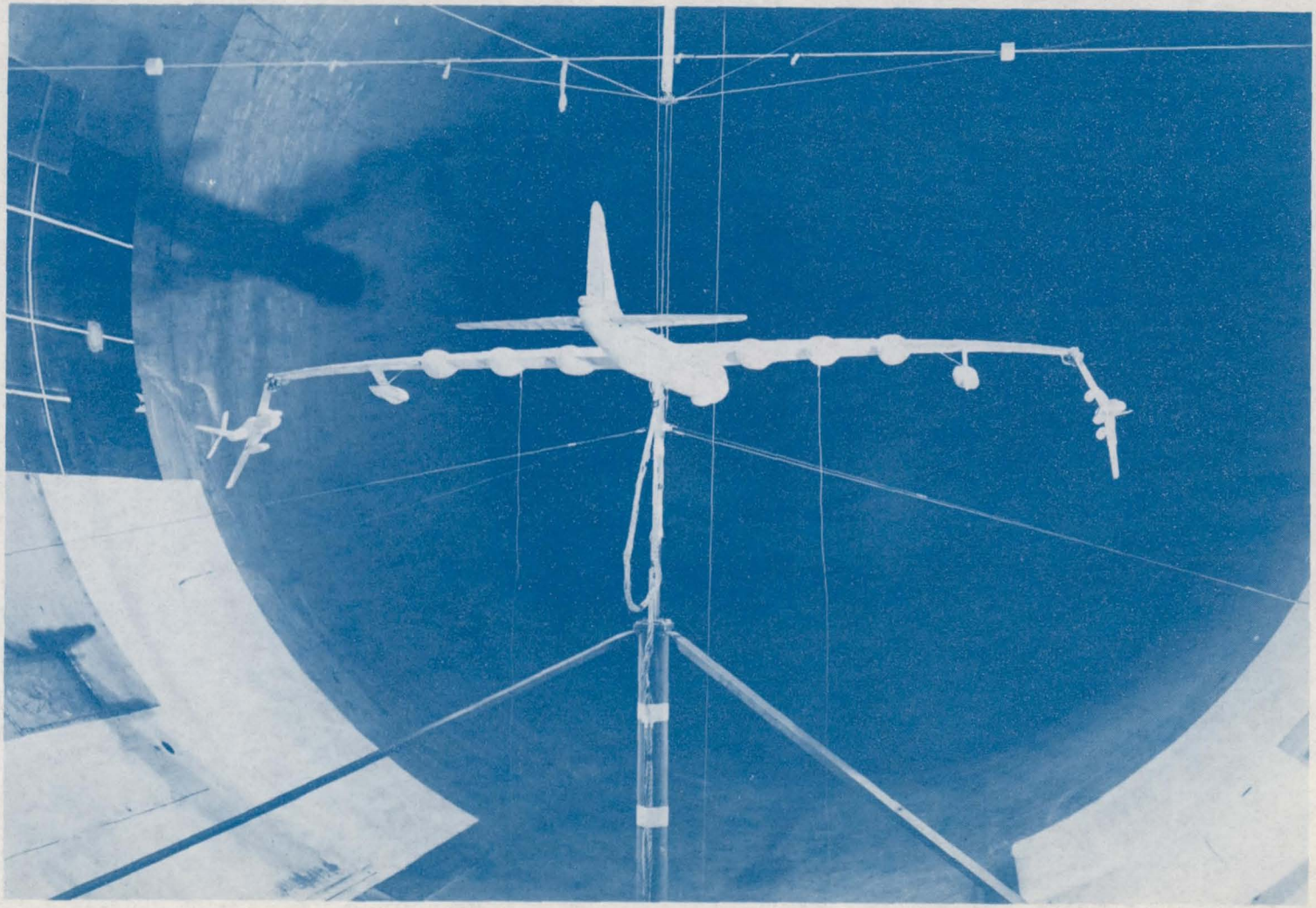

Figure 8.- Continued. L-38498

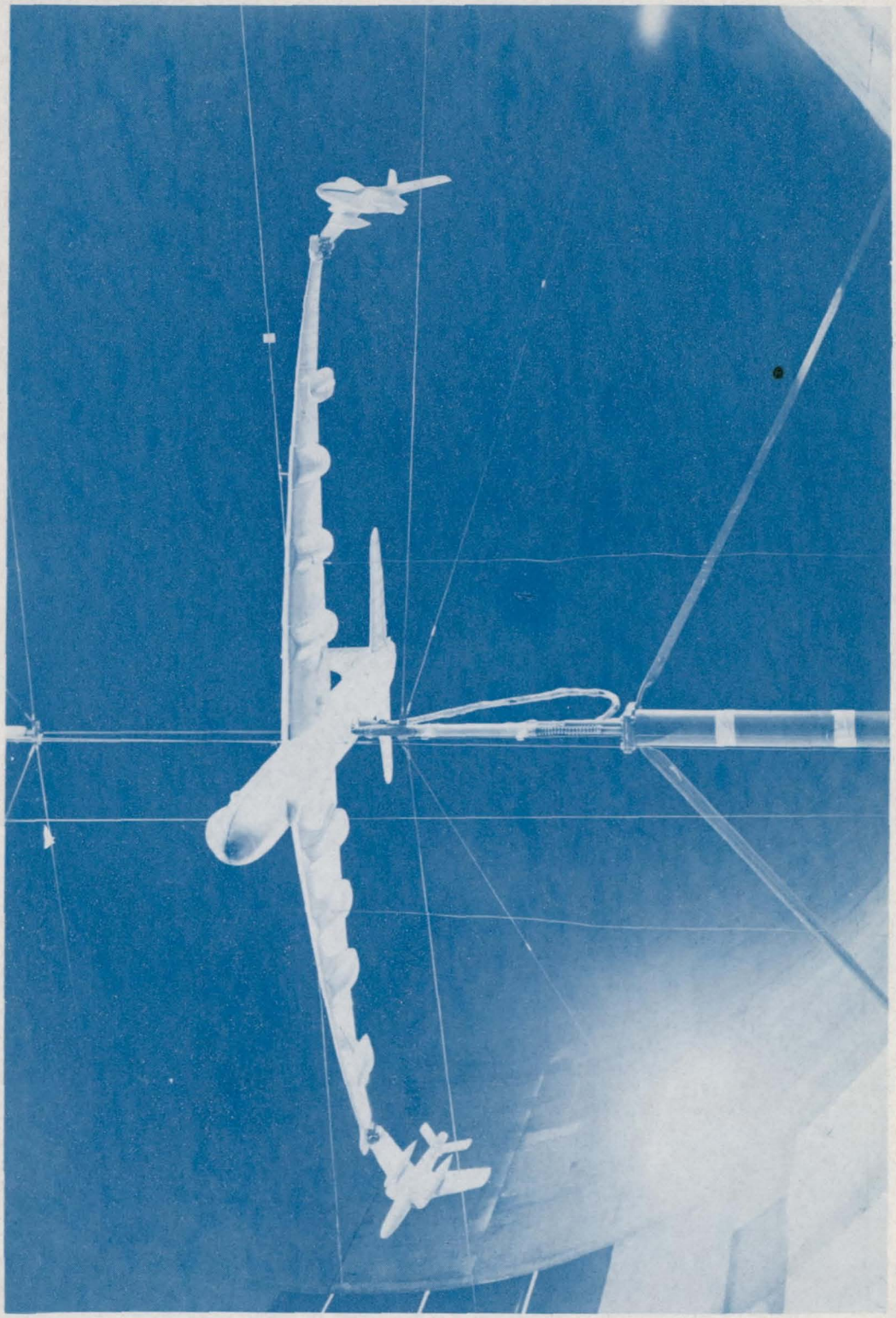

L-38494

Figure 8.- Concluded.

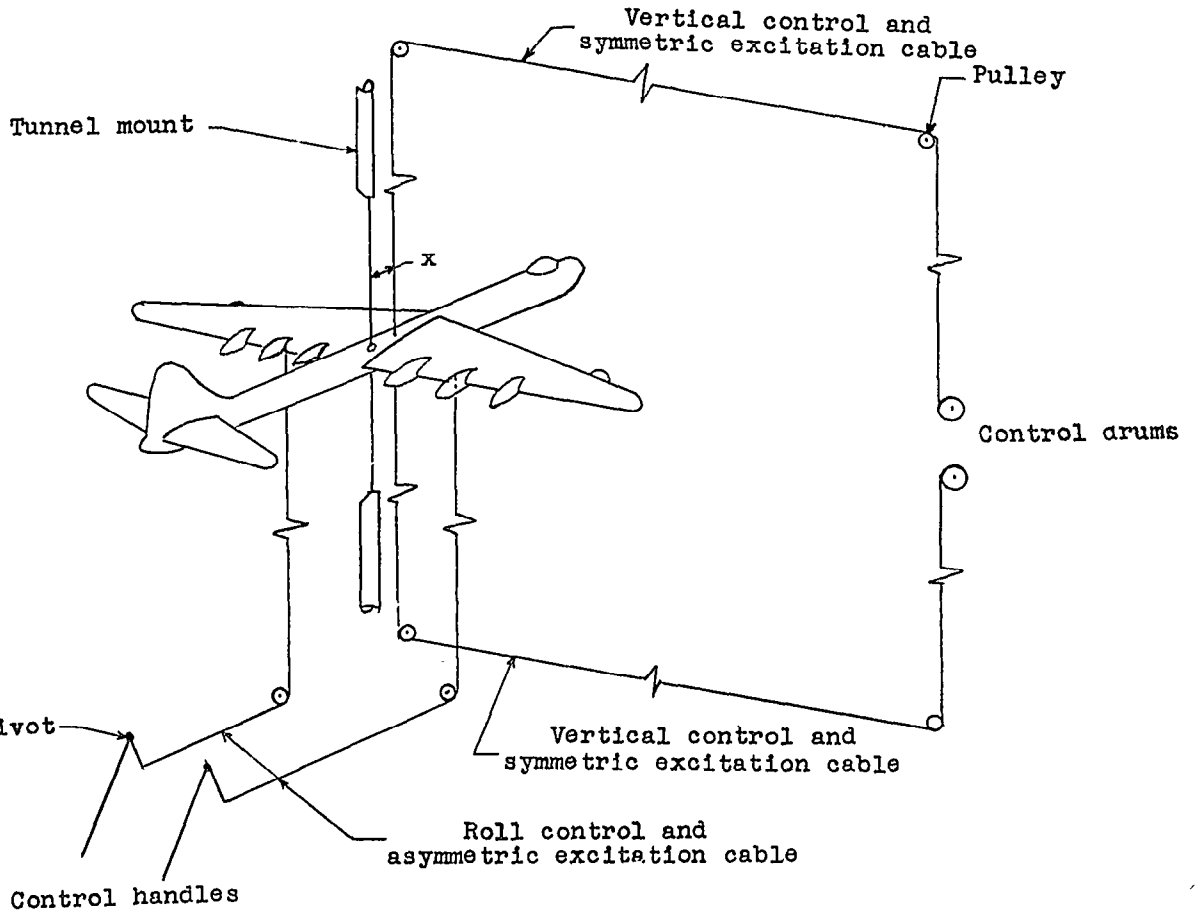

x

Light bomber -- 2.58 in.
Heavy bomber -- 3.72 in.

Figure 9.- Schematic diagram of the control and excitation cables.

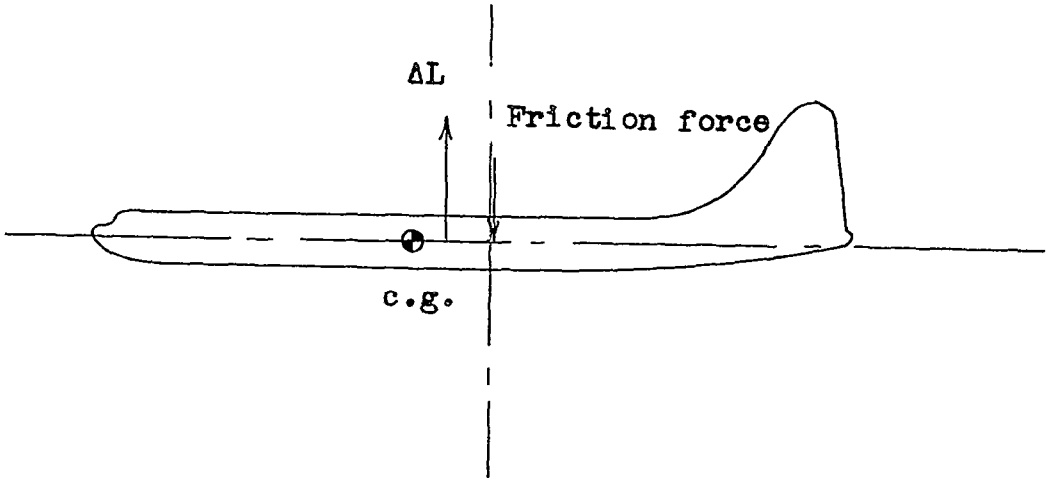

(a) Moment due to friction.

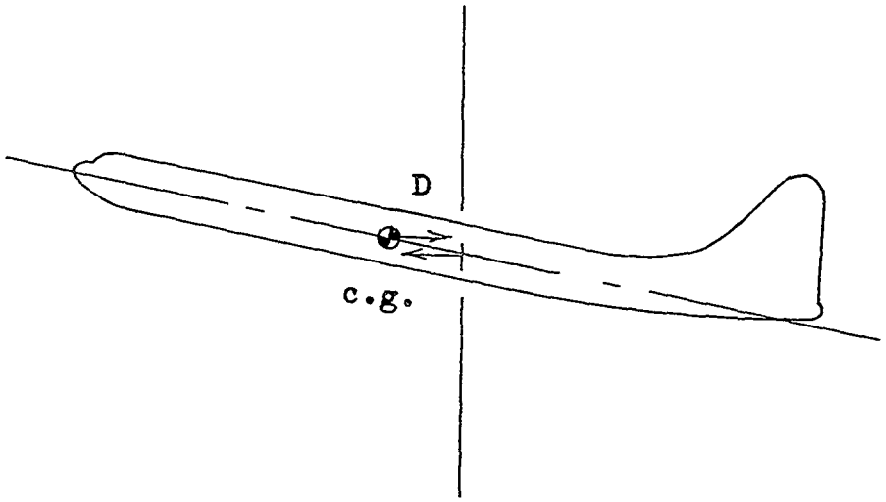

(b) Moment due to drag.

Figure 10.- Additional pitching moments resulting from center of gravity being located forward of gimbal.

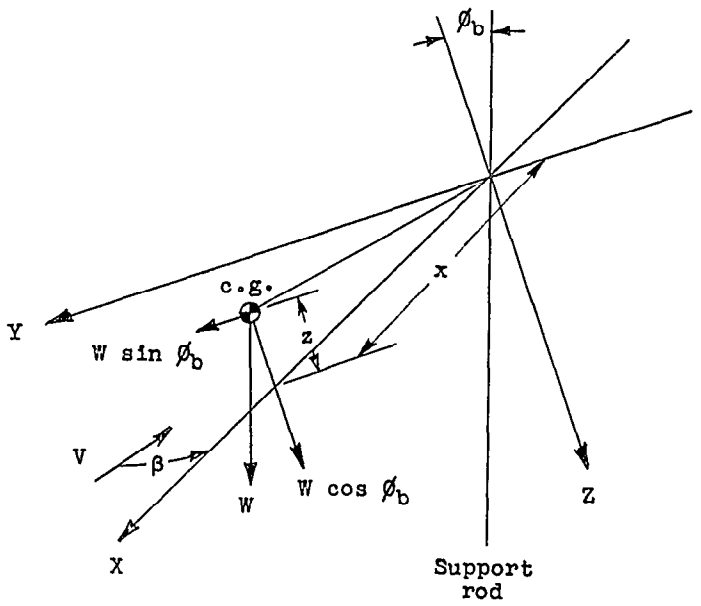

Roll: $-W \sin \phi_b z + L_\beta \beta = 0$

Yaw: $W \sin \phi_b x + N_\beta \beta = 0$

For static equilibrium,

$$\frac{z}{x} = -\frac{L_\beta}{N_\beta}$$

For stability,

$$\frac{z}{x} > -\frac{L_\beta}{N_\beta}$$

(a) Force diagram.

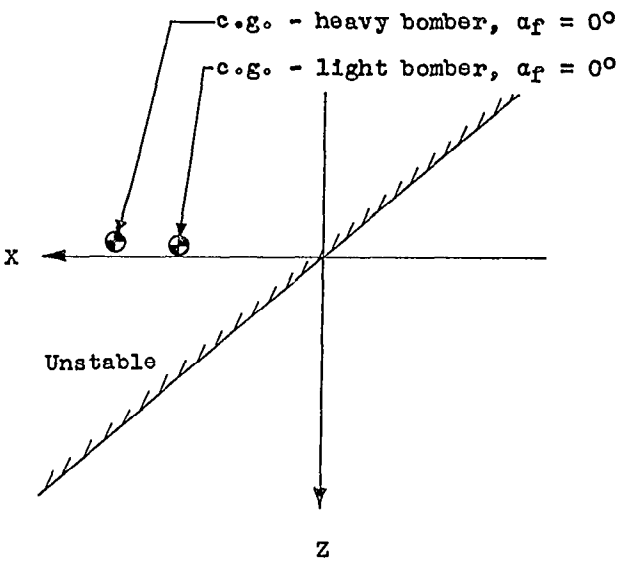

(b) Stability boundary.

Figure 11.- Analysis of lateral moments resulting from center of gravity being located away from gimbal.

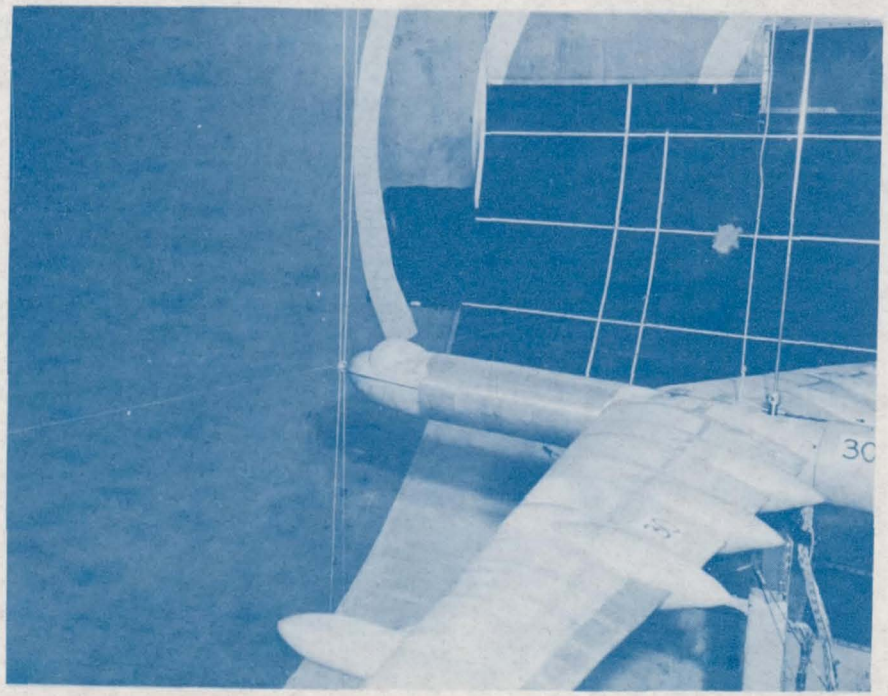

L-89575

Figure 12.- Model installation for bomber-fixed condition. Bomber is free in roll only.

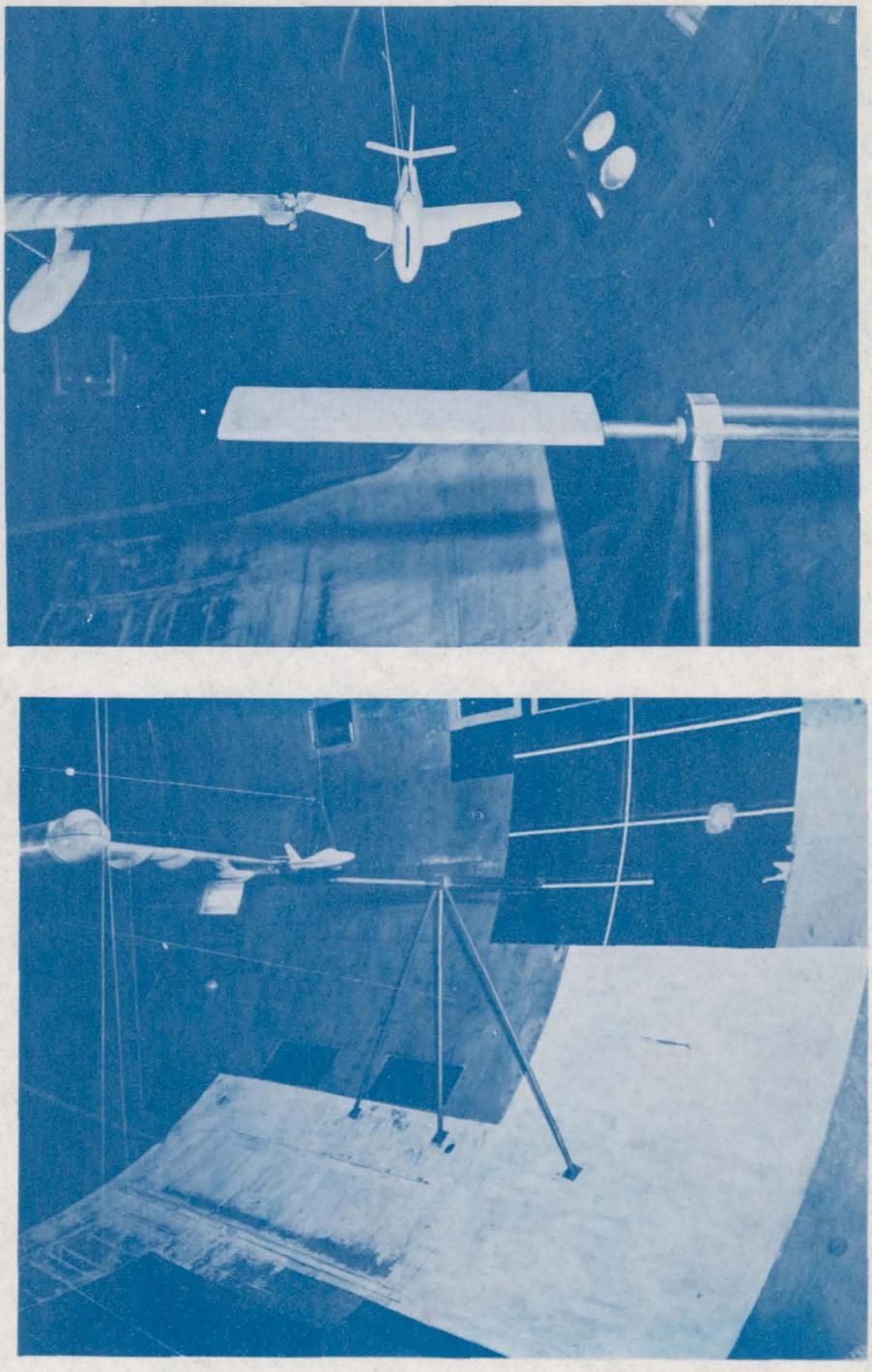

L-89576

Figure 13.- Setup showing airfoil for producing gusts.

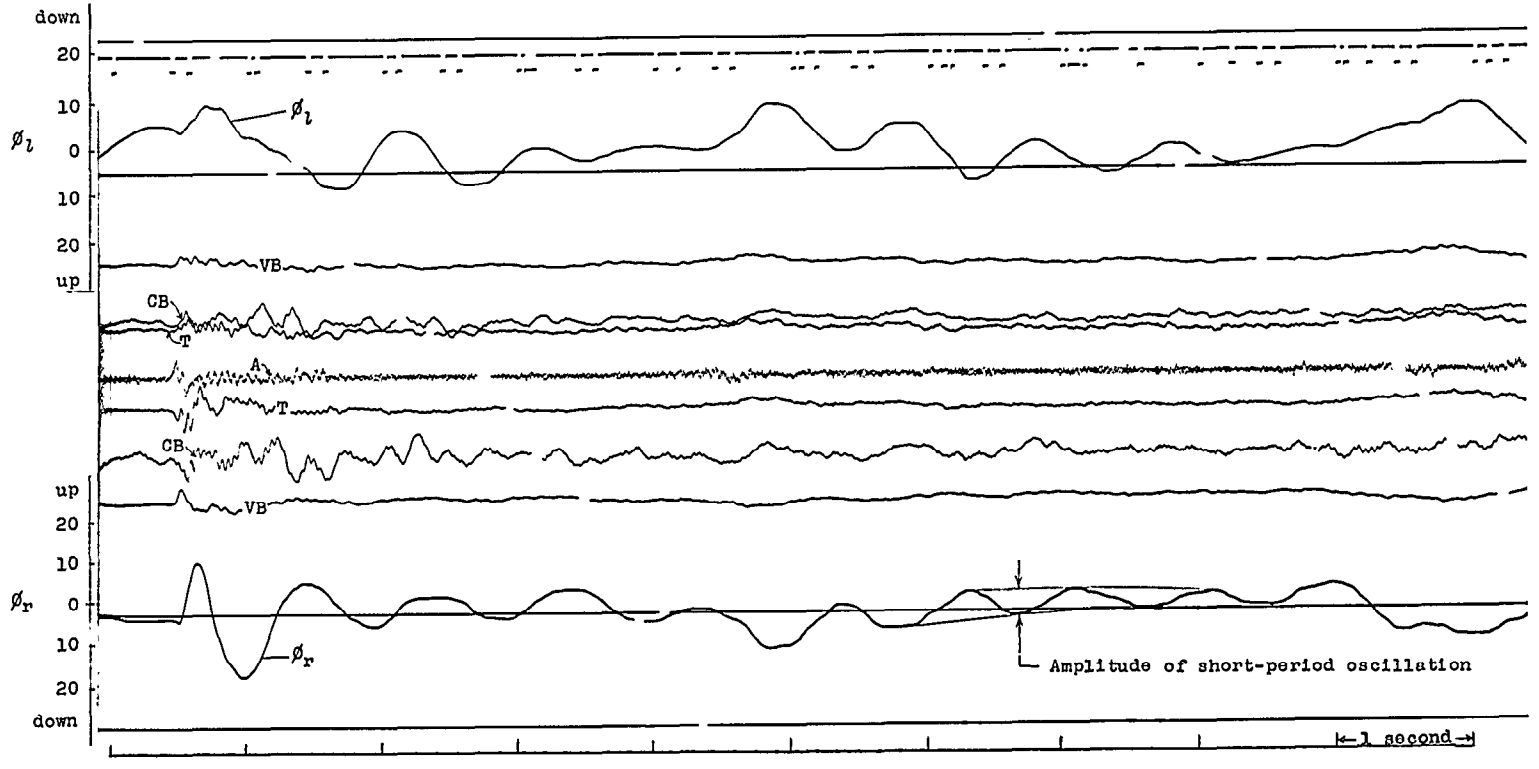

Figure 14.- Sample oscillogram.

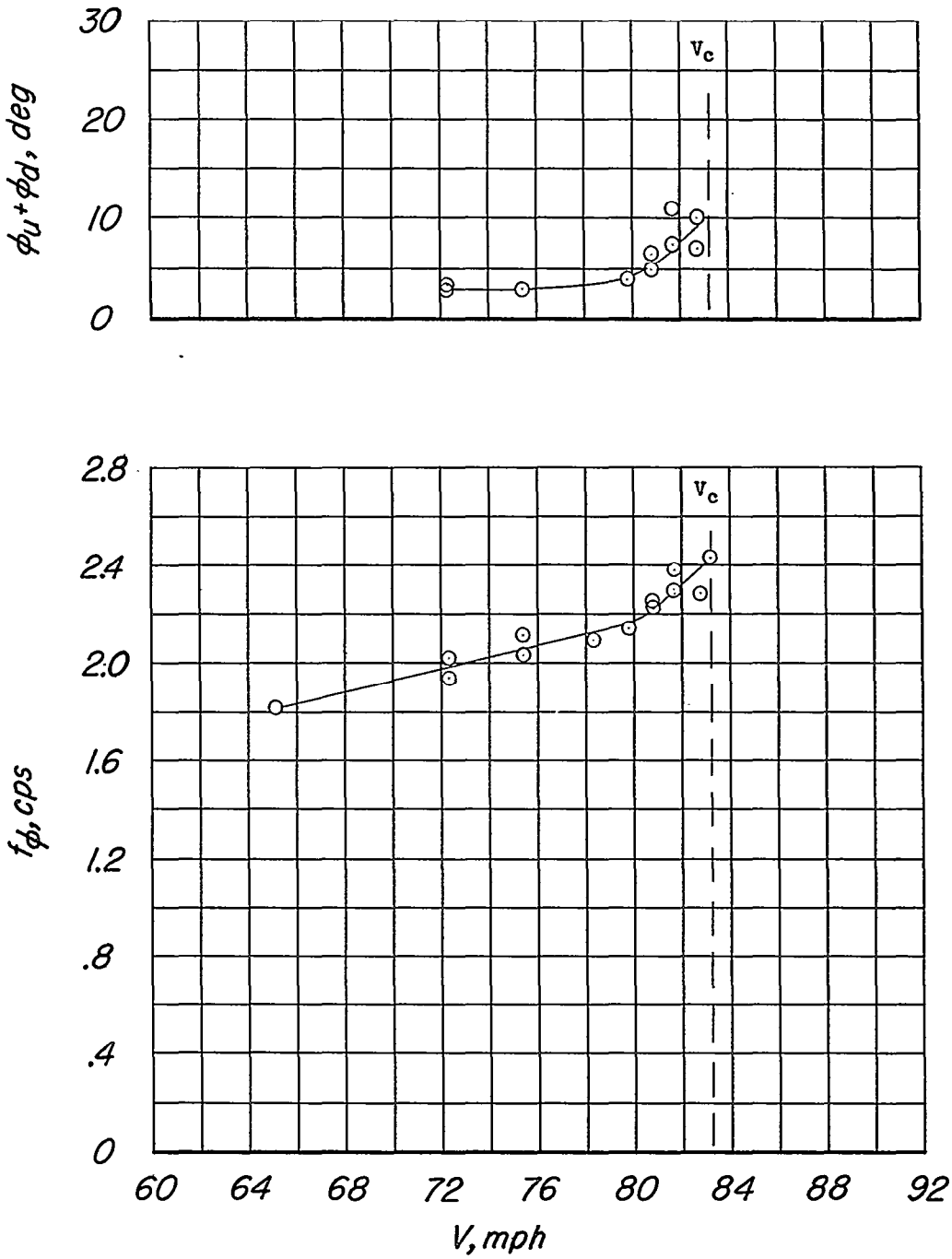

(a) $\delta = 15^{\circ}$; light fighters.

Figure 15.- Variation of amplitude and frequency of fighter roll oscillation with airspeed. Fighters aft; light bomber.

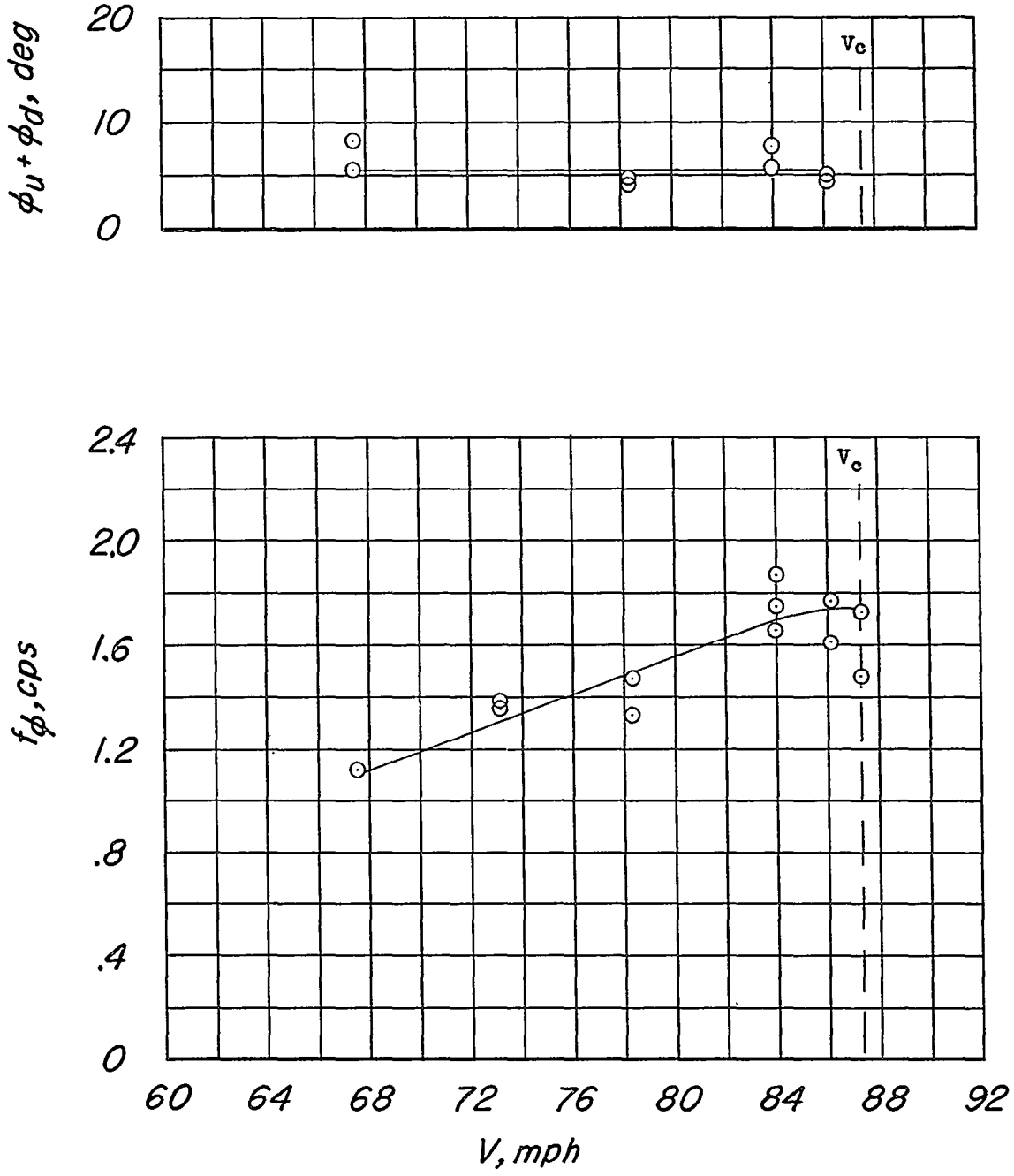

(b) $\delta = 15^{\circ}$; heavy fighters.

Figure 15.- Continued.

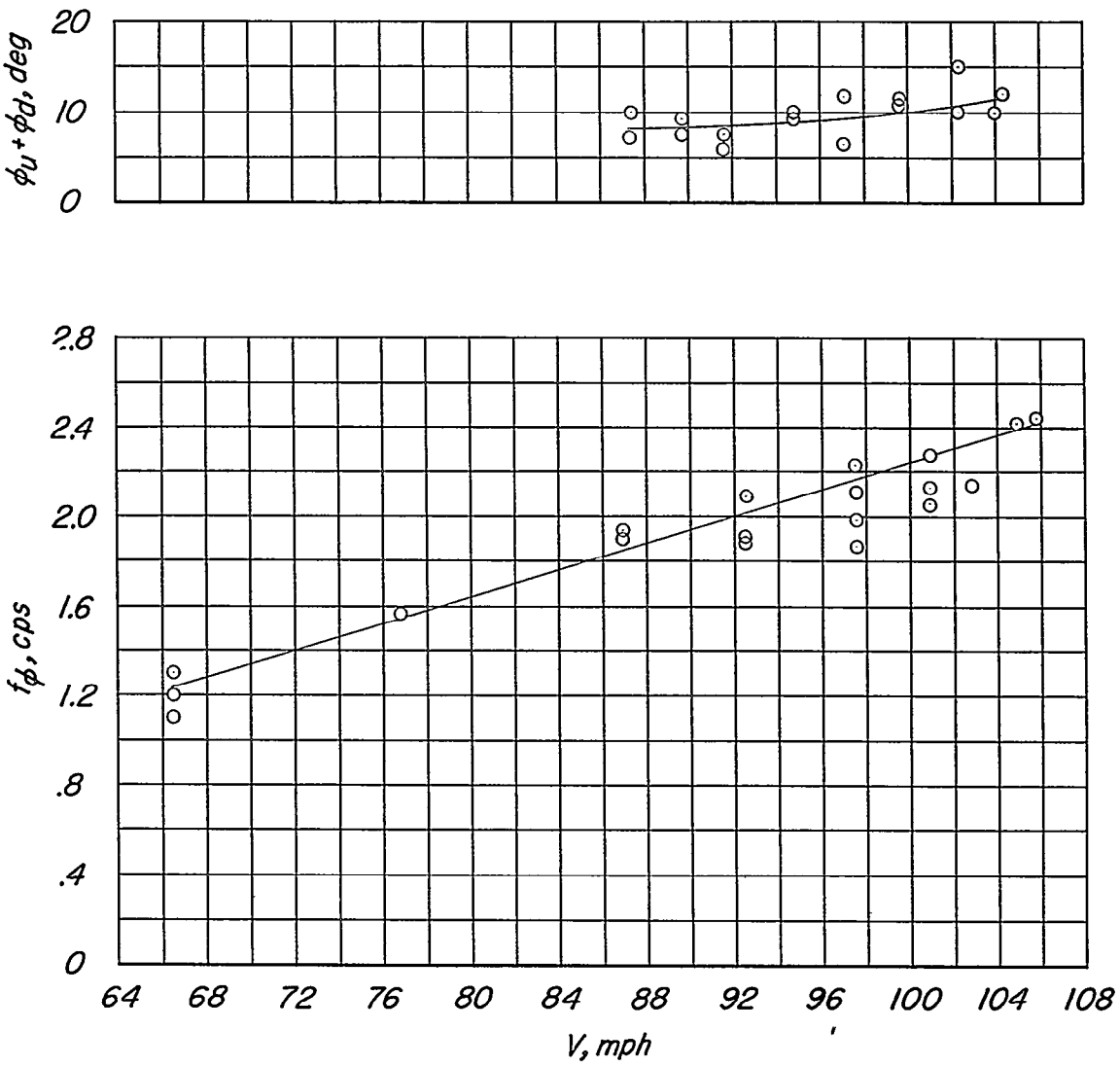

(c) $\delta = 8^{\circ}$; light fighters.

Figure 15.- Continued.

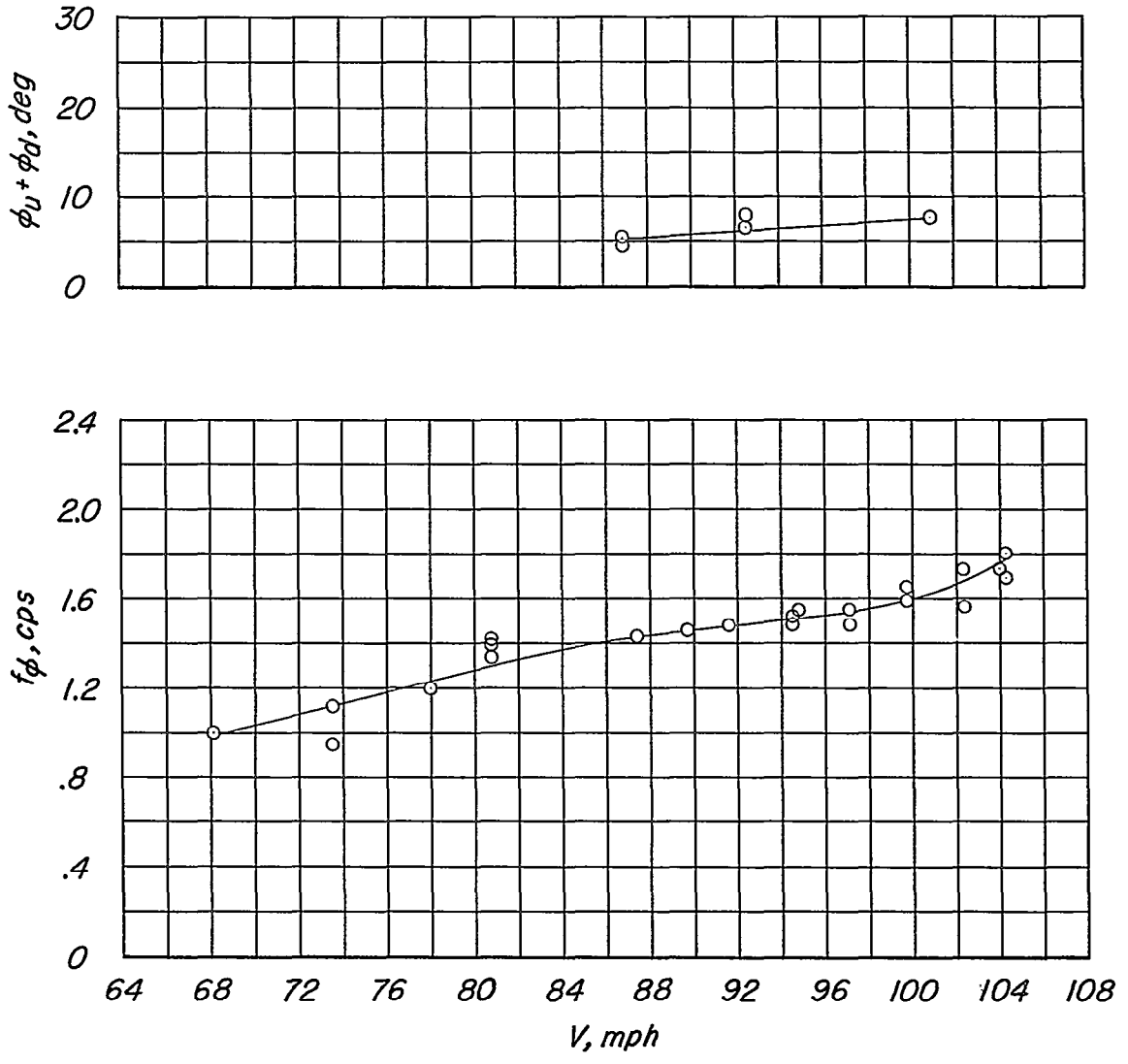

(d) $\delta = 8^{\circ}$; heavy fighters.

Figure 15.- Concluded.

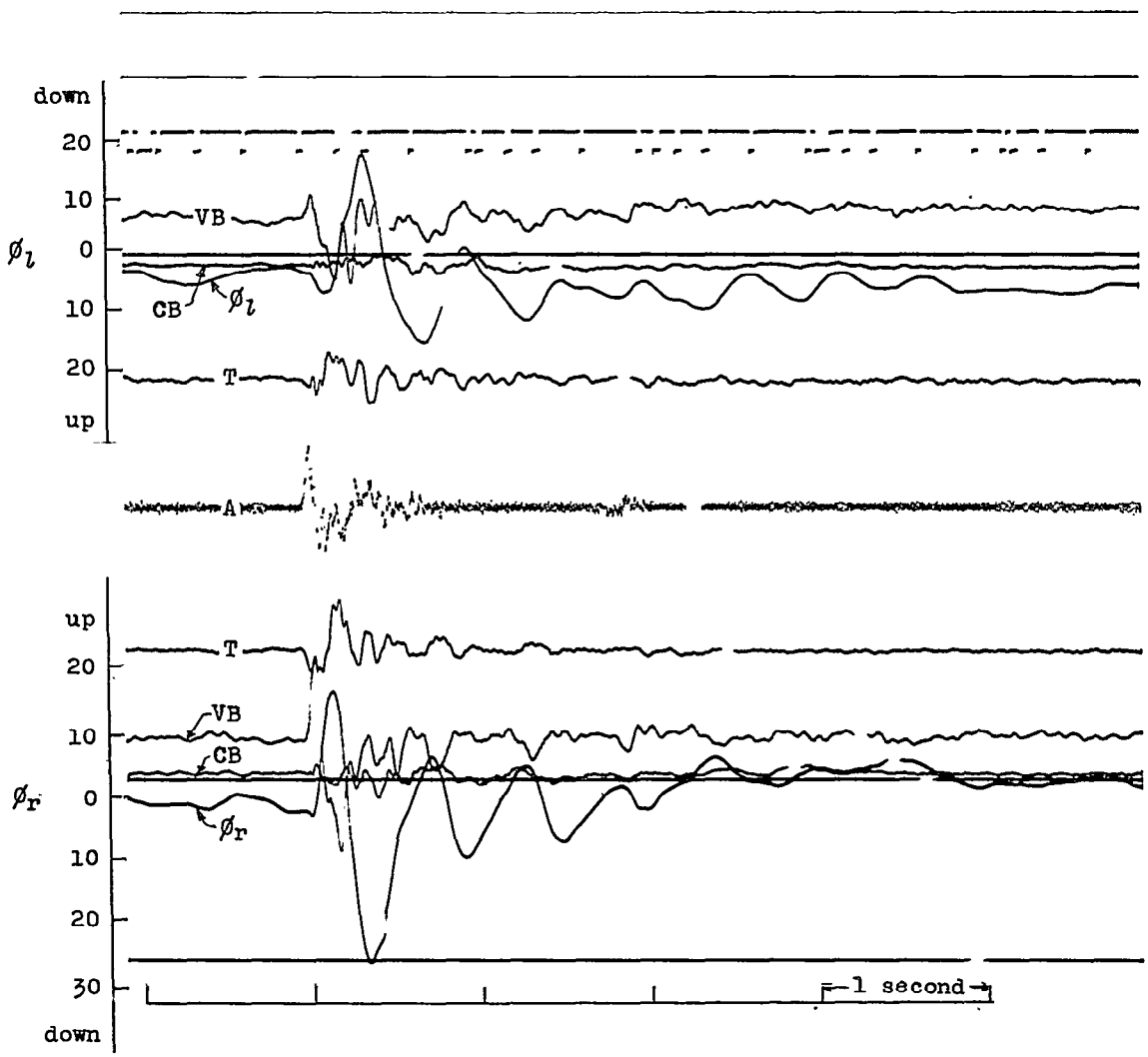

(a) V = 65.1 mph; symmetric excitation.

Figure 16.- Oscillograms for light fighters with $\delta = 15^{\circ}$. Fighters aft; light bomber.

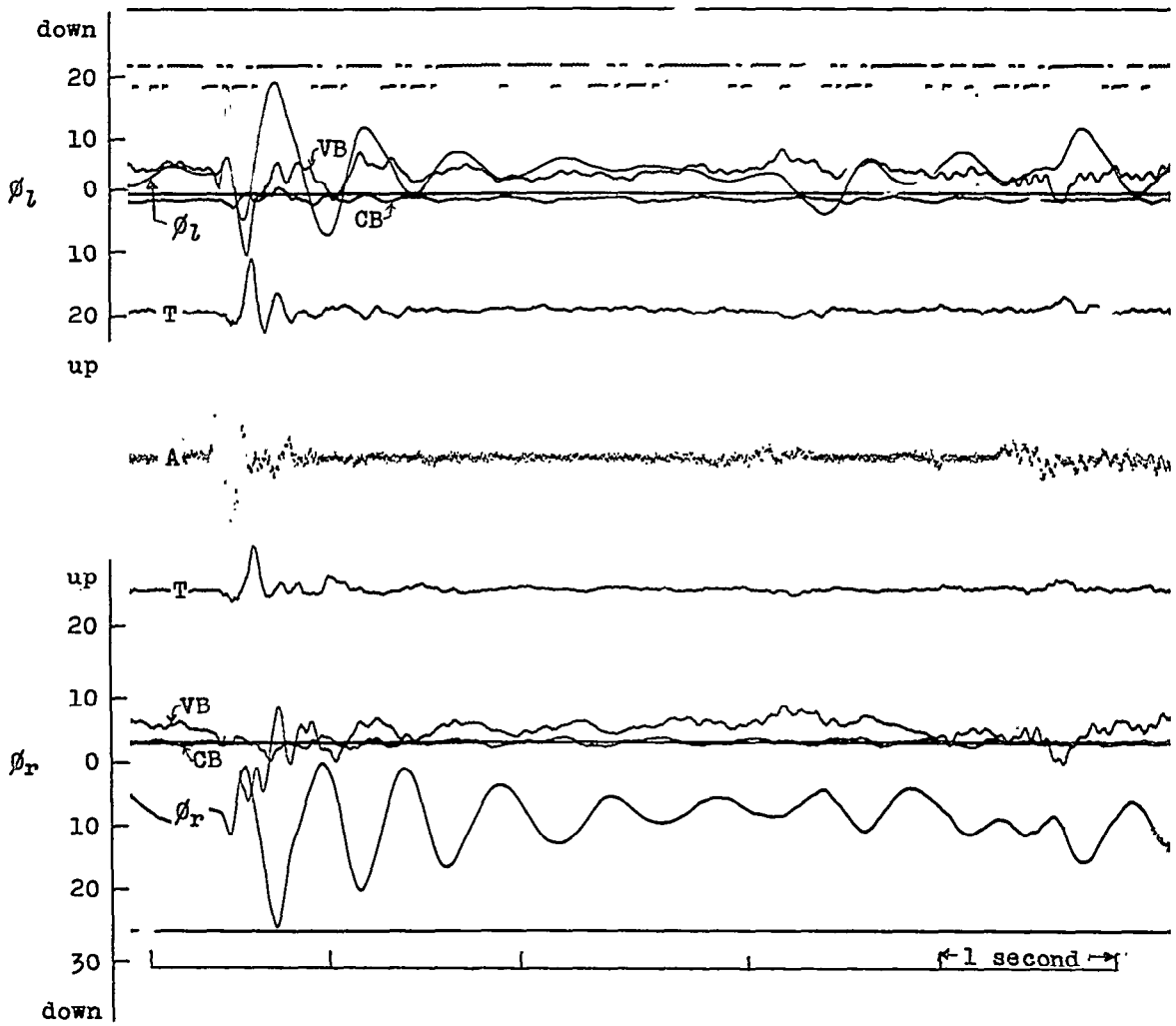

(b) V = 78.3 mph; symmetric excitation.

Figure 16.- Continued.

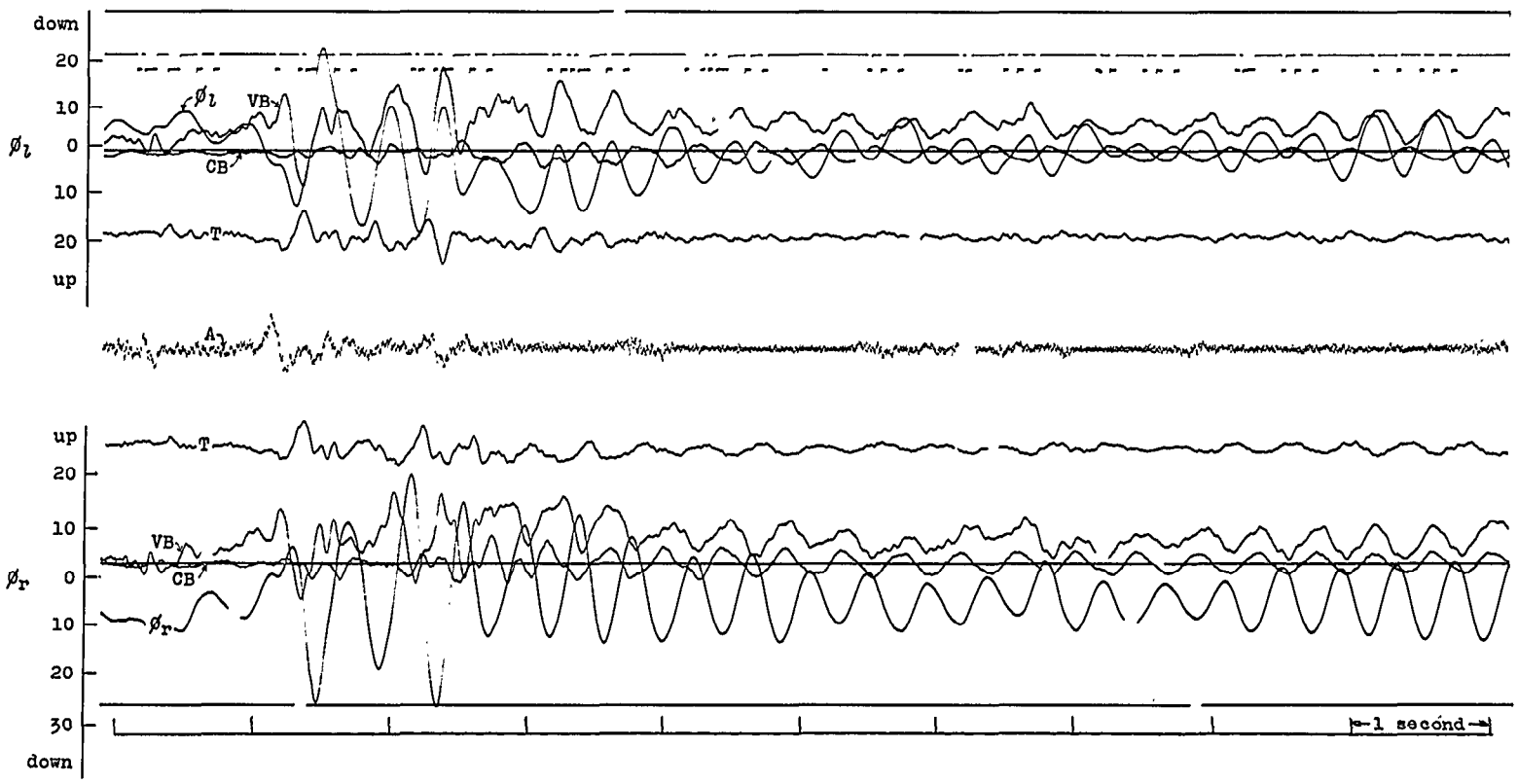

(c) V = 81.7 mph; symmetric excitation.

Figure 16.- Concluded.

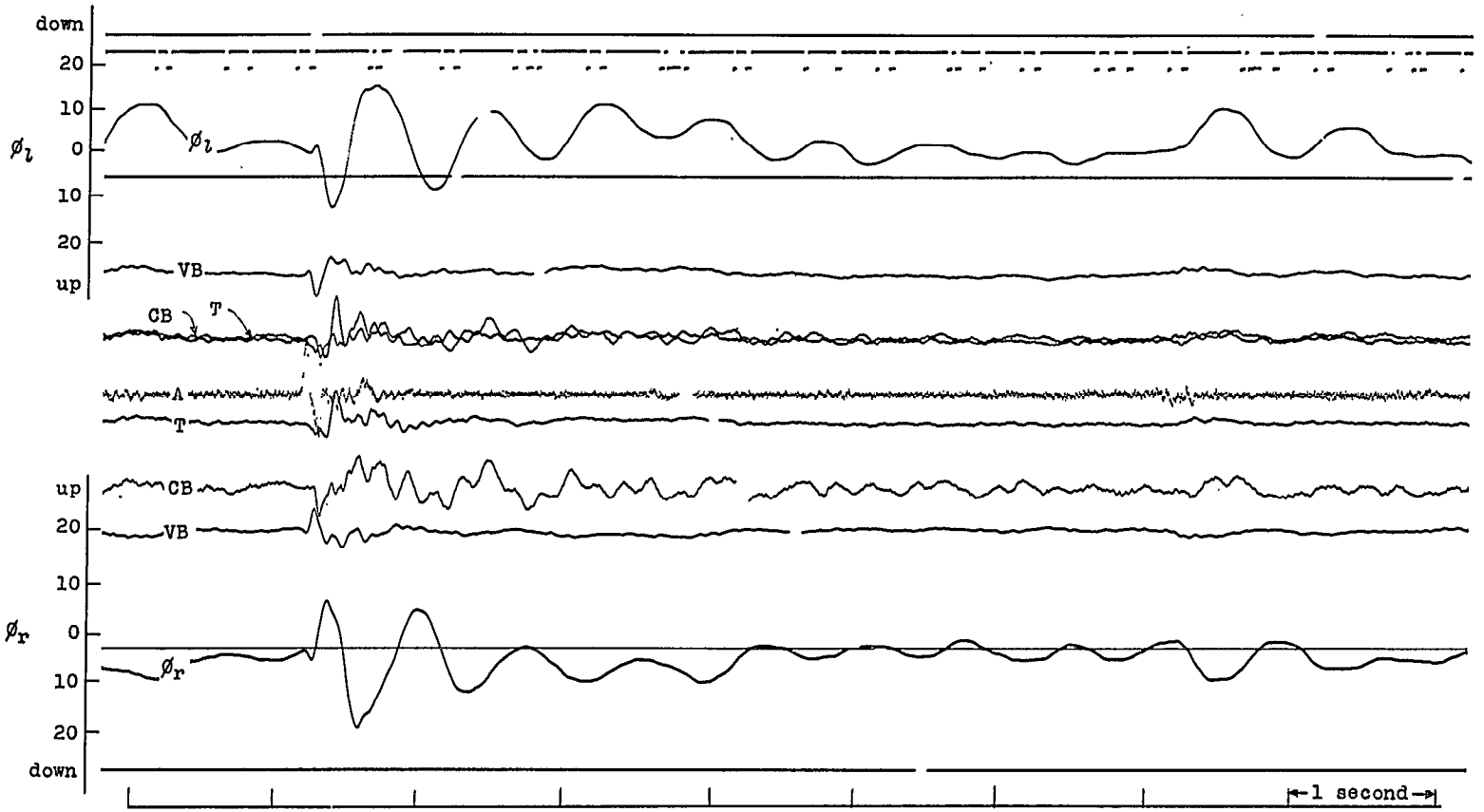

(a) V = 73.1 mph; symmetric excitation.

Figure 17.- Oscillograms for heavy fighters with $\delta = 15^{\circ}$. Fighters aft; light bomber.

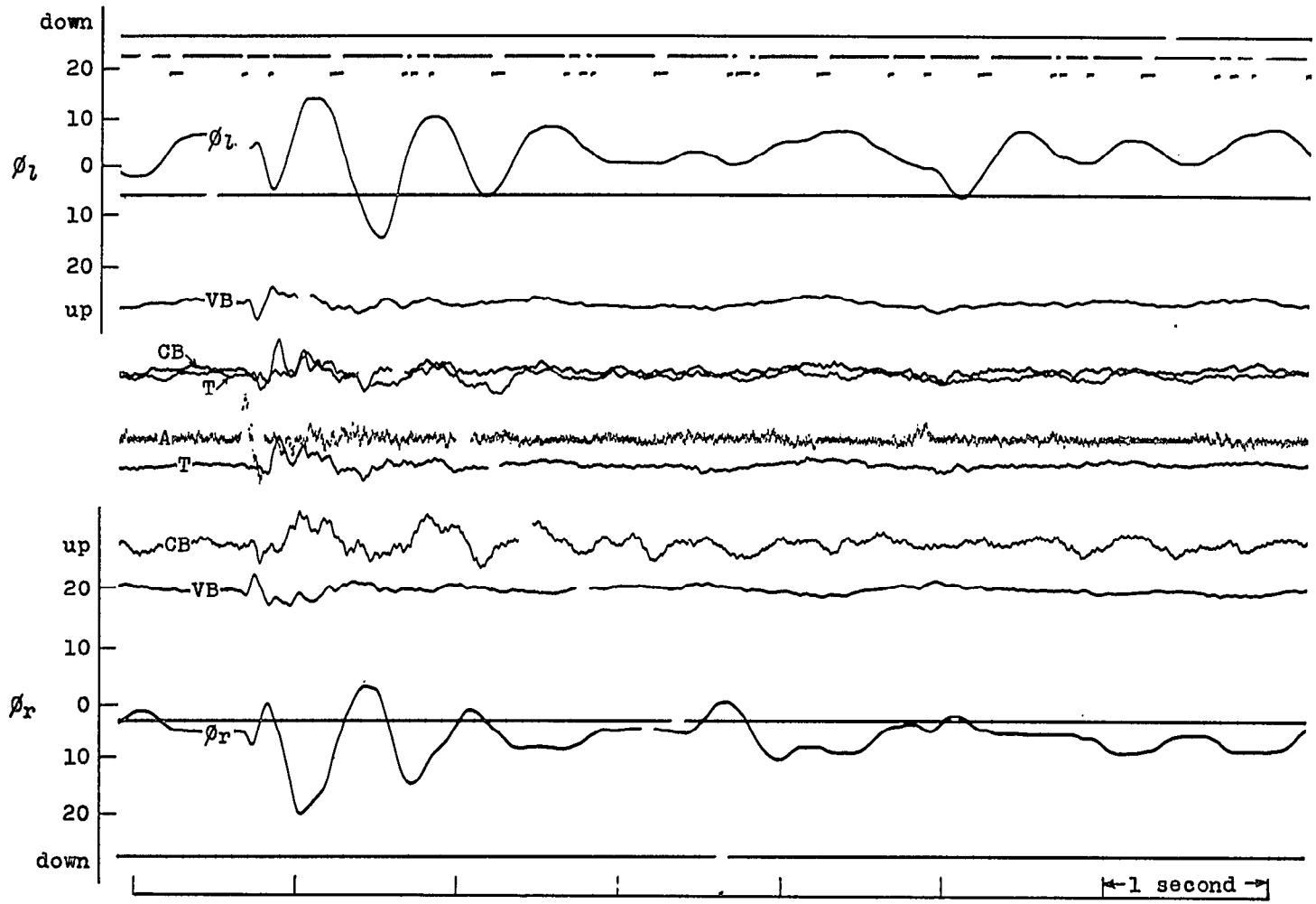

(b) V = 78.3 mph; symmetric excitation.

Figure 17.- Continued.

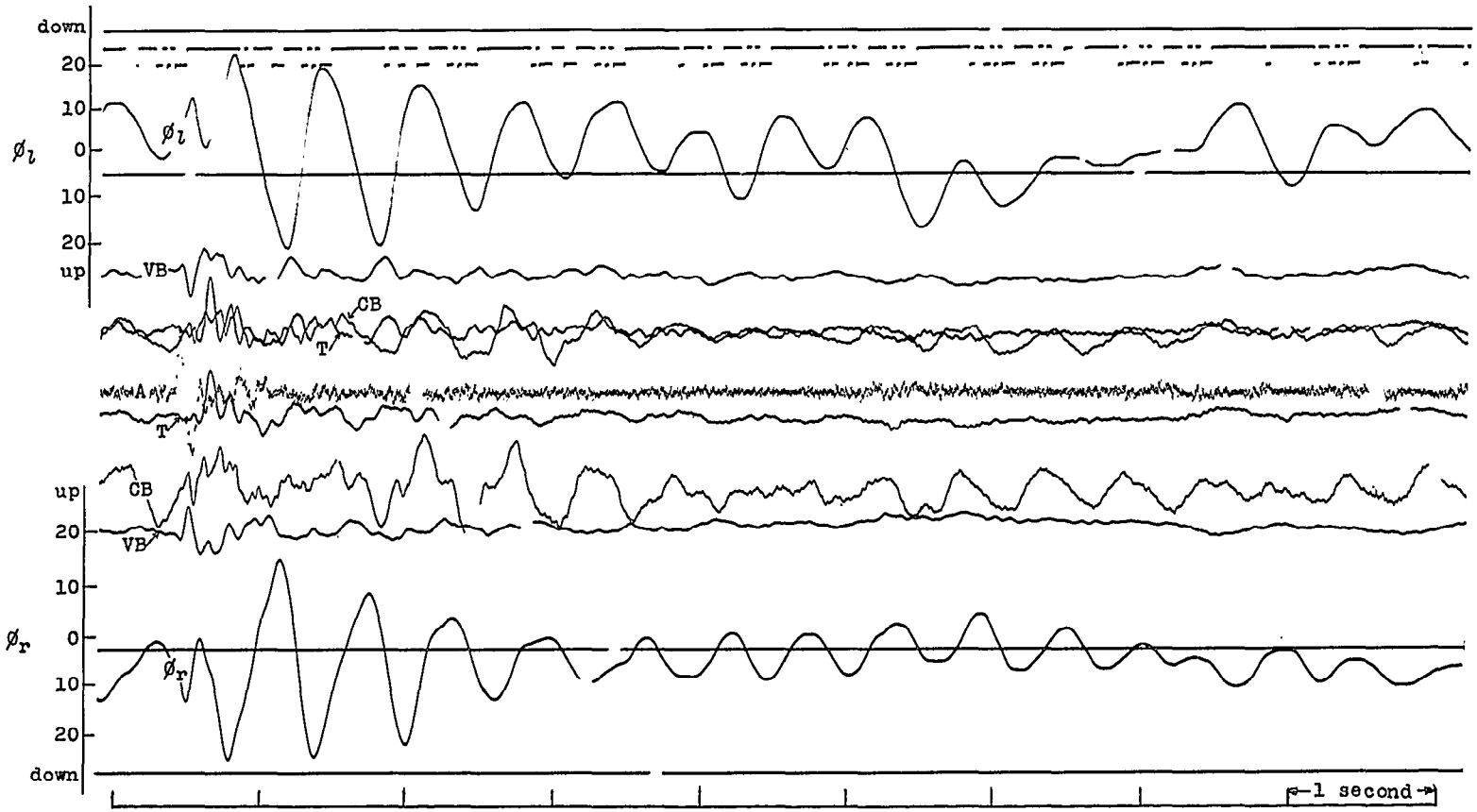

(c) V = 84.0 mph; symmetric excitation.

Figure 17.- Concluded.

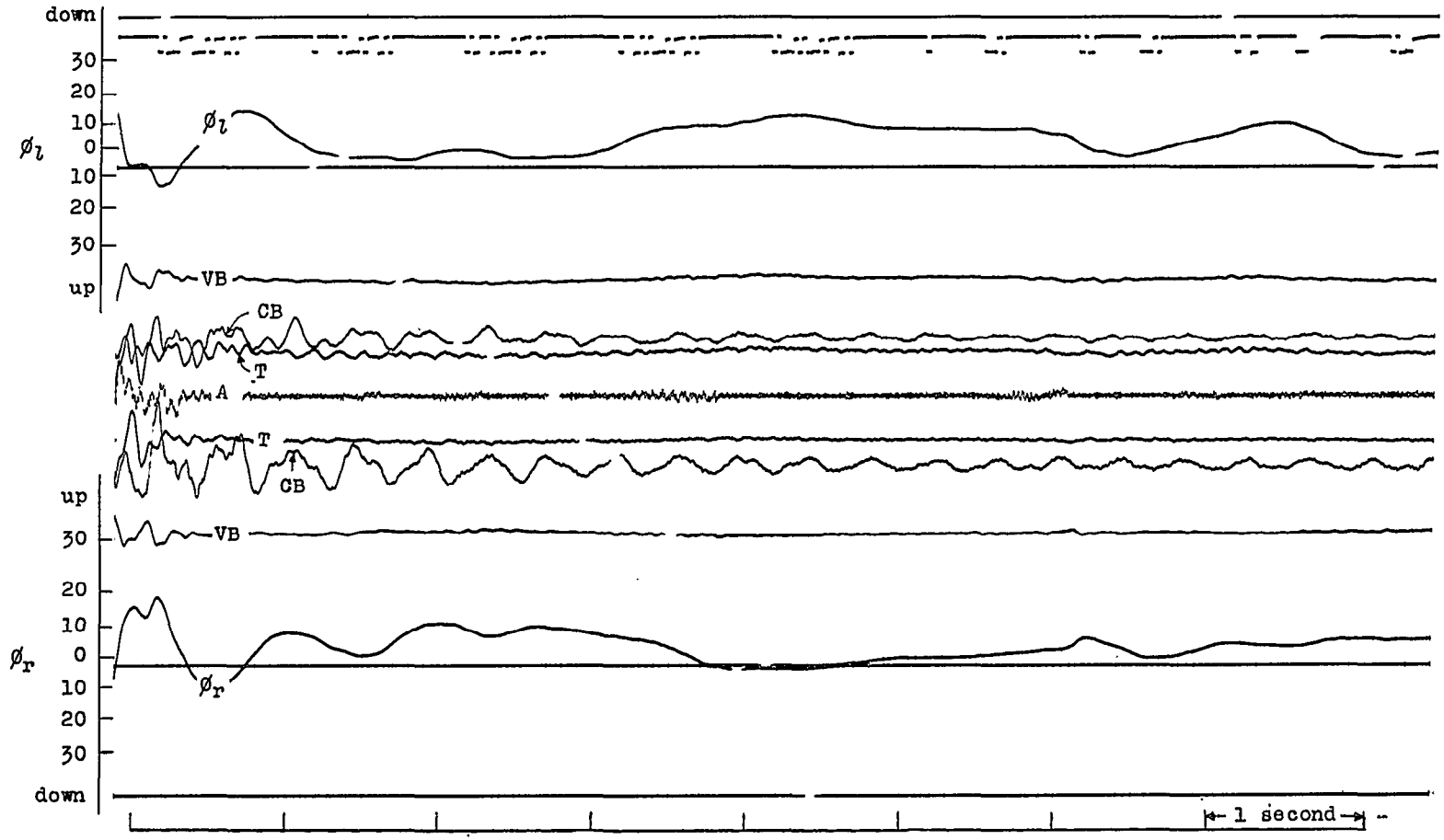

(a) V = 57.3 mph; symmetric excitation.

Figure 18.- Oscillograms for light fighters with $\delta = 8^{\circ}$. Fighters aft; light bomber.

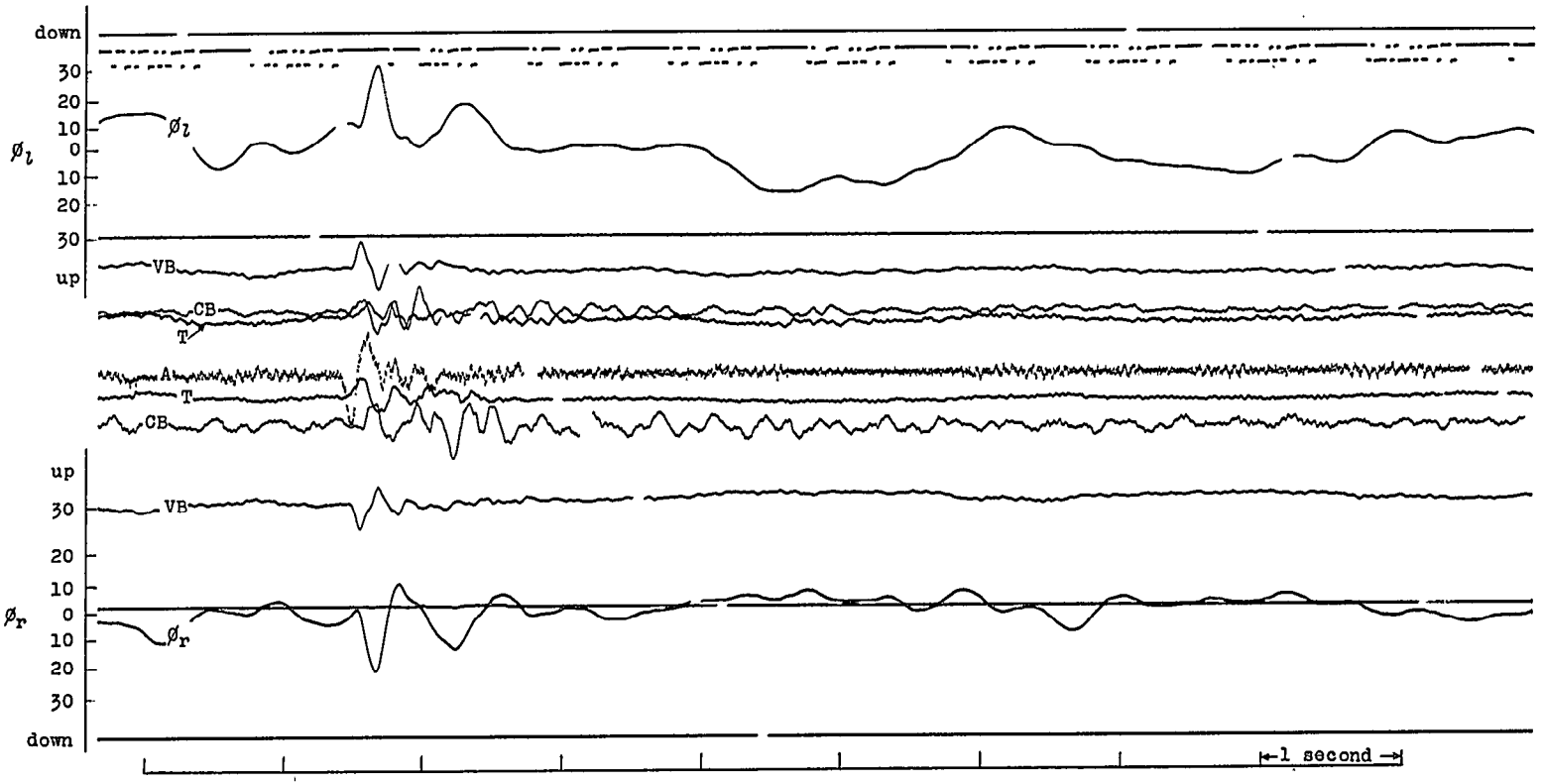

(b) V = 86.9 mph; symmetric excitation.

Figure 18.- Continued.

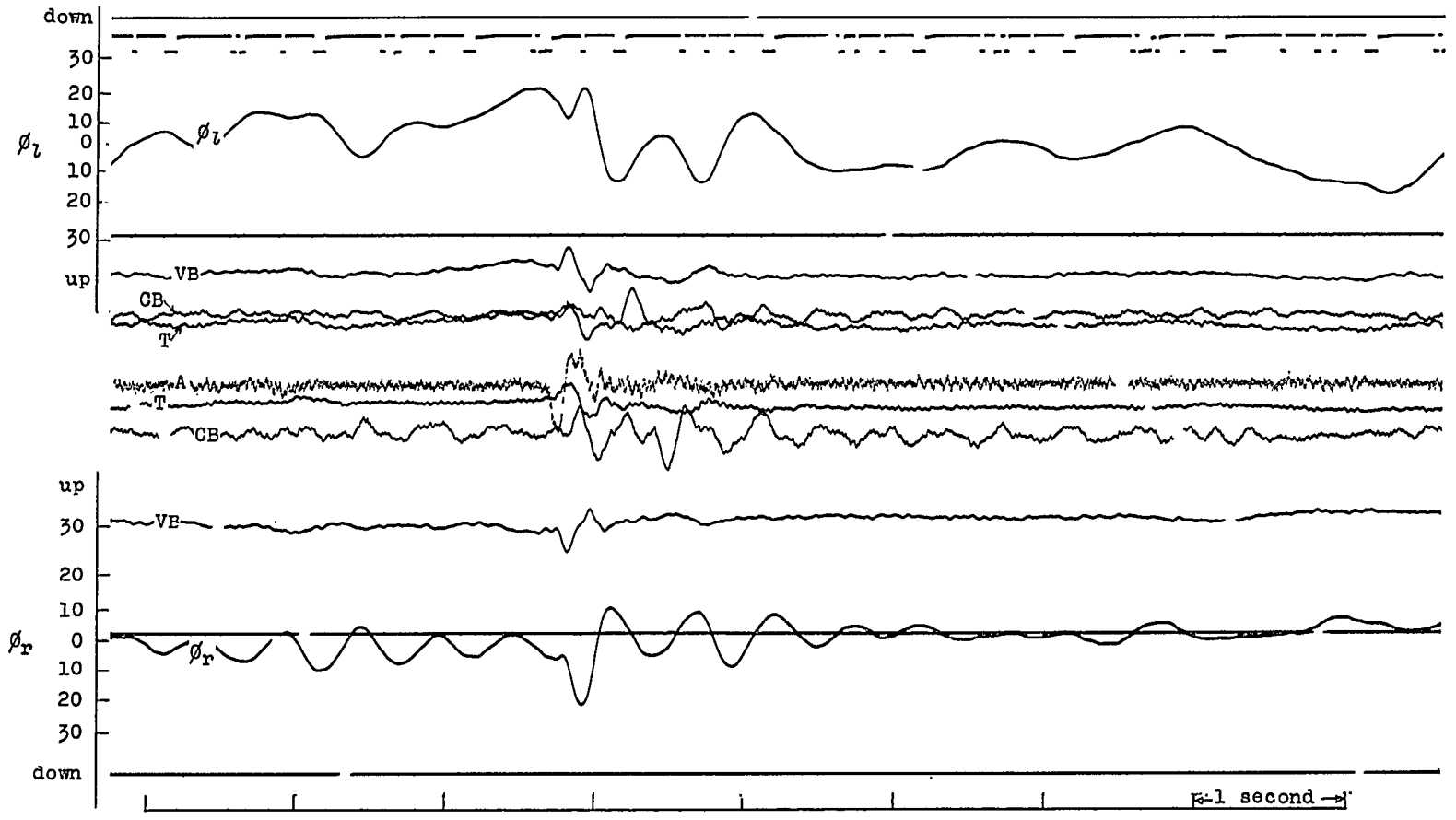

(c) V = 92.5 mph; symmetric excitation.

Figure 18.- Continued.

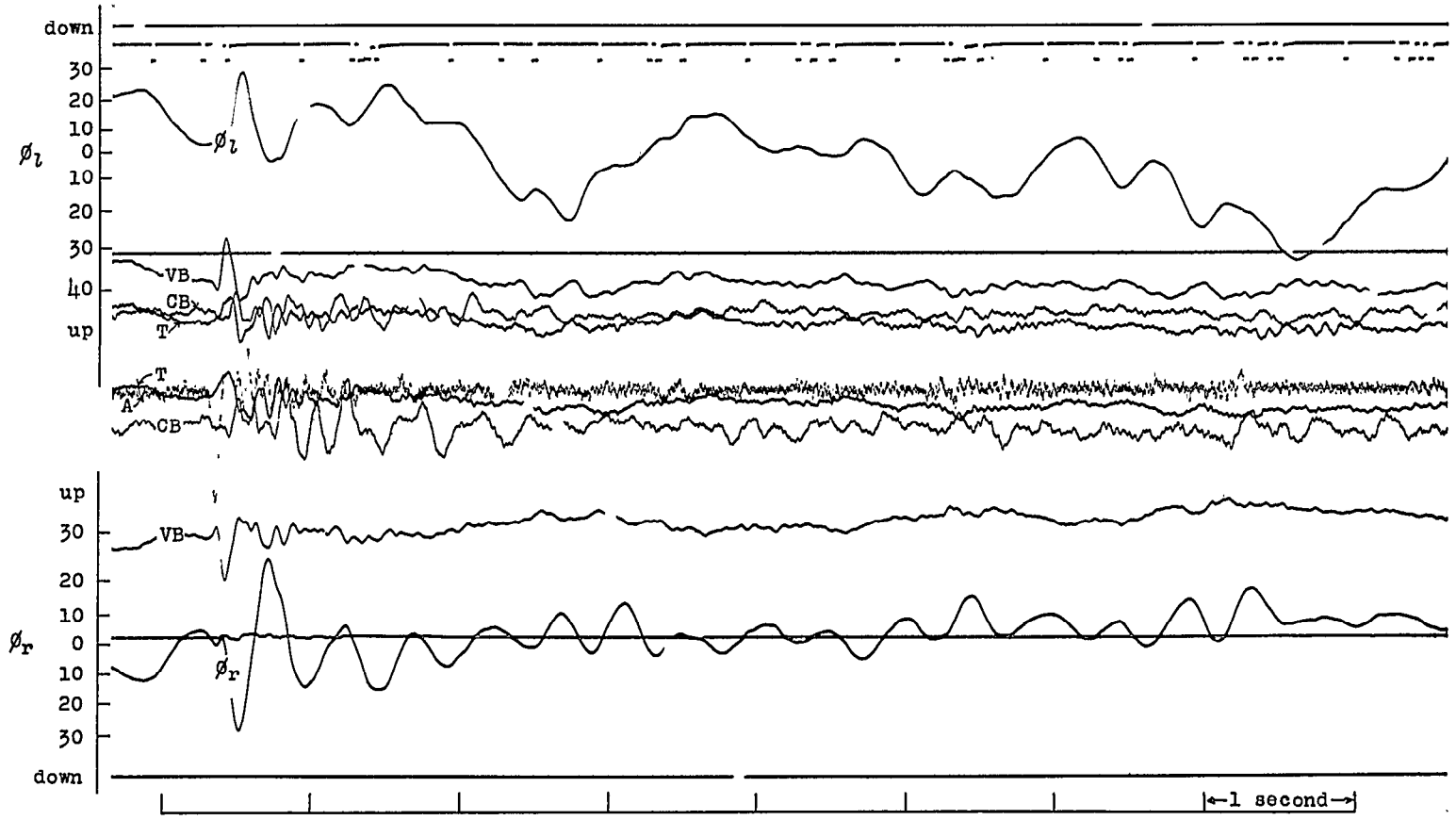

(d) V = 102.8 mph; symmetric excitation.

Figure 18.- Concluded.

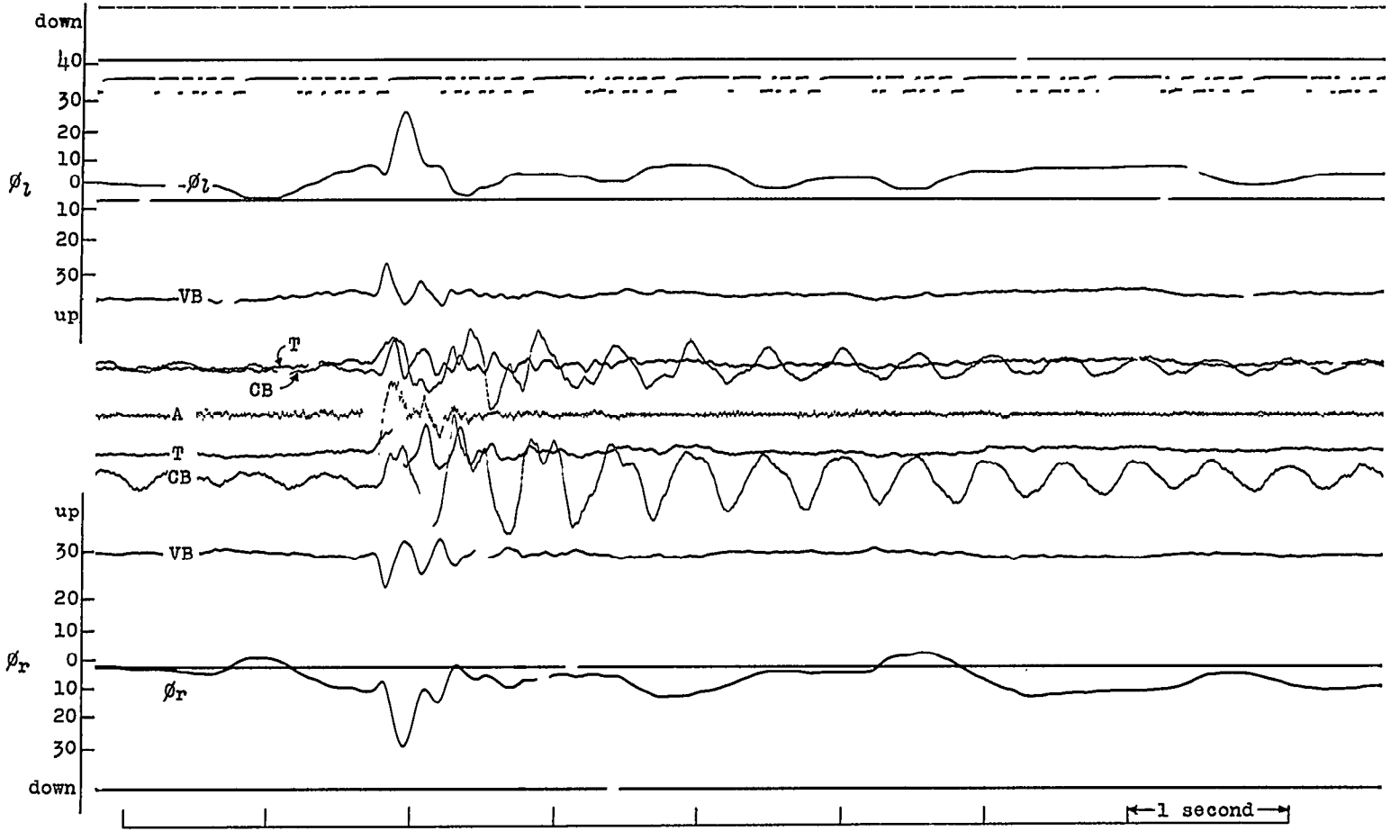

(a) V = 68.1 mph; symmetric excitation.

Figure 19.- Oscillograms for heavy fighters with $\delta = 8^{\circ}$. Fighters aft; light bomber.

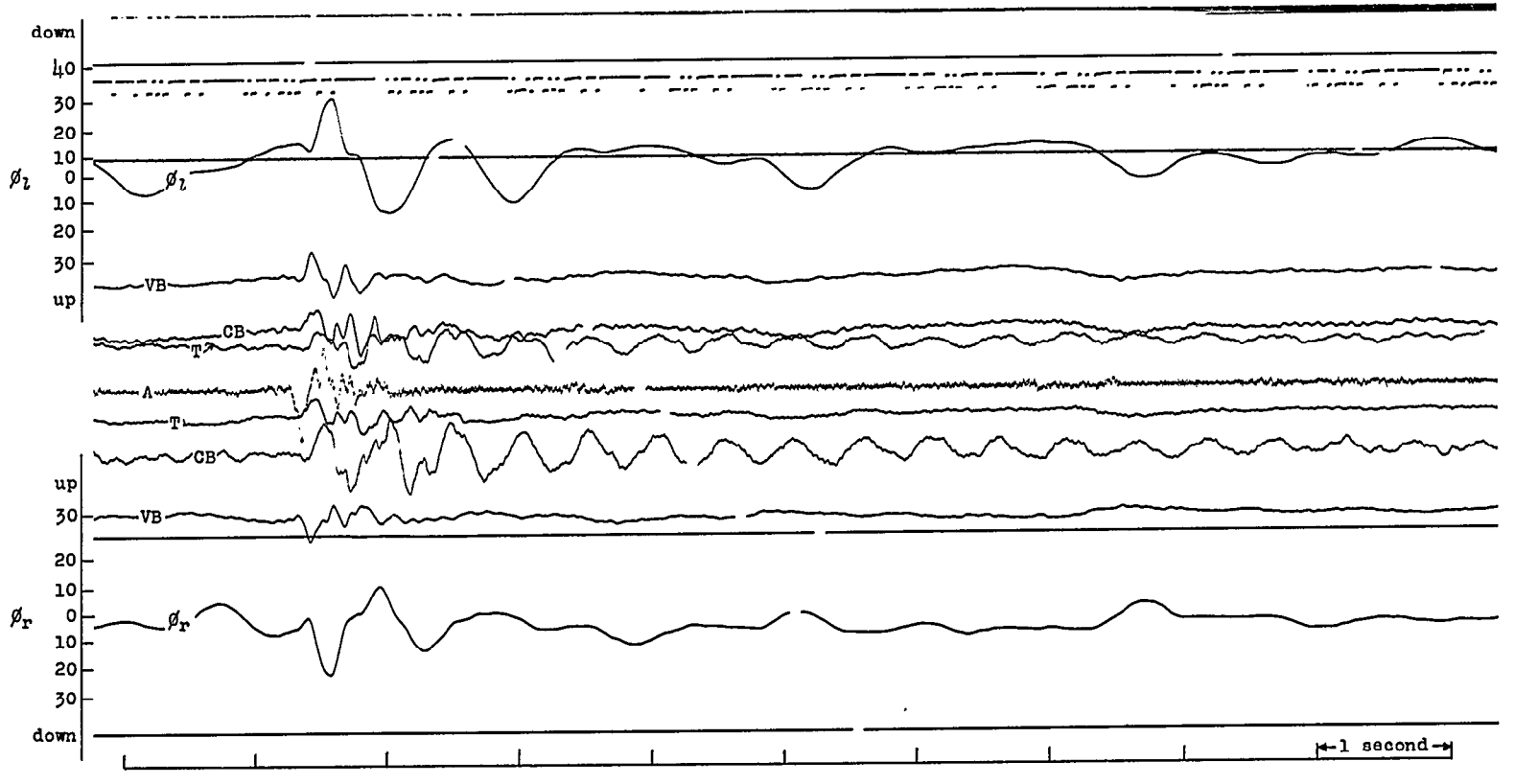

(b) V = 80.8 mph; symmetric excitation.

Figure 19.- Continued.

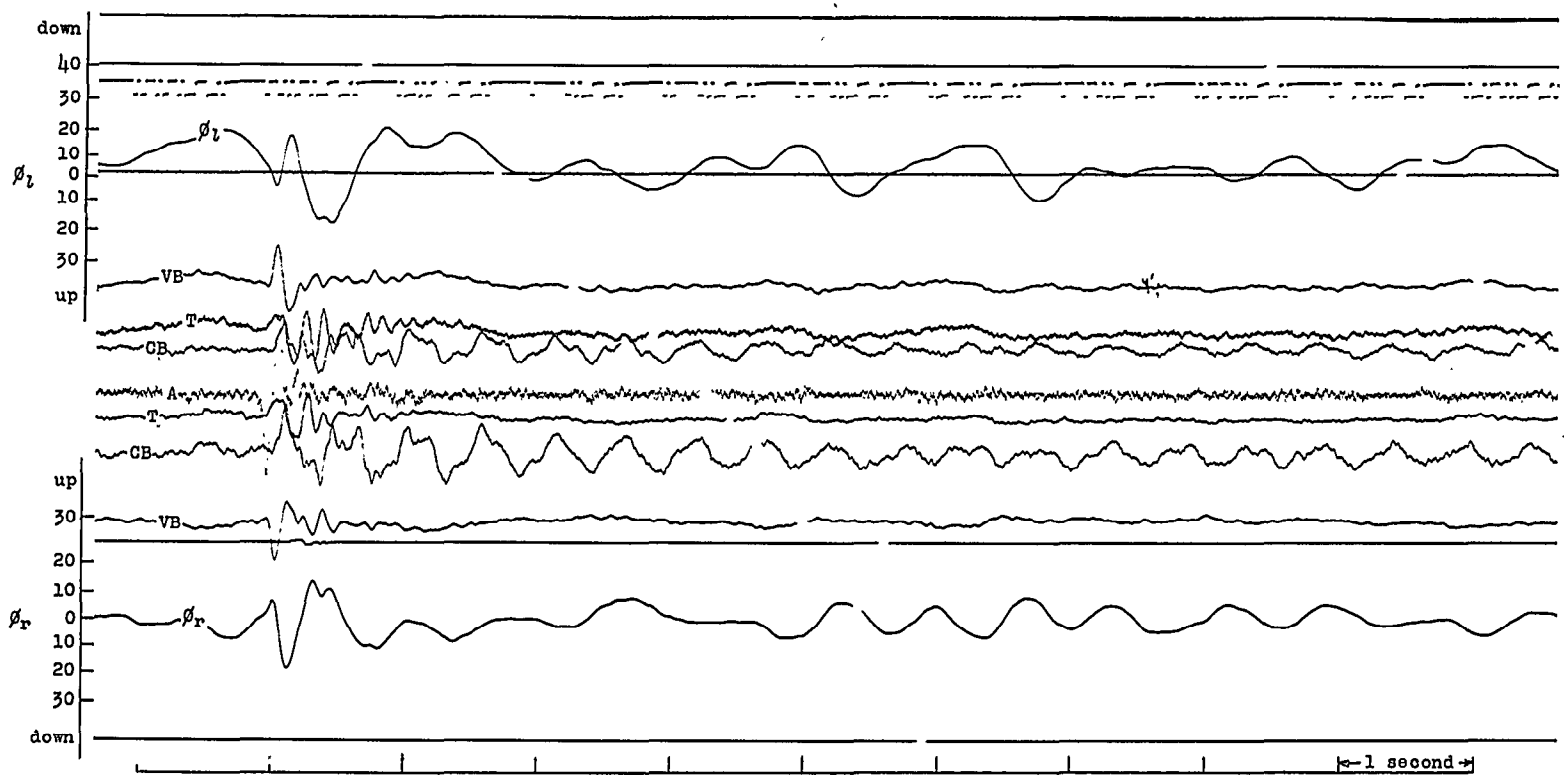

(c) V = 89.7 mph; symmetric excitation.

Figure 19.- Continued.

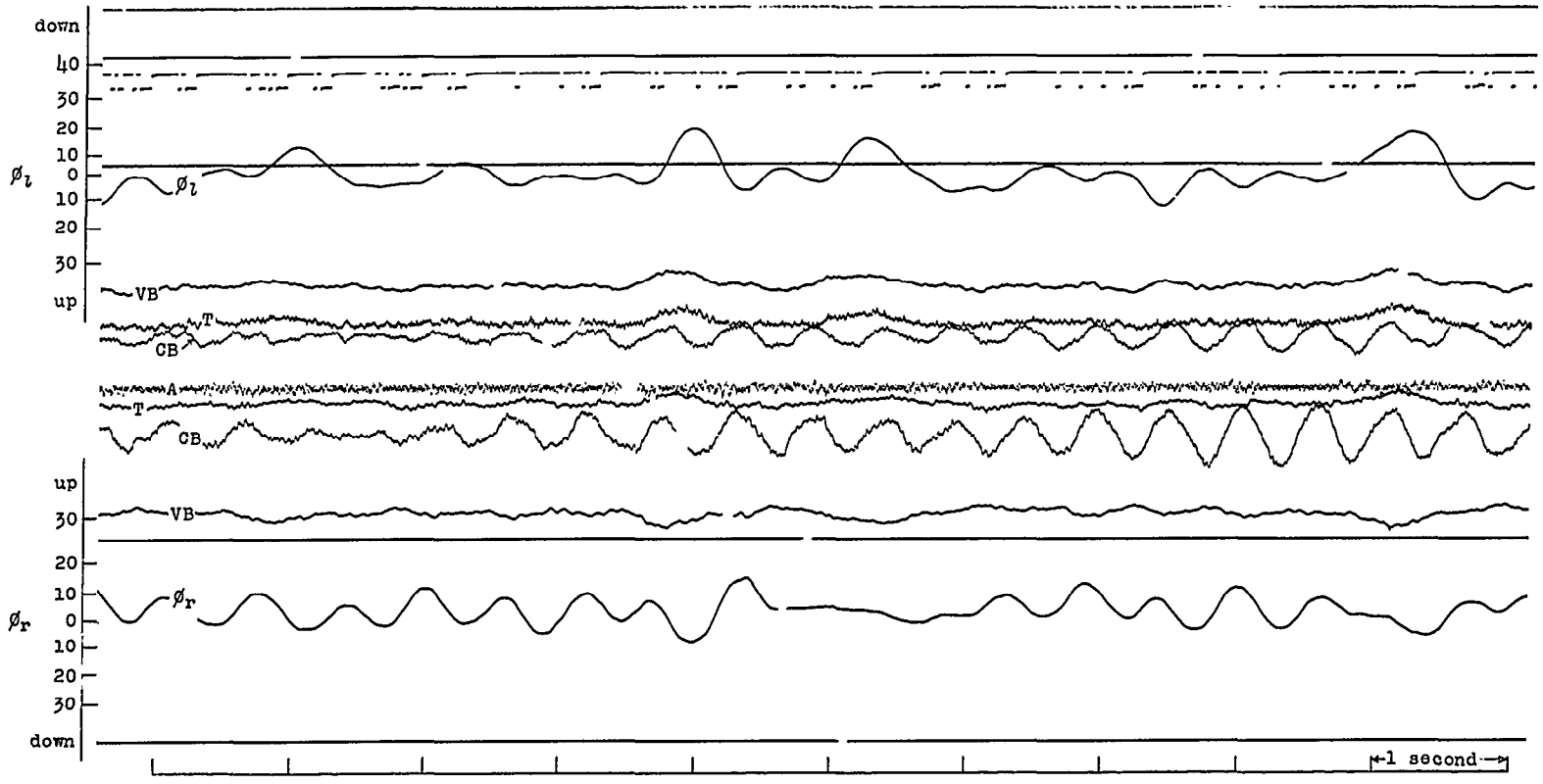

(d) V = 104.3 mph; symmetric excitation.

Figure 19.- Concluded.

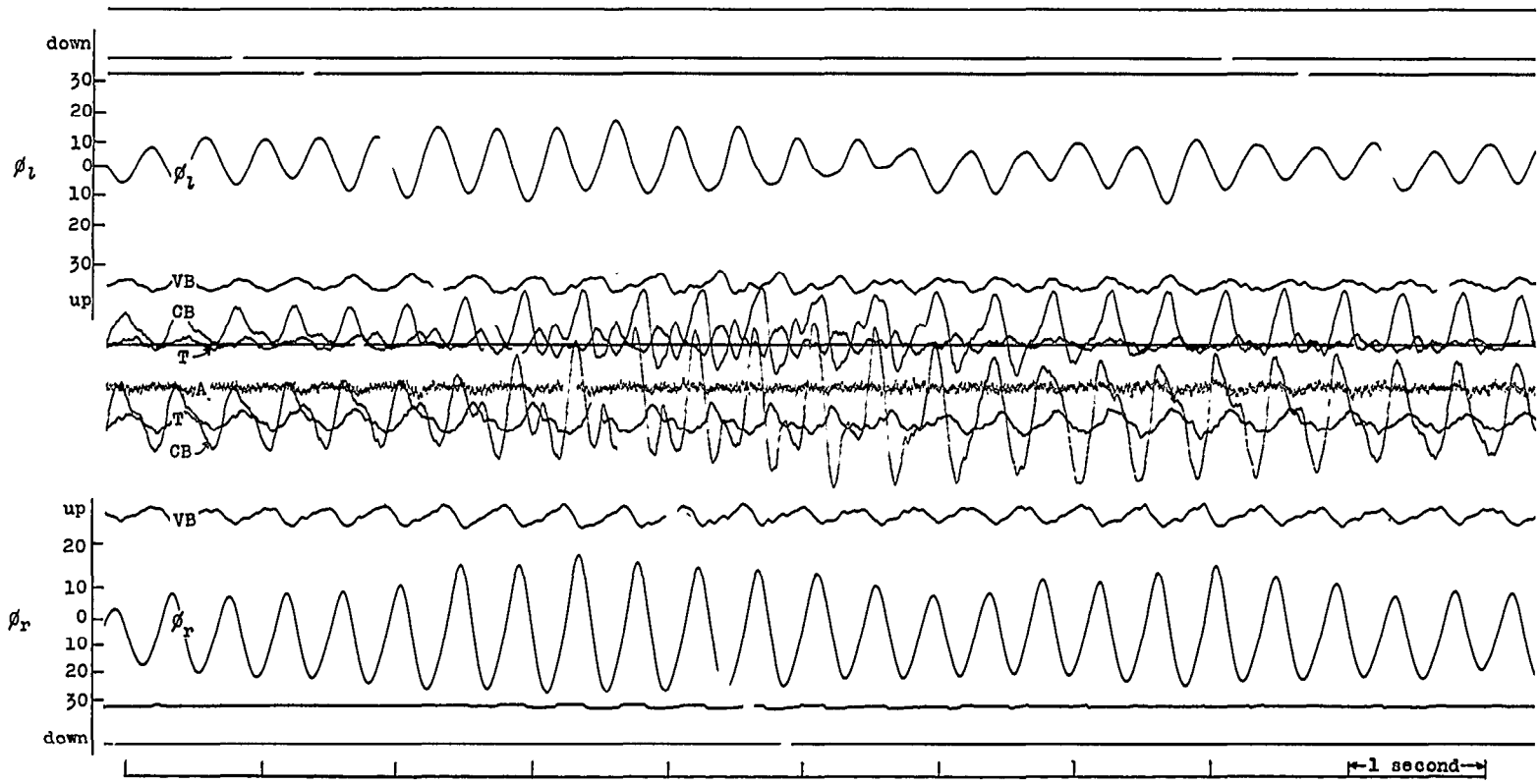

(a) Light fighters forward; $\delta = 15^\circ$; heavy bomber.

Figure 20.- Oscillograms obtained during instability.

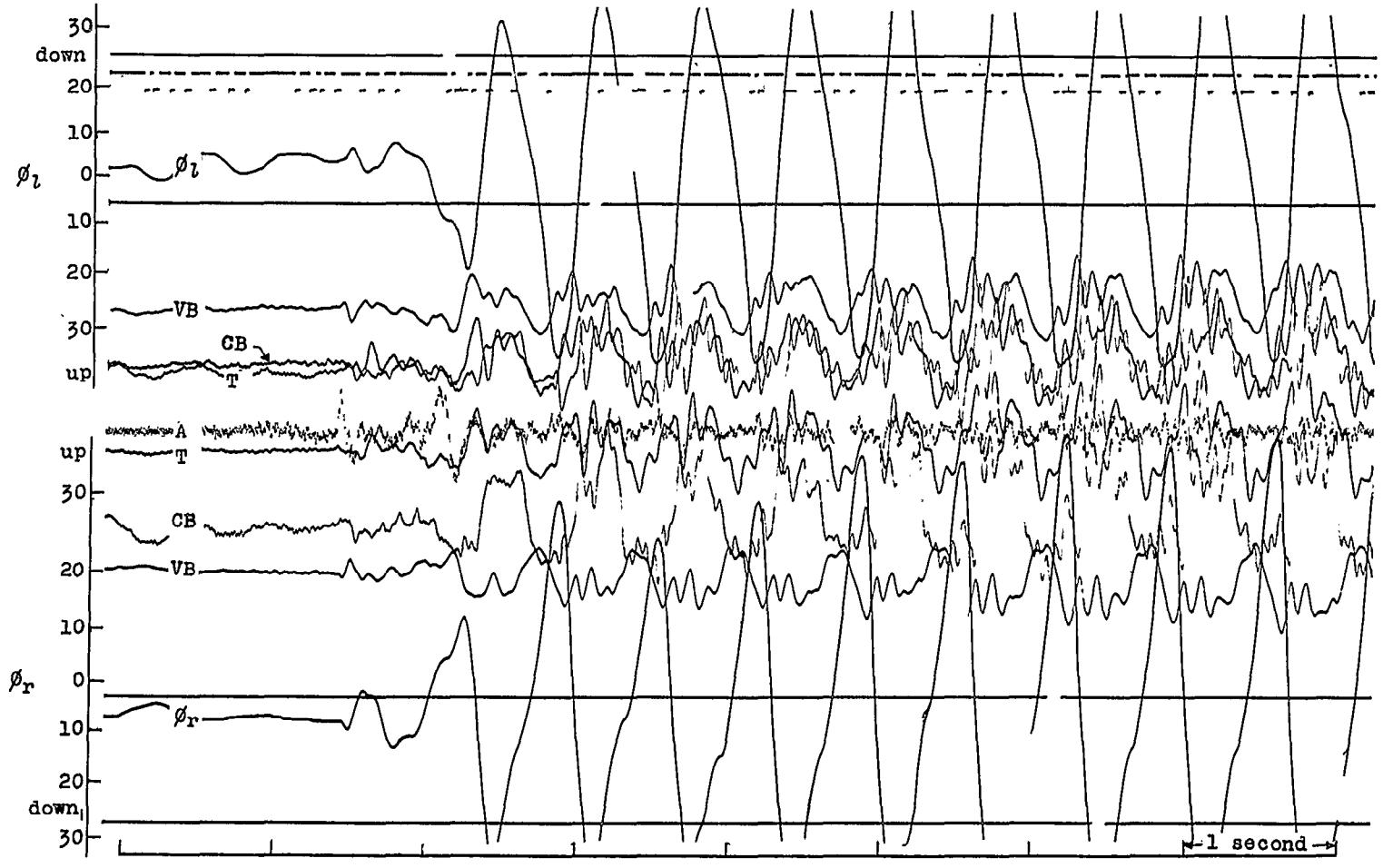

(b) Heavy fighters aft; $\delta = 15^{\circ}$; light bomber.

Figure 20.- Continued.

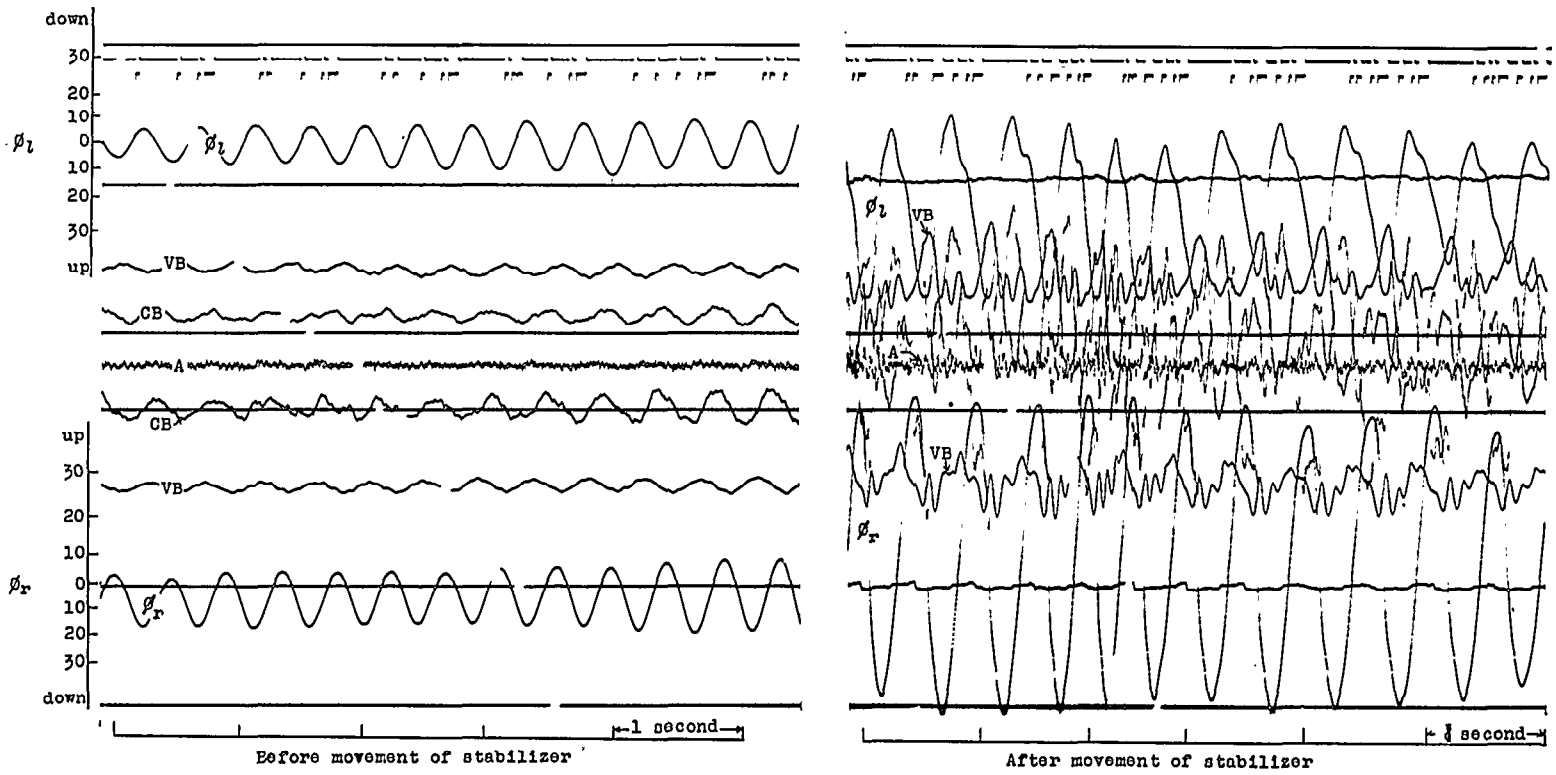

(c) Light fighters forward; $\delta = 15^{\circ}$; light bomber.

Figure 20.- Concluded.

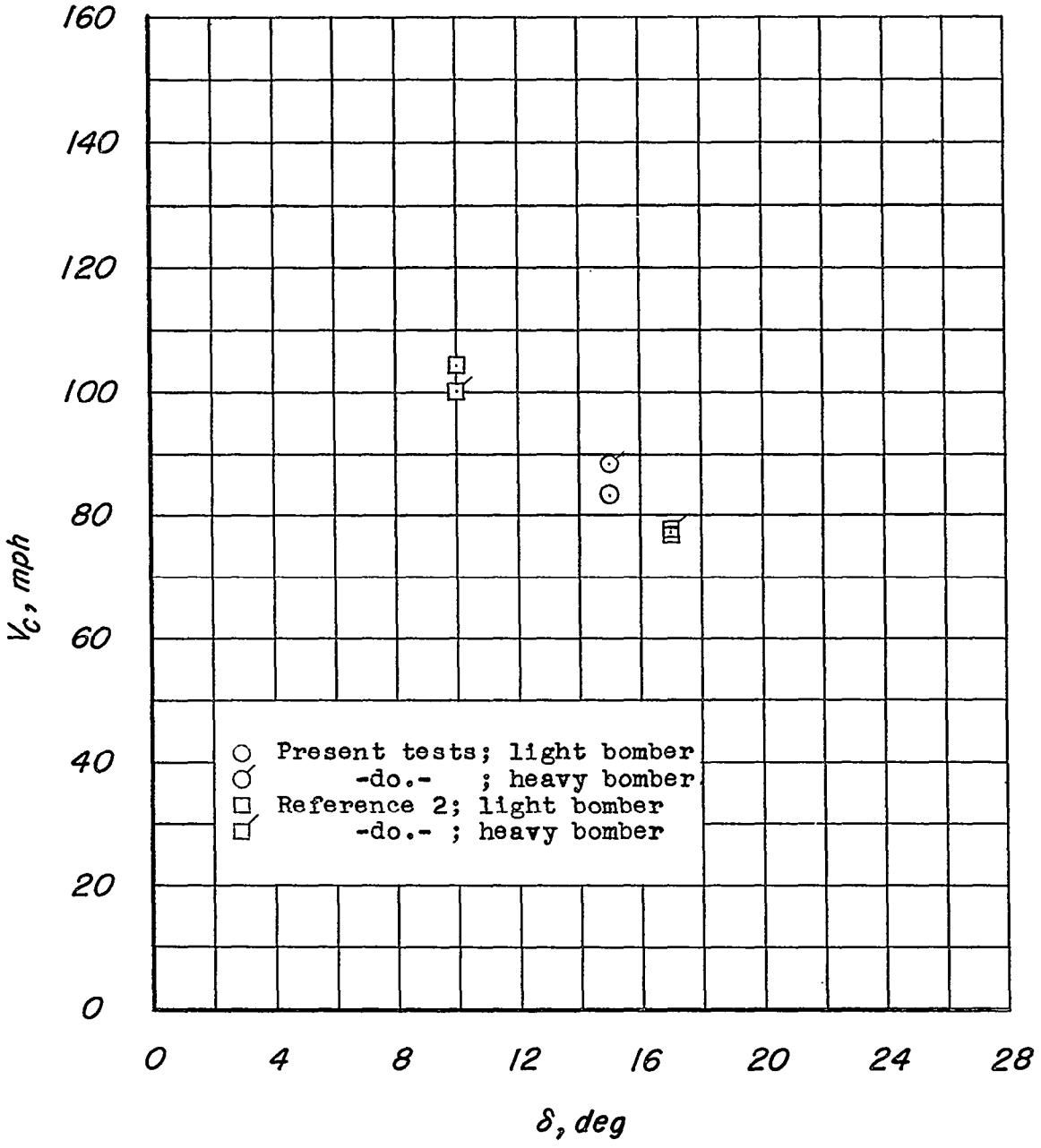

(a) Light fighters in aft position.

Figure 21.- Variation of flutter speed with hinge skew angle.

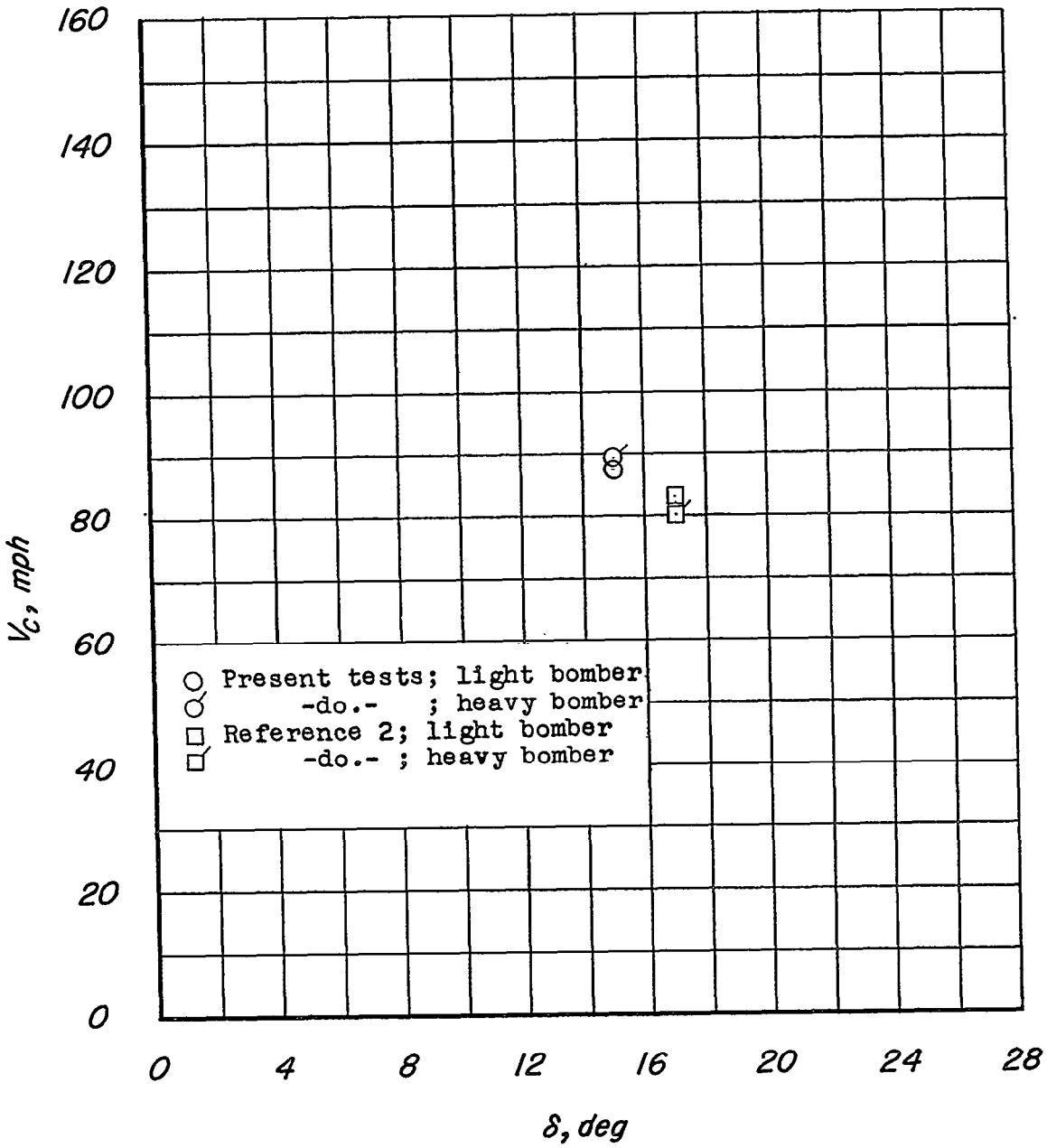

(b) Heavy fighters in aft position.

Figure 21.- Continued.

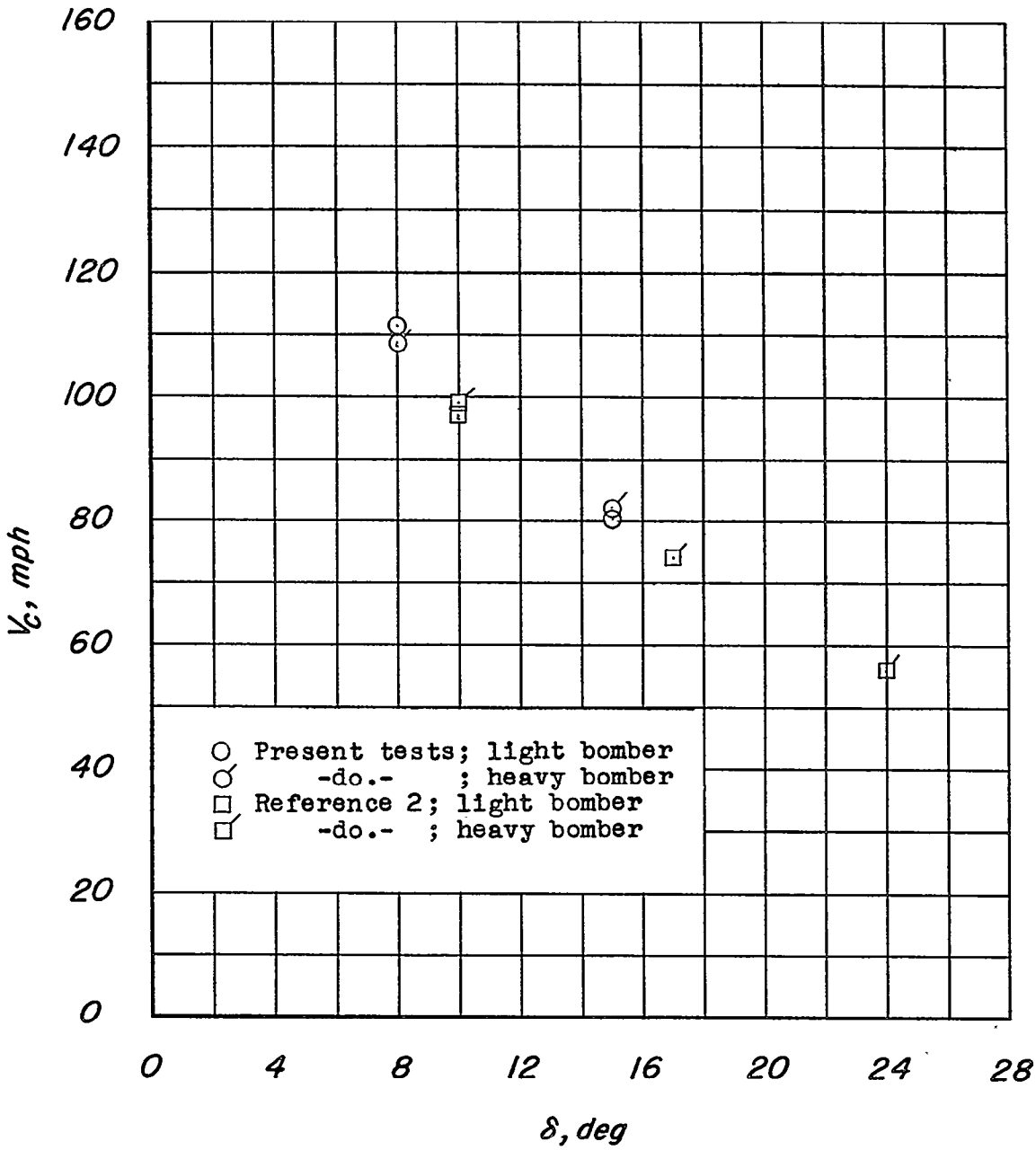

(c) Light fighters in forward position.

Figure 21.- Continued.

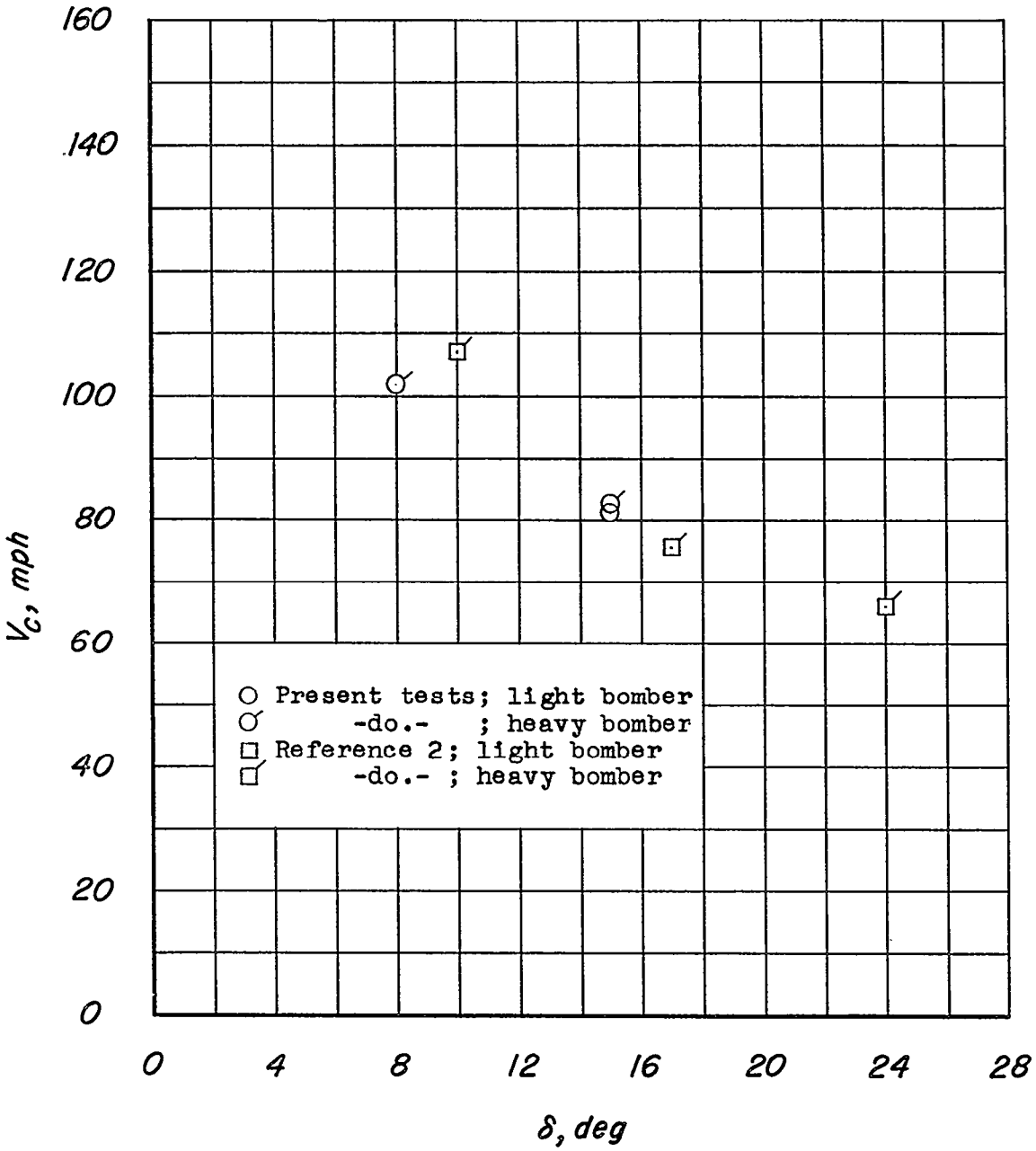

(d) Heavy fighters in forward position.

Figure 21.- Concluded.

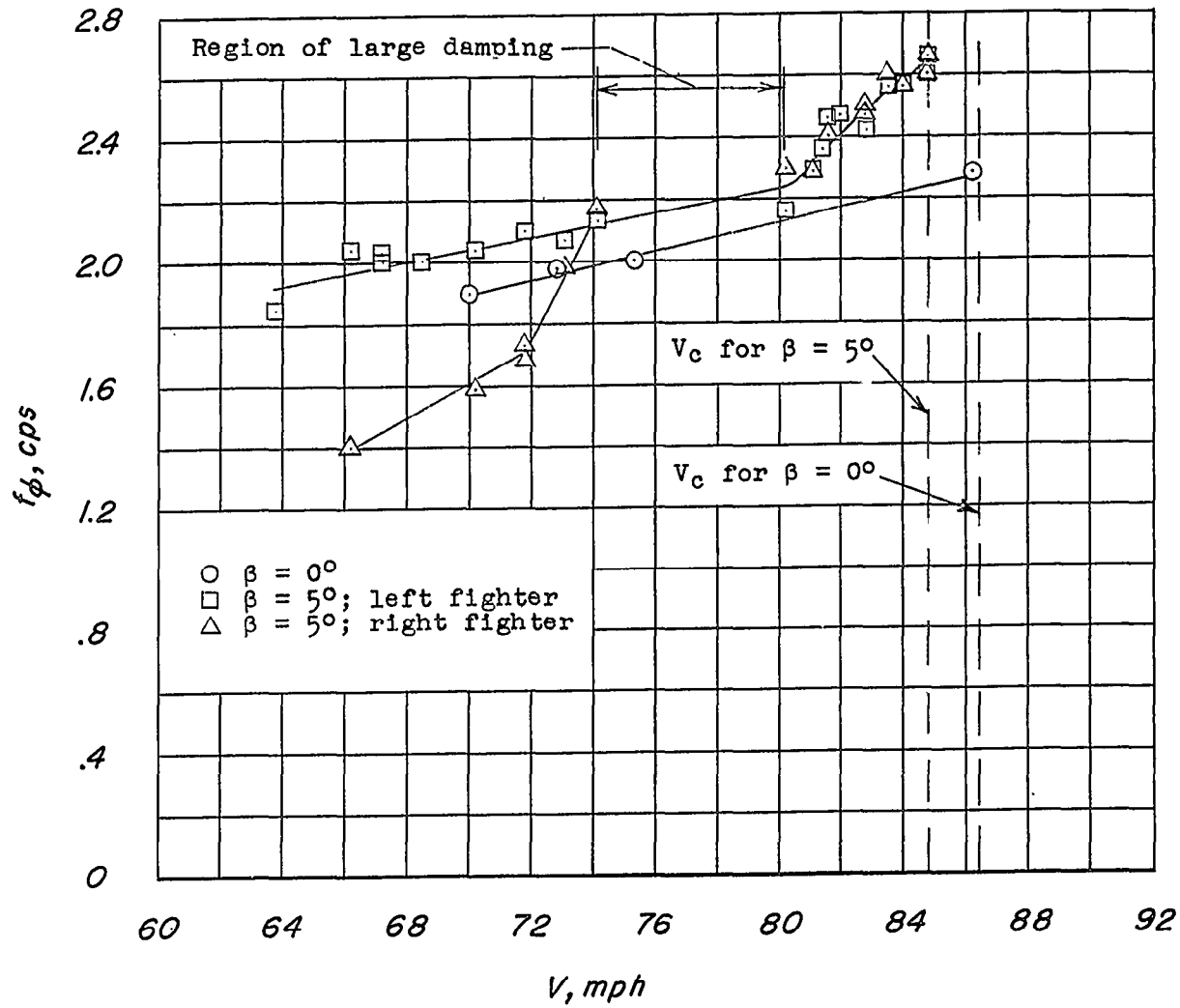

Figure 22.- Effect of sideslip angle on frequency of fighter roll oscillation. Light fighters in aft position; light bomber in fixed condition.

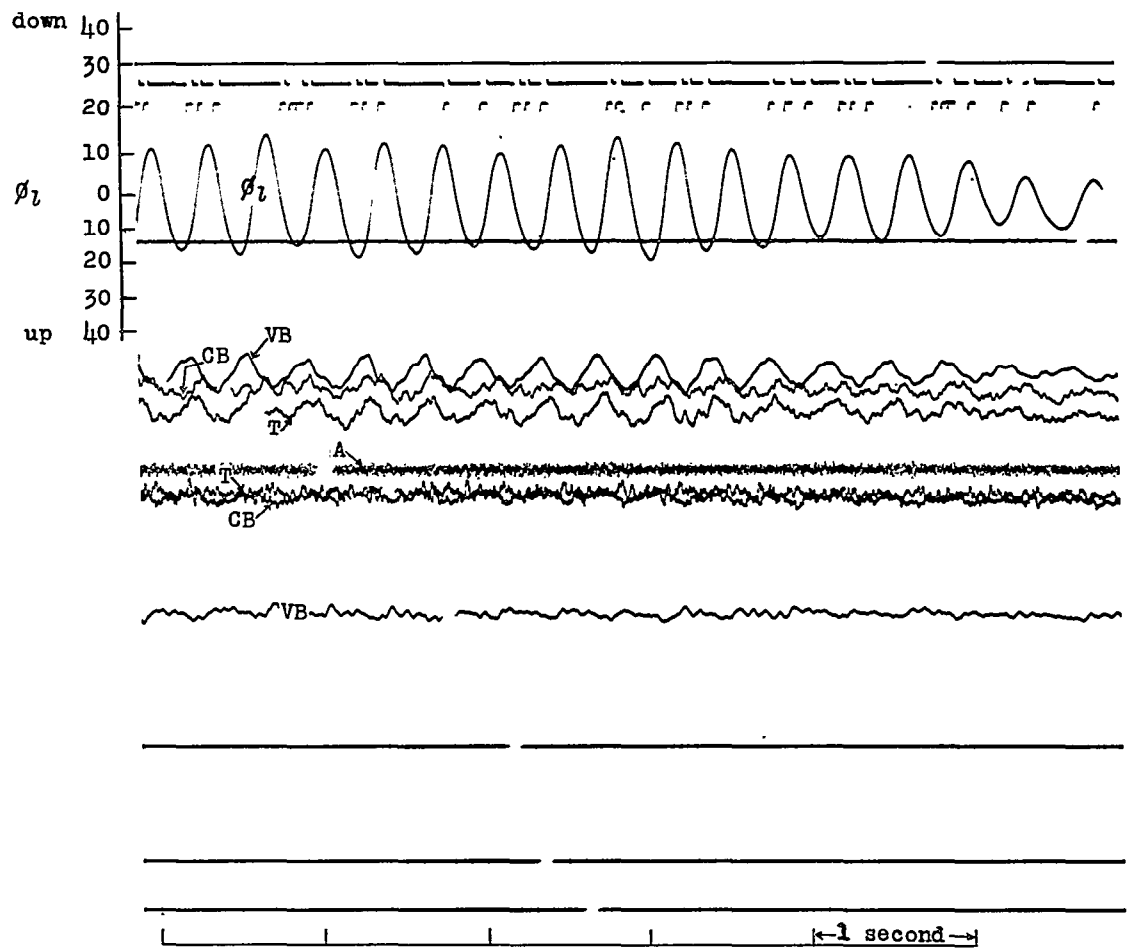

Figure 23.- Oscillogram showing flutter for single fighter configuration. Light fighters aft; $\delta = 15^{\circ}$; $\beta = 0^{\circ}$.

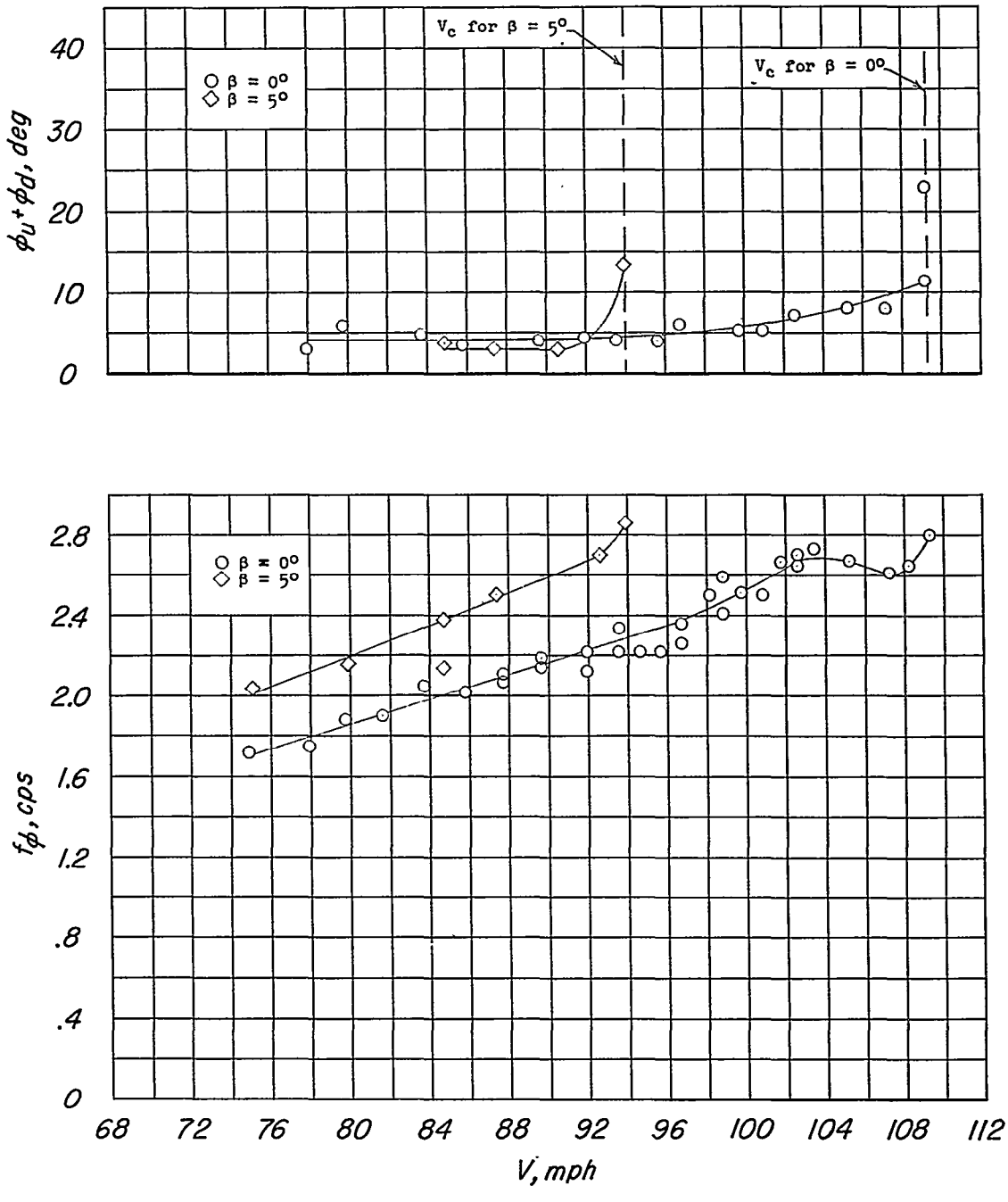

(a) Light fighter.

Figure 24.- Variation of amplitude and frequency of fighter roll oscillation with airspeed for single fighter configuration. $\delta = 15°$; left fighter in aft position; light bomber in fixed condition.

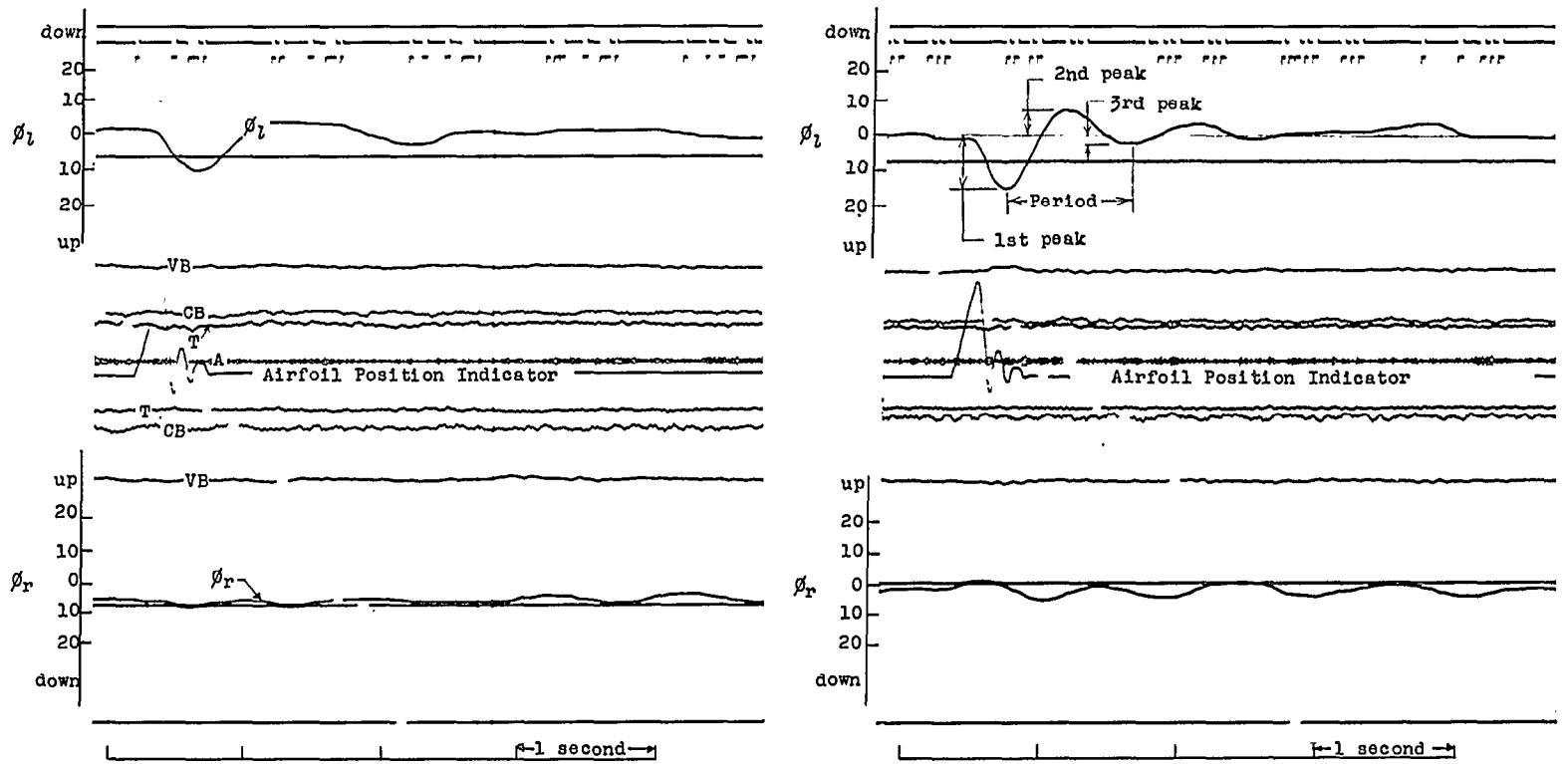

(c) $\delta = 8^{\circ}$; heavy fighters.

(d) $\delta = 8^{\circ}$; light fighters.

Figure 25.- Concluded.

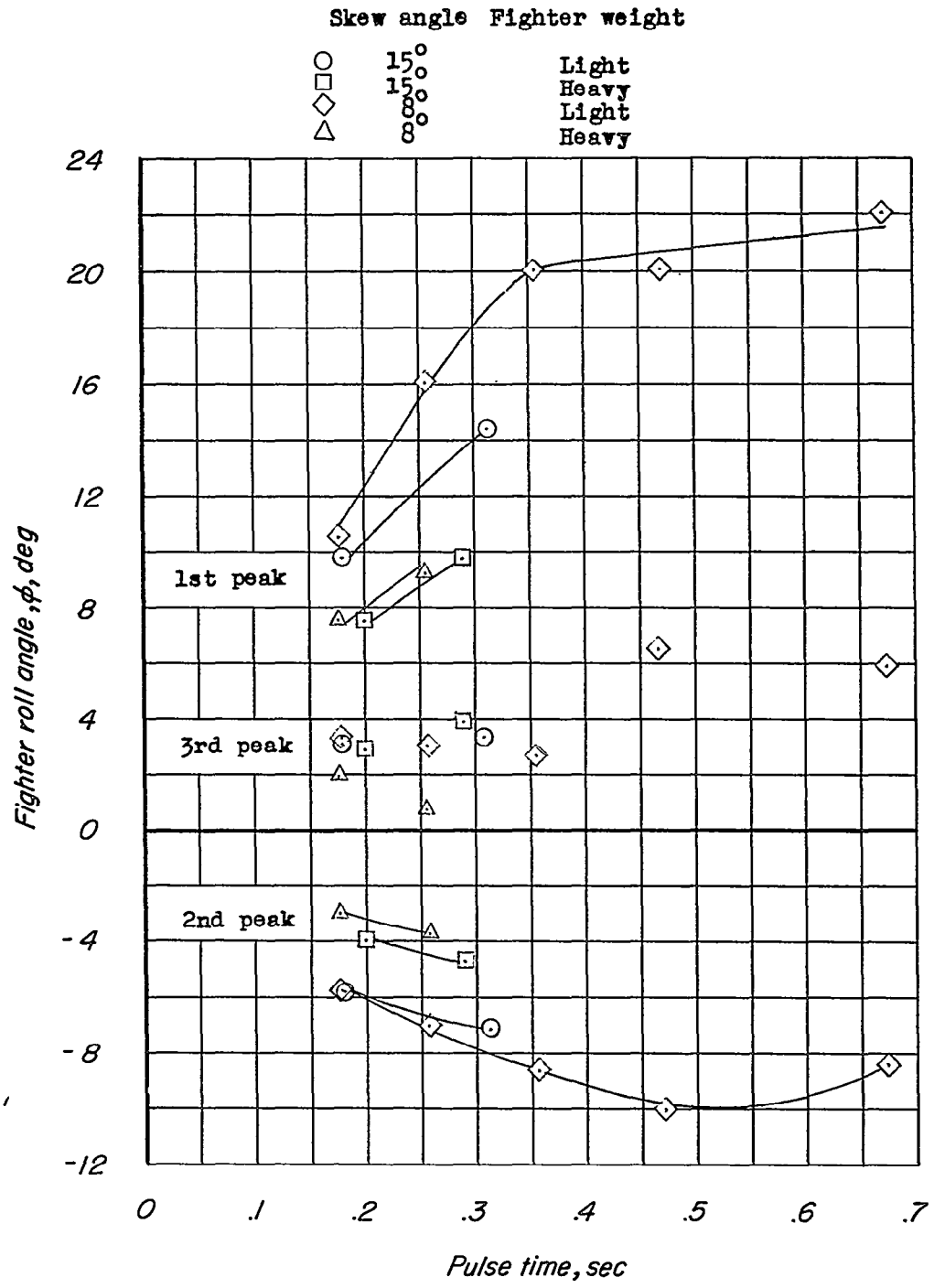

(b) V = 70 mph.

Figure 26.- Continued.

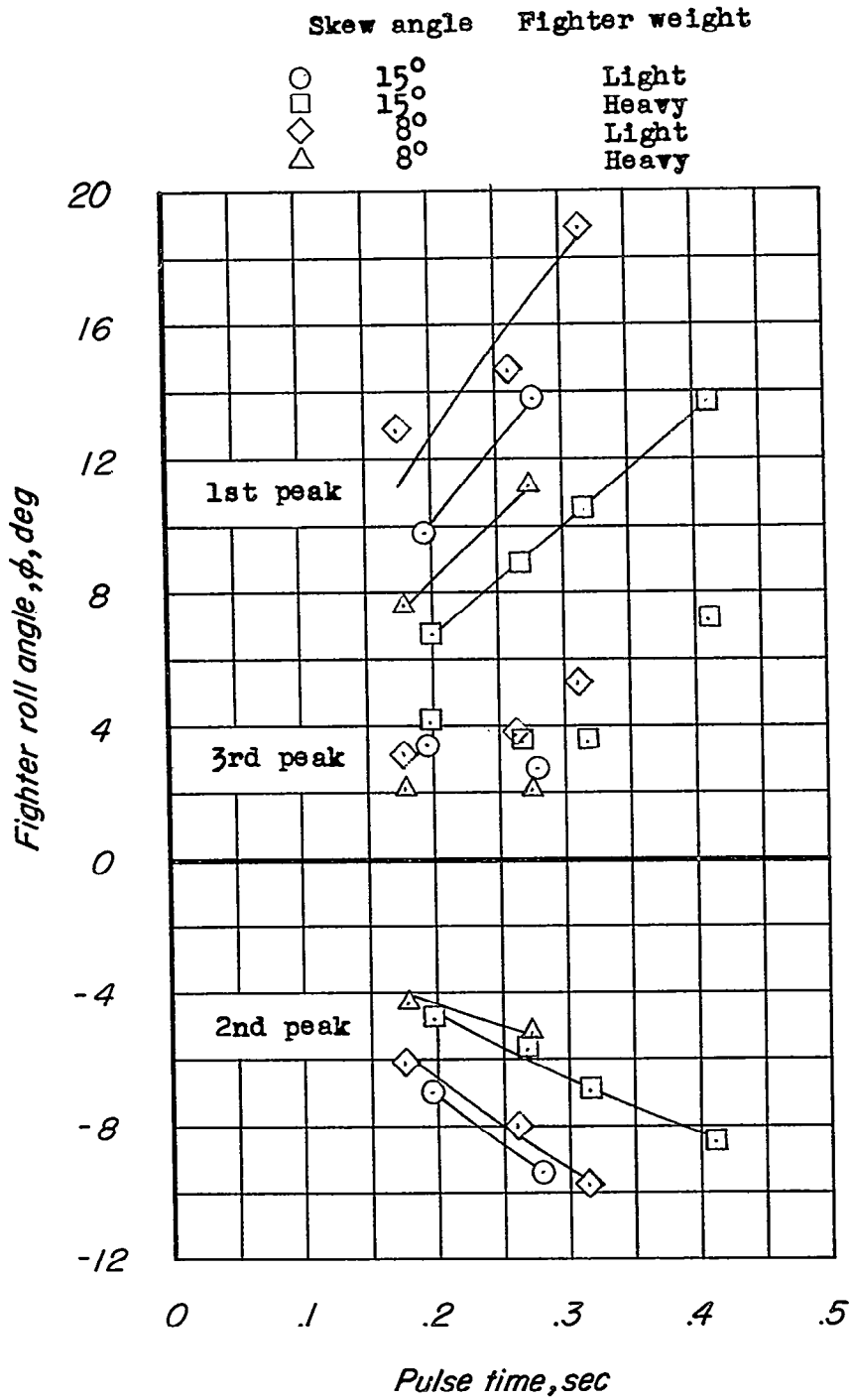

(c) V = 75 mph.

Figure 26.- Concluded.

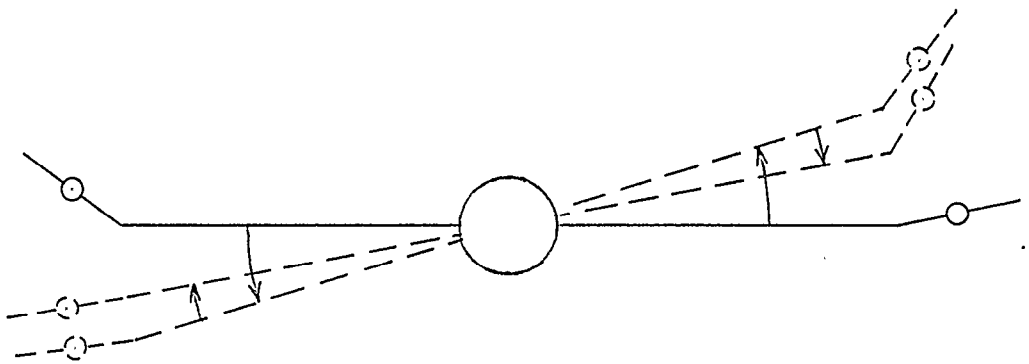

Figure 27.- Schematic drawing illustrating bomber-fighter roll oscillation obtained with fighters banked up. Light bomber in fixed condition; light fighters aft; $\delta = 8^{\circ}$.

INDEX

ABSTRACT

Tests of a 1/25-scale model of a B-36J/RF-84F tip-coupled airplane were made in the Langley 19-foot pressure tunnel in order to evaluate the flutter characteristics where bomber-body freedoms are allowed and to obtain an indication of the dynamic stability characteristics of the configuration. The bomber model was supported by a gimbal which moved on a vertical rod and permitted four degrees of body freedom. Both the fighter and bomber models were scaled in geometry, mass and inertia; in addition, the bomber model was elastically scaled. The variables studied in the investigation were the skew angle of the fighter-bomber coupling, fighter longitudinal position, fighter and bomber loading, angle of sideslip, degrees of body freedom, and the number of fighters.